Pullback Force Evaluation of Pipes Installed via Horizontal Directional Drilling

by

Montazar Rabiei

A thesis submitted in partial fulfillment of the requirements for the degree of

Doctor of Philosophy

in
Structural Engineering

Department of Civil and Environmental Engineering
University of Alberta

Abstract

Since its first application in the 1970s, Horizontal Directional Drilling (HDD) has steadily become one of the fastest growing trenchless construction methods for utility and conduit installation under surface obstacles. This rapid growth in HDD application could not have been accomplished without major development in engineering and design procedures, which take into account the unique characteristics of this technology. As a result, the most current HDD design references, at least to some extent, rely on studies carried out in other industries, e.g., oil well drilling and utility cable installation. These adoptions are often made without making proper adjustments, leading to inaccurate pipe designs.

This dissertation aims to identify and address the shortcomings that exist in current pullback determination methods during pipe installation by HDD. Throughout the study, special attention is paid to the investigation and refinement of the proposed procedures by the two reference design documents used widely in North America: the ASTM F1962 method and the Pipeline Research Council International (PRCI) method, used for HDPE and steel pipe design, respectively.

The dissertation is heavily tilted toward investigating the pipe-drilling fluid interaction since several studies have emphasized the necessity of refining the current practice of fluidic drag calculation. Two new methods for calculating fluidic drag are introduced: one applicable to power-law fluids and the other one for Herschel-Bulkley fluids. The latter accounts for pipe eccentricity and is based on the application of Finite Volume Method (FVM) to the HDD drilling fluid flow problem. Also, a series of simple methods for fluidic drag estimation are proposed, which are suitable for HDD practitioners to use and can be incorporated into future standards.

For estimating the non-fluidic drag component of pullback force, two different models have been developed: one for steel pipes and the other for HDPE pipes. Unlike the PRCI method, the former doesn't involve an iterative procedure and, contrary to the ASTM F1962 method, the latter is not limited to crossings with specific bore geometry.

For verification of the developed methods and models, pullback data collected on different crossings has been used. The data is provided by The Crossing Company (TCC), the industry partner of the Consortium for Engineered Trenchless Technologies (CETT) at the University of Alberta, and collected on different project sites for crossings executed in Alberta, Canada. The new proposed models have been able to simulate the recorded pullback forces, while the PRCI method failed to do so.

It has been observed that the fluidic drag changes almost linearly with the installation progress; therefore, simple methods based on adaption of the pipe annulus to a slot can be used for estimating the fluidic drag. Furthermore, the fluidic drag is not a direct function of hydrokinetic pressure and, as a result, methods like ASTM F 1962 fail to predict the fluidic drag changes accurately. The FVM results revalued that the effect of eccentricity on the drag is insignificant, and its effects can be disregarded for practical application. The new proposed methods in this dissertation enables the HDD contactors/practitioners to predict drilling fluid flow within bore hole during pipe installation operation, so they can fine-tune their plans for drilling fluid collection and recovery.

Preface

This thesis is an original work by Montazar Rabiei. The field data used in chapters 5 to 7 for verification of developed methods has been collected and provided by The Crossing Company in Nisku, Alberta, Canada.

Chapter 3 of this thesis has been published as Rabiei, M., Yi, Y., Bayat, A., and Cheng, R. (2016). "General Method for Pullback Force Estimation for Polyethylene Pipes in Horizontal Directional Drilling". Journal of Pipeline Systems Engineering and Practice, 10.1061/(ASCE)PS.1949-1204.0000230, 04016004. I was responsible for developing the MATLAB code and composing the manuscript. Dr. Yi and Dr. Cheng reviewed the manuscript and provided feedback for its improvement. Dr. Bayat was the supervisory author and was involved with concept formation and manuscript composition.

Chapter 4 of this thesis has been published as Rabiei, M., Yi, Y., Bayat, A., Cheng, R., and Osbak, M. (2015). "New Method for Predicting Pullback Force for Pipes Installed via Horizontal Directional Drilling (HDD)". Proc., NASTT No-Dig Show Conference, Denver, Colorado. I was responsible for developing the MATLAB code and composing the manuscript. Dr. Yi, Dr. Cheng, and Mr. Osbak reviewed the manuscript and provided feedback for its improvement. Dr. Bayat was the supervisory author and was involved with concept formation and manuscript composition.

Chapter 5 of this thesis has been submitted to the Journal of Pipeline Systems Engineering and Practice as Rabiei, M., Yi, Y., Bayat, A., Cheng, R., and Osbak, M. " Estimation of Hydrokinetic Pressure and Fluidic Drag Changes during Pipe Installations via HDD Based on Identifying Slurry Flow Pattern Change within Borehole". I was responsible for developing the MATLAB code and composing the manuscript. Dr. Yi reviewed the manuscript and provided

feedback for its improvement. Mr. Manley provided the field data used for verification of proposed method. Dr. Bayat was the supervisory author and was involved with concept formation and manuscript composition.

Chapter 6 of this thesis has been submitted to the Journal of Pipeline Engineering as Rabiei, M., Yi, Y., Bayat, A., Cheng, R., and Osbak, M. "Fluidic Drag Estimation in Horizontal Directional Drilling using Finite Volume Method". I was responsible for developing the MATLAB code and composing the manuscript. Dr. Yi reviewed the manuscript and provided feedback for its improvement. Mr. Manley provided the field data used for verification of the proposed method. Dr. Bayat and Dr. Cheng were the supervisory authors and were involved with concept formation and manuscript composition.

Chapter 7 of this thesis will be submitted to the Journal of Pipeline Engineering as Rabiei, M., Yi, Y., Bayat, A., Cheng, R., and Osbak, M. "Simple Methods for Fluidic Drag Estimation during Pipe Installation via HDD". I was responsible for developing the MATLAB code and composing the manuscript. Dr. Yi reviewed the manuscript and provided feedback for its improvement. Mr. Manley provided the field data used for verification of the proposed method. Dr. Bayat and Dr. Cheng were the supervisory authors and were involved with concept formation and manuscript composition.

Dedicated

To

Faedeh, my mom and first teacher,

who taught me the lesson of love and patience

Jaber, my dad,

who left me the most valuable heritage a father can give his son ”the freedom”

Kamran, my brother,

for his never-ending support

Acknowledgment

First, I would like to thank Dr. Bayat, my supervisor, for his support through my studies and providing a medium for me and other students to do research. The weekly meetings we had were useful in terms of delivering the research project on time, developing presentation skills, and getting feedback from the research group members.

I would like to sincerely thank Dr. Roger Cheng, my co-supervisor, for his thoughtful guidance during my program. The meetings we had benefited me a lot both academically and personally.

I also like to extend my gratitude to Dr. Mohammad Najafi, from the University of Texas at Arlington, and Dr. Dave Chan for serving on my PhD defense committee.

I would also like to thank Dr. Yaolin Yi, the postdoc fellow with our research group, for his positive attitude and good comments during reviewing my research work. I also need to thank our technical writers, Sheena Moore and Lauren Wozny, for their wonderful job of editing papers and theses.

I am very grateful to Manley Osbak, The Crossing Company vice president of engineering, for giving me the opportunity to do my internship in their company and granting me access to the company's projects database. The conversations we had helped me to develop a more realistic and deeper understanding of HDD operations.

I am indebted to thank my friends Sadegh, Hadi, Amir, Pouya, Saeideh, and Meisam for being next to me during all the ups and downs we had together over the past four years.

Finally, I would like to thank the Natural Sciences and Engineering Research Council of Canada (NSERC), The Crossing Company, and the Consortium for Engineered Trenchless Technologies (CETT) at the University of Alberta for providing financial support for this project.

Table of Content

List of Tables

List of Figures

List of Symbols

A_p : Pipe's surface area in contact with drilling fluid per meter, m^2

D_p : Product pipe outer diameter, m

D_b : Borehole diameter, m

e : Normalized pipe eccentricity

EI : Pipe bending stiffness, $N.m^2$

E_s : Steel modulus, Pa

E_{HDPE} :High Density Polyethylene modulus, Pa

f : Dimensionless pressure drop gradient

$frict_c$: Frictional force developed between a curved pipe segment and borehole surface, N

F_{fluid} : Fluidic drag, N

H : Depth of bore hole from ground surface, m

K : Consistency index in Herschel-Bulkley model, $Pa.sec^n$

L_c : Length of curved pipe segment, m

m : Power-law consistency index, $Pa.sec^n$

n : Power-law behavior index

Q : Flow rate, m^3/sec

Q_{dis} : Volume of slurry displaced by product pipe advancement per unit time, m^3/sec

Q_D : Dimensionless flow rate

Q_{pump} :Drilling fluid flow rate pumped from the rig into the bore, m^3/sec

Q_1 : Flow rate moving within product pipe annulus, m^3/sec

Q_2 : Flow rate moving within drill pipe annulus, m^3/sec

R : Borehole radius, m

R_P : Product pipe radius, m

s : Reciprocal of the Power-law behaviour index

v : Fluid annular velocity, m/sec

v_a : Friction coefficient between the pipe and ground surface/rollers

v_b : Friction coefficient between the pipe and bore wall

V_D : Dimensionless velocity

V_p : Pullback velocity, m/sec

w_a : Pipe weight on the ground surface per unit length, N/m

w_b : In-bore pipe effective (buoyant) weight per unit length, N/m

μ_{mud} : Fluidic drag coefficient, Pa

L_s : Length of straight pipe segment, m

θ : Angle of the pipe/borehole axis with respect to the horizontal

θ_s : Angle of straight pipe segment with respect to the horizontal

θ_c : Angle of the line bisecting a curved pipe segment with respect to the horizontal

φ : Angle between the radial line passing through the curved segment mid-point and the horizontal

ΔP : Hydrokinetic pressure, Pa

σ : Normalized radius of the annulus' inner bounding surface

λ : Normalized radial location of the maximum velocity within annulus

τ_z : Shear stress on pipe's outer surface, Pa

τ_0 : Yield stress, Pa

μ_D : Dimensionless viscosity

γ_D : Normalized shear rate

τ_D : Normalized shear stress

1- Chapter 1: Introduction

With the sharp increase in the number of large congested urban areas over the last several decades, a rise in the of level of awareness on environmental issues, and the increasing cost of normal vehicular/marine traffic and business disruptions, the demand for new construction methods with minimal impact on the surrounding environment has increased within the underground utility installation industry. This need has been the main driving force behind the development of different trenchless (no-dig) installation techniques, where the underground utility lines and conduits are laid without trenching the ground from the surface. Usually, different trenchless methods are divided into two main broad areas: construction methods, used for placing new pipes and utility lines; and rehabilitation methods, used for rehabilitating/replacing existing, old, or host pipeline or utilities systems. Figure 1-1 lists some of the techniques falling under either category. Originating from the oil well drilling industry, Horizontal Directional Drilling (HDD) is a technology for new pipe or conduct installation under obstacles using a steerable and trackable bit. These obstacles can be a wide river, a preserved natural habitat, or the deep foundations of a skyscraper in a congested metropolitan downtown area.

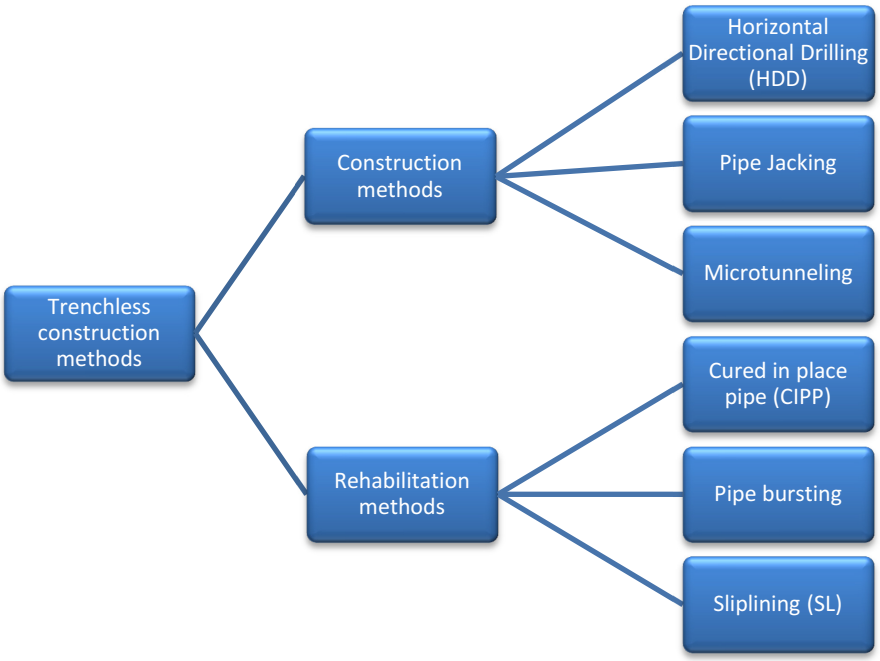

Figure 1-1- Trenchless construction areas and some of the corresponding methods

To place a pipe using HDD, first a small diameter hole is drilled along the planned path using a downhole assembly with steering and tracking capabilities, as shown in Figure 1-2a. This assembly is launched and placed at a shallow angle (8 to 20 degrees) with respect to the ground surface via a ground-mounted rig. For drilling through hard formations, the downhole assembly typically involves a drill bit, a downhole mud motor, a bent sub, and a non-magnetic collar. To drill within softer formations, such as sand, the same assembly is used, but since the torque demand at the bit is lower, the mud motor is taken off the assembly. The mud motor converts the drilling fluid hydraulic energy into mechanical energy at the bit. Using a mud motor can significantly increase the service life of drill pipes and, indirectly.

Over the second stage of installation, called reaming, the bore is widened to a dimeter typically 50 percent larger than the final product pipe size. This is achieved by passing a reamer (hole opener) over one or multiple passes, depending on the final bore size. Finally, the product pipe is pulled back into the enlarged hole. In the HDD literature, the discussed three construction phases of HDD are often referred to as pilot hole drilling, reaming, and pullback stages, respectively, as shown in Figure 1-2.

During all three HDD construction stages, drilling fluid, a mixture of water, bentonite, and polymers, is continuously circulated within the bore from the rig. The drilling fluid circulation serves several functions: a) transporting the drilled cuttings out of the bore, b) maintaining the bore stability by balancing the overburden pressure, c) cooling the cutting head during the pilot bore drilling stage, and d) lubricating the passage of the product pipe.

HDD-installed pipes are subjected to two types of loadings, namely installation loads and post-installations loads (ASCE 2014). For an HDD installation to be successful, it is necessary that the pipe is able to sustain all probable installation and post-installation loads within allowable limits, as specified by relevant design standards. Unlike open trench construction, the forces developed through the product pipe during the HDD installation stage are often the greatest and govern the pipe design; therefore, the majority of studies in HDD literature have been focused on identifying and quantifying these loads. This happens due to pulling a long prefabricated pipe string into the reamed hole at once.

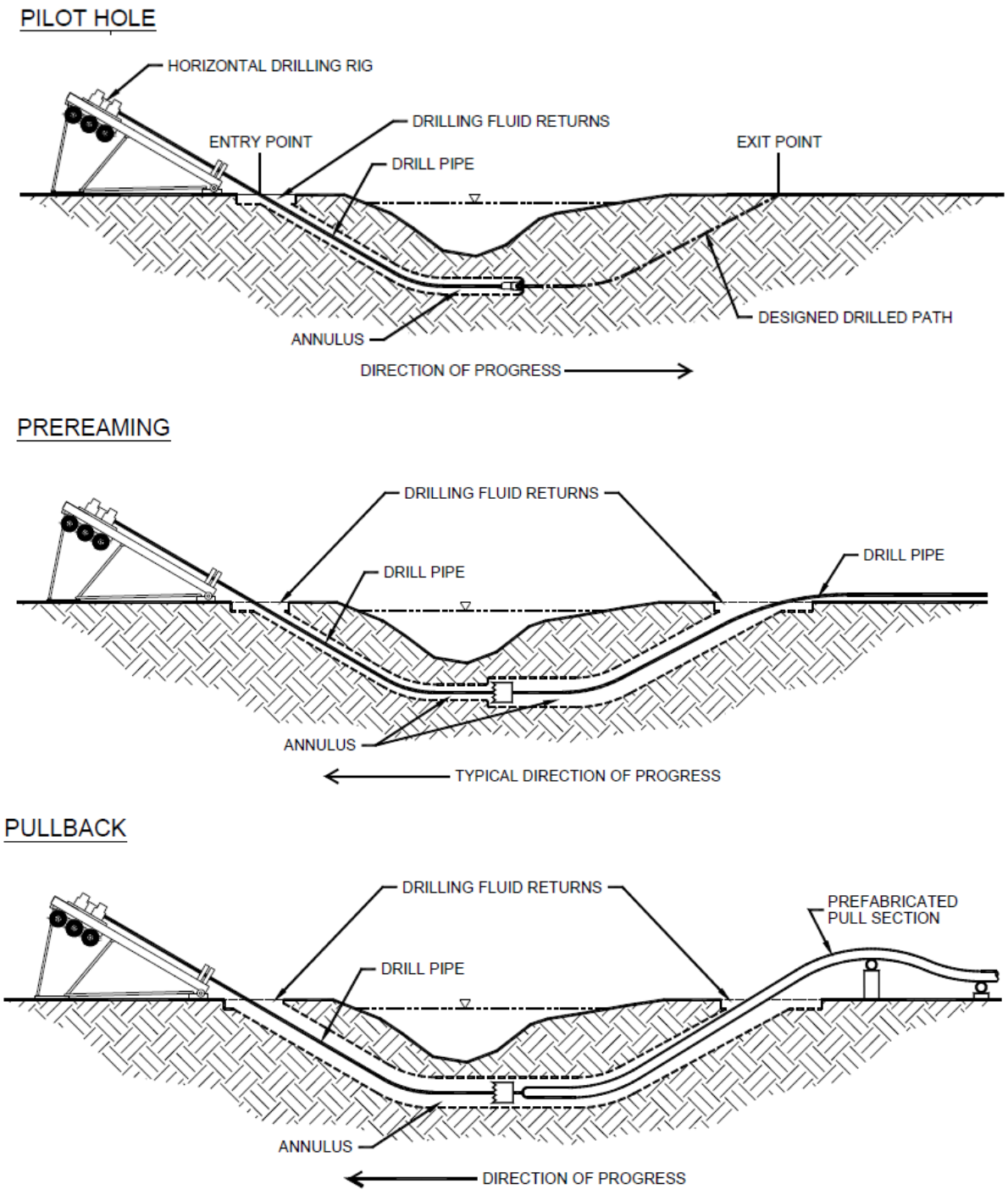

Figure 1-2 – Typical stages of an HDD pipe installation operation (www.fws.gov)

In spite of HDD's growth in popularity, the interaction of the installed pipe with the surrounding soil and slurry medium during the pipe installation phase is not well understood, leading to conservative pipe design (Baumert et al. 2005). Due to a lack of relevant investigations, current HDD design references rely on studies completed in other industries, like oil well directional drilling and utility cable installation industries (Slavin and Petroff 2010). Subsequently, in current design references, such as ASTM F1962 (2011) and Pipeline Research Council International (PRCI) (Huey et al. 1996), unique HDD characteristics are sometimes ignored.

1-1- Objective and Scope

The main objective of this study is to improve and address the gaps existing in current practices of pullback force estimation in HDD installations. This study aims to better understand the physics of the pullback problem and quantify the components of pullback force requiring modification for a more rational design. The scope of the investigation consists of:

- Identifying the gaps currently exist in theoretical pullback force evaluation of steel and high density polyethylene (HDPE) pipes installed via HDD;
- Developing a general method for evaluating the HDPE pipes pullback force applicable to all installations regardless of bore geometry;
- Proposing a new simple method for predicting the pullback force in steel pipe installations;
- Investigating the pipe-drilling fluid interaction problem in HDD and how drilling fluid returns to the ground surface as installation progresses;
- Developing new refined methods for estimating fluidic drag and hydrokinetic pressure that account for a wider range of parameters;
- Developing a practical industry-oriented method for calculating fluidic drag;

1-2- Methodology

In order to identify areas requiring in-depth study, a literature review on pullback force has been performed. This review includes two parts: a review of studies dealing with frictional drag, and a review of studies centred on the fluidic component of pullback force. For frictional drag evaluation of HDPE pipes, the proposed ASTM F1962 equations will be investigated in detail first as they are the current industry standard. Following this, a general procedure for evaluating frictional drag of pullback force in HDPE pipes will be developed. This is achieved by analytically solving equilibrium equations of a pipe segment negotiating a curved bore segment and satisfying the corresponding boundary conditions. For steel pipes, assuming a pipe segment within a curved bore to behave like a three-point beam, the theory of beams with large deflections is implemented for frictional drag estimation. By knowing the fictional beam (pipe) mid-span deflection from the bore geometry, the beam reactions and mid-span point load associated with pipe frictional drag can be calculated.

To predict the fluidic drag and hydrokinetic pressure changes of a Power-law slurry, a series of coupled equations governing drilling fluid flow within the borehole will be derived and solved numerically. These equations are obtained by applying the solution to the generalized annular Couette flow problem to the flow in the product pipe and drill rod annuli, assuming zero fluid loss during the pipe installation process. The underlying assumption in this phase of the study is that both the product pipe and drill rod are placed concentrically within the bore.

To investigate the fluidic drag for Herschel-Bulkley fluids, a MATLAB code will be developed, which is based on solving the annular flow problem using FVM. Through an iterative process, the code solves the continuity equation within the borehole and during the installation operation, and it return the associated hydrokinetic pressure and shear stress on the pipe's outer surface. The code will also be used to study the effects of eccentricity on the estimated values. Finally, having investigated the estimated fluidic drag changes by FVM, a set of practical simple solutions will be developed.

1-3- Thesis Outline

This thesis is organized as the following:

Chapter 1 – Introduction: In this chapter, a background on trenchless construction and, specifically, HDD is presented. The importance of trenchless construction methods to the utility construction/rehabilitation industry is highlighted by reviewing some survey results and statistics. The objectives and scope of the thesis, the implemented methodologies for achieving the specified objectives, and the thesis outlie are also discussed.

Chapter 2 – Literature Review: In this chapter, a review of major studies on fluidic drag is carried out. The chapter is divided into two sections: a review of studies focused on developing methods for evaluating non-fluidic drag component of pullback force, and a review of researches centred on estimating fluidic drag component. At the end, a table is presented, which summarizes the gaps in the discussed studies.

Chapter 3 – General Method for Pullback Force Estimation for Polyethylene Pipes in Horizontal Directional Drilling: In this chapter, a general method for evaluating the pullback force of HDPE pipe is developed. The method is called general since, in contrast to the ASTM F1962 method, it can be applied to any crossing regardless of the bore geometry.

Chapter 4 – New Method for Predicting Pullback Force for Pipes Installed via Horizontal Directional Drilling (HDD): In this chapter, a model is developed for pullback estimation of pipe by adopting the theory of beam with large deflections. The model is applicable to both steel and HDPE pipes and, unlike the PRCI method, doesn't include an iterative process. For verification purposes, the estimated pullback forces by the new model for two installations are compared against those obtained from the ASMT and PRCI methods.

Chapter 5 – Estimation of Hydrokinetic Pressure and Fluidic Drag Changes during Pipe Installations via HDD Based on Identifying Slurry Flow Pattern Change within Borehole: This chapter sets out a new method for determining hydrokinetic pressure and fluidic drag changes, supposing the drilling fluid to behave as a Power-law fluid. In this method, in order to estimate the intended values, the bore length is divided into two sections, and then the governing equations of fluid motion for either section are derived and solved.

Chapter 6 – Fluidic Drag Estimation in Horizontal Directional Drilling using Finite Volume Method: This chapter introduces a new approach for determining the fluidic drag, which is applicable to Herschel-Bulkley fluids. The proposed method is based on using FVM for calculating the annular flow moving through the drill pipe and product pipe annuli as well as satisfying the continuity equation within bore-product pipe-drill pipe system. To verify the suggested method, pullback data of two actual installations has been used. Also, the effect of eccentricity on fluidic drag is investigated.

Chapter 7 – Simple Methods for Fluidic Drag Estimation during Pipe Installation via HDD: This chapter introduces a series of simple methods for fluidic drag evaluation using slot approximation of the annulus, which are applicable to both Power-law and Herschel-Bulkley fluids. The methods are suited for the HDD industry and can be incorporated into the future relevant standards.

Chapter 8 – Summary and Conclusions: This chapter summarizes the thesis and reviews the main findings of the carried-out research. Furthermore, it outlines the future works which can be done as a continuation of the current study.

2- Chapter 2: Literature Review

Originating from the oil well drilling industry, HDD has been utilized for about four decades and is one of the most promising trenchless methods (Najafi and Gokhale 2005). HDD is an ideal technique for pipe placement through urban areas, environmentally sensitive areas, traffic-heavy streets, and other high-risk regions (Sarireh et al. 2012; Willoughby 2004). The first HDD installation took place in 1971 to cross the Pajaro River near Watsonville, California, and since then, the number of completed HDD projects has been increasing steadily (Sarireh et al. 2012). Recently, the total number of HDD rigs manufactured worldwide reached more than 30,000 units, 80 percent of which were manufactured in the U.S. (Carpenter 2011). Among the different trenchless construction methods, HDD has a good standing applicability in most underground applications (Najafi and Gokhale 2005).

According to the 17th annual Underground Construction HDD Survey of the U.S. market, the four largest HDD niches in 2015 were telecommunication, gas distribution, water, and electric with a market share of 20.0, 19.6, 18.0, and 14.0 percent, respectively, as presented in Figure 2-1. Currently, the estimated HDD market size in North America is around USD 2.1 billion and expected to reach USD 4.6 billion by 2022, growing at a Compound Annual Growth Rate (CAGR) of over 14 percent from 2016 to 2022, as shown in Figure 2-2. Globally, HDD revenue is estimated to reach USD 14.95 billion by 2022 (Grand View Research 2015). The significant growth prospects for this market is mainly due to high demand originating from the telecommunications sector. Telecom companies have initiated putting some measures in place in order to make 4G and 5G services available to everyone.

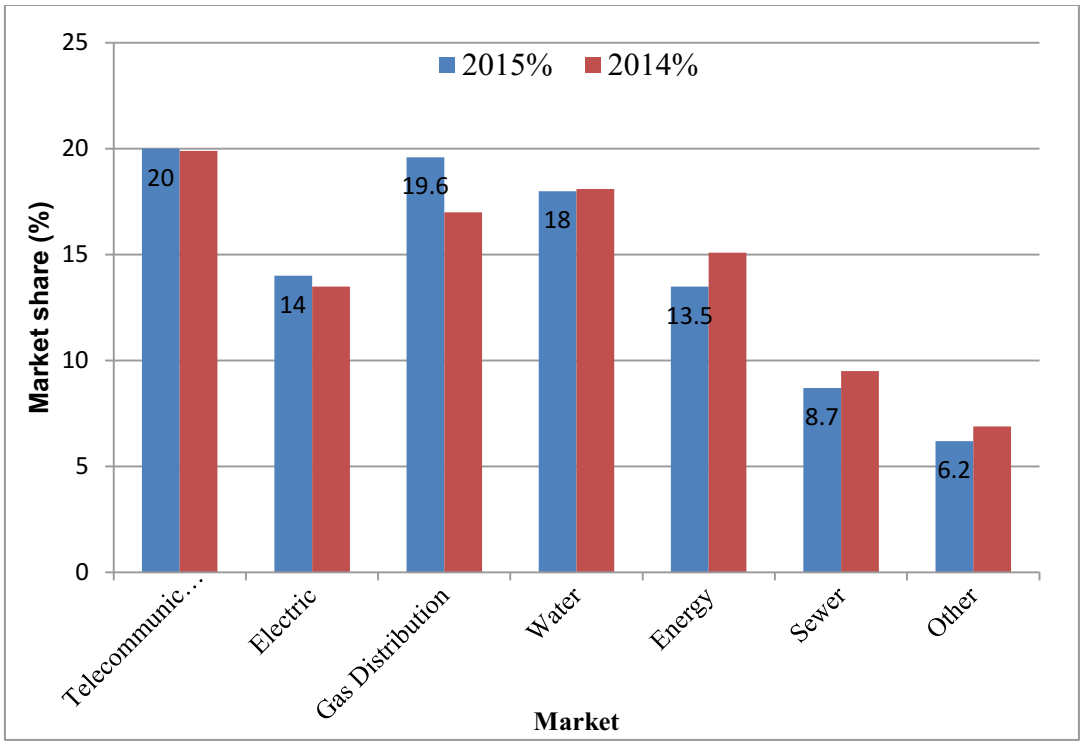

Figure 2-1- HDD markets breakdown in the U.S. (17th annual underground construction HDD survey of the U.S. market, www.uconline.com)

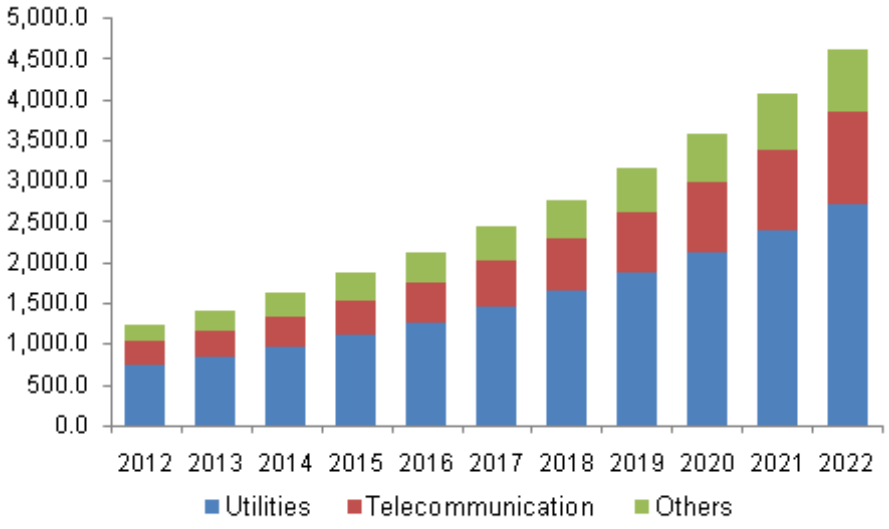

Figure 2-2- 2012-2022 North America HDD market in million USD (Grand View Research 2015)

This chapter reviews the studies carried out so far on pullback force estimation during the pipe installation stage via HDD. In order to be able to connect different investigations together and identify the exiting gaps that need further study, having a solid understanding of the nature of pullback force is necessary. Pullback force is the tensile force that must be applied at the pipe leading end in order to pull it into the reamed hole during the HDD installation stage. This force needs to be large enough to overcome the forces resisting pipe advancement into the bore: a) frictional drag between the out-bore portion of the pipe and ground surface, F_g; b) frictional drag between the in-bore portion of the pipe and bore wall, F_b; c) fluidic drag due to pipe-drilling fluid interaction, F_f; and d) fraction of pipe buoyant weight, F_w. For the segments of the pipe pulled upward in the bore, however, F_w turns into an assistive force since the component of pipe buoyant weight aligned along the pipe axis points toward the pipe exit point. Figure 2-3 demonstrates the total pullback force as well as its components, which are related as:

$$T_p = f(F_b + F_w) + F_g + F_f \tag{2.1}$$

The pullback force equation is written in this form because the frictional forces developed on the bore surface directly depend on the pipe buoyant weight. Most of the existing methods provide fairly similar equations for F_w and F_g components; however, they differ in their approach to estimating F_b and F_f components, as well as in the way they treat function f.

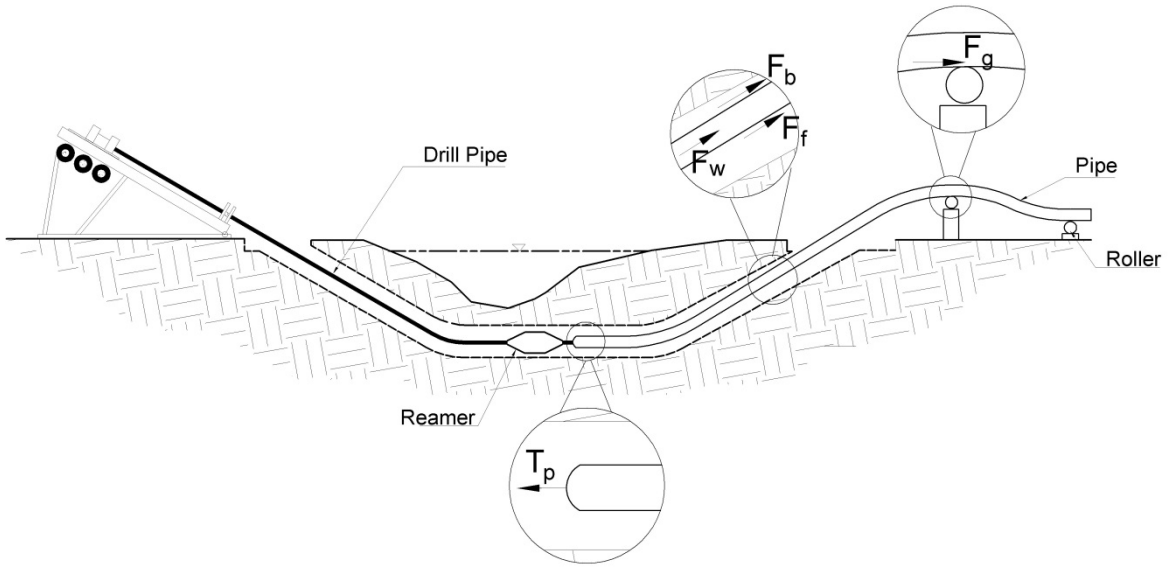

Figure 2-3 – Pullback force and its components

To estimate the pullback force at a specific stage of a pipe placement operation, all methods follow similar steps:

1) Divide the pipe into a series of straight and curved segments.
2) Determine the tensile force increment along each individual segment using corresponding equations provided by the method.
3) Sum all force increments from pipe tail to pulling head.

In the next two sections, exiting methods for estimating non-fluidic and fluidic drag components of pullback force, terms $f(F_b + F_w) + F_g$ and F_f in equation (2.1) will be reviewed. At the end of this chapter, studies dedicated to verifying the exiting pullback models will be discussed.

2-1- Non-Fluidic Drag

The Driscopipe method (Baumert and Allouche 2002) is one of the earliest methods that attempted to tackle pullback force estimation problems back in 1993. In this numerical method, pipe curvature effects on pullback force are neglected and the entire pipe length is treated as a series of straight-line segments along its centreline that are linked together. To determine the force increment along each segment, the equation for static equilibrium of forces applied on the pipe segment is solved. The final equation for total pullback force has the following form:

$$T_p = \sum_{i=1}^{i=n} w_b L_i (v_b \cos\theta \pm \sin\theta) \tag{2.2}$$

where i is the segment number; n is the total number of segments comprising the pipe, w_b (N/m) is the pipe buoyant weight per unit length; θ (rad) is the angle of the pipe/borehole axis with respect to the horizontal; and v_b is the friction coefficient between the pipe and bore wall. Although simplicity of this method makes it favorable for practical uses, it has substantial shortcomings, which include ignoring pipe bending rigidity and the effects of pipe-drilling fluid interaction on pullback force amplification.

As part of a study carried out for the American Gas Association (AGA) in 1996, Huey et al. developed a method that would come to be known as the Pipeline Research Council International

(PRCI) method (Huey et al. 1996) for estimating pullback forces in steel pipes. The method assumes that the force at the pipe entry point is always zero, or $F_g = 0$ in equation (2.1), and that it gradually increases as the leading end approaches the exit point. Representing a curved pipe segment as a three-point beam undergoing large deflections, with the maximum centre deflection of $h = R(1 - \cos(\alpha / 2))$ where α (rad) is the included angle of the curved segment, the PRCI method provides the following equation for estimating tensile force increment along a curved pipe segment:

$$\Delta T_c = 2\left|frict_c\right| + F_{fluid} \pm w_b \times L_c \times Sin(\theta_c) \tag{2.3}$$

where $frict_c$ (N) is the frictional force developed between the pipe and borehole surface evaluated using an iterative procedure (Huey et al. 1996); L_c (m) is the length of the pipe's curved segment; θ_c (rad) is the angle of the line bisecting the pipe segment with respect to the horizontal; and F_{fluid} (N) is the fluidic drag component of the pullback force, as defined in Section 2-2-. Unlike the Driscopipe method, the PRCI method accounts for pipe rigidity through the term $frict_c$. The main shortcoming of this method is being iterative, which makes it unsuitable for quick estimation of pullback force.

Cheng and Polak (2007a) proposed a model that was incorporated into the numerical program Pipeforce 2005. The model takes the recorded drill head coordinates during pilot bore drilling stage as an input, and based on that, it predicts the pipe deformed shape within the reamed hole and estimates the pullback force. To determine the force amplification along different pipe segments, the pipe inside the bore was assumed to behave like a flexible bar and the corresponding equations were used. Comparing the method to methods like PRCI, its required computational effort is much more, and the authors did not comment on the additional accuracy achieved by using this method. Also, similar to PRCI, the fluidic drag was simply calculated by multiplying the pipe's surface area by a constant coefficient; however, the authors had previously noted the necessity of performing additional research into this area (Polak and Chu 2005).

For installation of High Density Polyethylene (HDPE) pipes, the American Society of Testing and Materials' standard "ASTM F 1962" sets out the procedure for pullback force estimation (ASTM F1962 2011). The proposed procedure rests on some major assumptions: a)

the bore profile consists of only two terminal curved segments and one intermediate straight segment, b) the entry and exit points are at the same elevation, and c) the intermediate straight segment is horizontal. The ASTM's typical bore profile is demonstrated in Figure 2-4. Assuming the pullback force to reach its maximum value at one of the transition points A, B, C, or D, as shown in Figure 2-4, the following set of equations is suggested to determine the corresponding non-fluidic components of pullback force at these points:

$$\begin{aligned} T_A &= \exp(\nu_a \alpha)(\nu_a w_a (L_1 + L_2 + L_3 + L_4)) \\ T_B &= \exp(\nu_a \alpha)(T_A + \nu_b |w_b| L_2 + w_b H - \nu_a w_a L_2 \exp(\nu_a \alpha)) \\ T_C &= T_B + \nu_b |w_b| L_3 - \exp(\nu_b \alpha)(\nu_a w_a L_3 \exp(\nu_a \alpha)) \\ T_D &= \exp(\nu_b \beta)(\mathrm{T}_C + \nu_b |w_b| L_4 - w_b H - \exp(\nu_a \alpha)(\nu_a w_a L_4 \exp(\nu_a \alpha))) \end{aligned} \tag{2.4}$$

where ν_a and ν_b are the in-bore and out-bore coefficients of friction, respectively; w_a and w_b (N/m) are the in-bore and out-bore unit effective (buoyant) weight of the pipe, respectively; L_1 to L_4 (m) are the projected lengths of different pipe segments, as shown in Figure 2-4; and H (m) is the depth of installation.

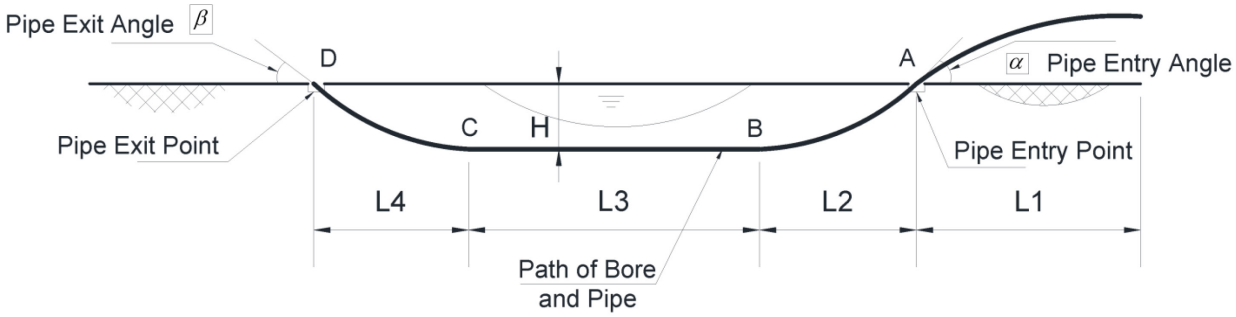

Figure 2-4 Typical bore profile geometry in ASTM F1962 (2011)

The major weakness of the ASTM method is in the restraints it imposes on the bore geometry, making it inapplicable to many actual crossings with different bore shapes.

Slavin et al. (2011) extended the ASTM equations for situations where the pipeline entry and exit points are not level, considering the straight intermediate segment of the bore profile to be horizontal. Their proposed equations considered the effects of possible anti-buoyancy measures (i.e., ballasting the pipe by filling it with water) and partial slurry drainage from the borehole. Based on the analysis of a sample installation, they concluded that pulling the pipe upgrade was less risky than pulling it downgrade when anti-buoyancy techniques were not employed.

However, in cases with liquid-filled pipes, downgrade installation was preferable. Later, the equations were extended to include cases where the intermediate pipe segment was positioned at a grade equal to the ground surface (Slavin and Najafi 2013). This demonstrated that for a pipe filled with water, the pullback forces for an upgrade or downgrade installation were greater than that of a similar level grade installation (Slavin and Najafi 2013). Although these studies made the ASTM F1962 equations more general, they can still be used for bores involving only three segments.

ASTM F1962 considers that the effects pipe bending rigidity have on pullback force are insignificant and, consequently, implements the Capstan effect basic equation to estimate pullback force amplification at bore bends. A study carried out in 2012, aimed to investigate the additional pullback forces produced due to pipe bending stiffness effects, revealed that these effects are a function of different factors: bending stiffness of the pipe, the nature of the bend(s) or path curvature, and the pipe and borehole sizes (Slavin and Najafi 2012). The results also showed that for the considered cases, the quantitative impact of the bending stiffness increases with pipe size, but is nonetheless low, especially for the relatively flexible HDPE pipes.

2-2- Fluidic Drag

In spite of HDD's growth, the interaction of the pipe with drilling fluid during installation is not well understood, resulting in conservative designs (Baumert et al. 2005). Some methods, such as PRCI, attribute a significant percentage of the total pullback force to the pipe interaction with the surrounding drilling fluid; while other methods, like ASTM, nearly ignore this component of pullback force. Because of a lack of relevant investigations, current HDD design references heavily rely on studies completed in other industries, like oil well directional drilling and utility cable installation (Slavin and Petroff 2010). Subsequently, HDD design references, such as ASTM F1962 (2011) and PRCI (Huey et al. 1996), sometimes disregard unique HDD characteristics.

In oil well drilling operations, the drilling fluid is pumped from the ground-mounted rig down into the drill string. After being discharged from the nozzle and getting mixed with cuttings, the resulting slurry flows back from the well bottom to the ground surface through the annular space between the drill string and the well. In terms of the slurry flow pattern, this process resembles

the pilot bore drilling phase, where the total slurry volume within annular space flows in a direction opposite to the pipe movement throughout the operation. During the pullback phase, however, since the total bore length has already been reamed to its final diameter, the slurry exits to the ground surface through the product pipe and/or drill rod annuli depending on the product pipe leading head location. This behaviour is demonstrated schematically in Figure 2-5. Similarly, lightweight utility cable installation via the blown-cable technique (Slavin 2009), which is the basis of current ASTM F1962 fluidic drag evaluation (Slavin and Petroff 2010), observes annular flow in a singular direction during installation.

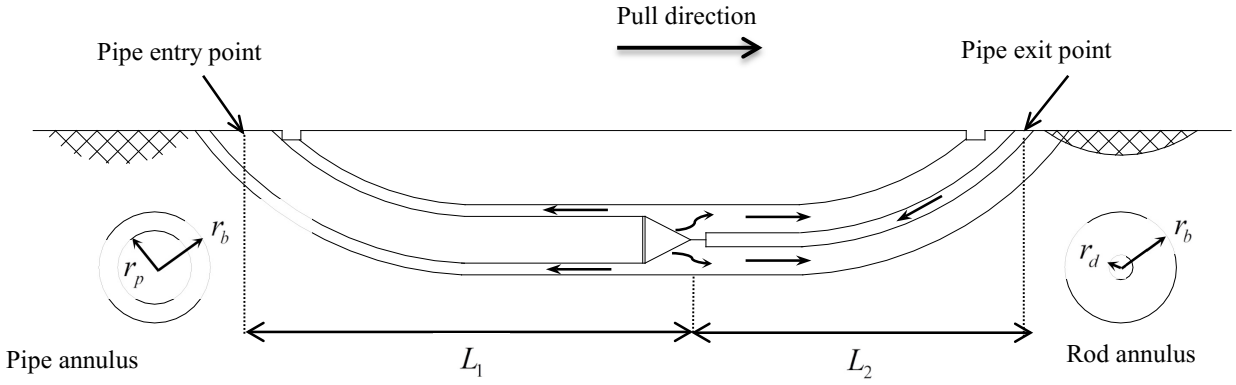

Figure 2-5- Drilling fluid circulation within the bore during pullback operation

At this time, ASTM F1962 and PRCI are the two design references HDD practitioners often use to estimate the fluidic drag for HDPE pipe and steel pipe installations, respectively. ASTM F1962 suggests using equation (2.5), which was originally used to calculate the drag force applied on a utility cable's outer surface (Slavin and Petroff 2010):

$$F_{fluid} = \Delta P \frac{\pi(R^2 - R_P^2)}{2} \tag{2.5}$$

where $R\,(\mathrm{m})$ and $R_P\,(\mathrm{m})$ are the bore and pipe radii, respectively, and $\Delta P\,(\mathrm{Pa})$ is the hydrokinetic pressure, with a suggested value of 70 kPa. The proposed equation provides no data on drag change as the installation develops, and the slurry rheology is considered in the pressure implicitly. In contrast, PRCI provides no value for the hydrokinetic pressure, but it suggests that fluidic drag can be calculated by multiplying the pipe's outer surface area in contact with the slurry by a fluidic drag coefficient:

$$F_{fluid} = 2\pi R_P L_1 \mu_{mud} \tag{2.6}$$

where L_1 (m) is the in-bore length of the product pipe, and μ_{mud} (Pa) is the fluidic drag coefficient with a value of 350 Pa taken from the Dutch standard NEN 3650, *Requirements for Pipeline Systems* (NEN 2007). Unlike ASTM, PRCI accounts for installation progress (in-bore pipe length), but it disregards the impact of slurry rheology and annulus size. Table 2-1 summarizes the features of both ASTM and PRCI methods in determining fluidic drag.

Table 2-1 Comparison of fluidic drag treatment by the ASTM and PRCI methods

Method	Drilling fluid characteristics	Length of pipe installed	Annulus size	Pullback rate
ASTM F1962	×	×	✓	×
PRCI	×	✓	×	×

In an attempt to model the fluidic drag component of the pullback force more realistically, Duyvestyn (2009) implemented the slot flow approximation and considered the slurry flow direction to change during the pullback stage. Duyvestyn assumed that in an installation, with the pipe leading head between the pipe entry and crossover points, the total slurry volume flows to the surface through annular space between the product pipe and bore. Then, once the crossover point has been reached, the slurry flow direction switches, and the slurry moves in front of the product pipe toward the rig. To determine the crossover point location, the hydrokinetic pressure required for exhausting the slurry via product pipe and drill rod annuli were calculated in terms of in-bore pipe length. After equating these pressures and solving for the in-bore pipe length, the crossover point was calculated. The major shortcoming of this study was ignoring the fact that in a typical installation, the slurry returns to the surface through both the product pipe and drill rod annular spaces over a considerable length. Furthermore, the pullback rate effects were not considered.

Supposing the drilling fluid to be characterized as a non-Newtonian Power-law fluid, a more recent study by Faghih et al. (2015b) proposed using the solution of the general annular flow problem to determine the fluidic drag. The strongest point of this study is accounting for

pullback velocity. Similar to previous investigations (Polak and Lasheen 2001), this research also assumed that the whole drilling fluid volume flows to the ground through the space between pipe and borehole and against the pipe pull over the entire installation course.

2-3- Pullback Force Models Validation

So far, several investigations have tried to validate the current practice of pullback force estimation by comparing the rig recorded forces with those obtained from different theoretical models (Baumert and Allouche 2002; Baumert et al. 2004; Duyvestyn 2009). Using the recorded forces of two actual installations, Baumert and Allouche showed that there is a significant discrepancy between predicted forces, via models such as the PRCI, and recorded ones in terms of both the maximum pull force value and trend of pullback force change with in-bore pipe length. Through a sensitivity analysis, it was demonstrated that the PRCI fluidic drag has strong influence on the predicted forces and the HDD practitioners were advised to be cautions when accounting for fluidic drag using the PRCI model, a conclusion which was supported by a later study (Baumert et al. 2005).

A team of researchers developed three different monitoring tools for collecting in-bore pressure and pullback force data during an HDD pullback operation at the University of Western Ontario, and then implemented them on 19 commercial HDD projects (Baumert et al. 2004). After comparing the recorded forces against the Driscopipe and PRCI models' predictions, it was concluded that: a) the exiting pullback force models are based on the assumption of having an ideal bore during installation and, therefore, fail to estimate the pullback force for crossings with an unideal bore; b) the PRCI fluidic drag coefficient of 350 Pa is independent from project specification and needs to be modified; c) the in-bore pipe resistance is a function of bore condition at the initiation of pullback operations, which can be defined as a percentage of solids removed from the bore and soil type. To address the problem of high fluidic drags in the PRCI model, Puckett (2003) suggested reducing the fluidic drag coefficient by half to 175 Pa. This suggestion was made based on a comparison of estimated forces against measured values for only two case studies without the provision of any further justification.

Recently, some studies have tried to emphasize the importance of including site-specific factors, such as soil type and drilling fluid characteristics, into the pullback force estimation process (Hassan et al. 2014; Faghih et al. 2015a), a significant aspect which is ignored by both

the PRCI and ASMT F1962. Via a lab testing program, Hassan (2014) investigated and quantified the effect of soil type on the friction developed at the pipe-soil interface. It was observed that the friction coefficient at the interface varies with the applied normal force on the soil/bore surface as well as soil type, and it falls in the range 0.27-0.45 for surfaces with filter cake. A comparison of estimated and measured pullback forces for 50 HDD installations revealed that the PRCI tend to overestimate the pullback forces for large HDD crossings while for the case of small crossings a reversed observation was made (Faghih et al. 2015a).

Table 2-2- Shortcoming(s) of different studies on pullback force and/or fluidic drag

Method/Researcher(s)	Description	Shortcoming(s)
Driscopipe, 1993	-	• Ignoring pipe bending stiffness • Neglecting fluidic drag
PRCI, 1996	Applicable to steel pipes only	• Being iterative • See Table **2-1** for fluidic drag
ASTM F 1962, 2011	Applicable to HDPE pipes only	• Limited to installations with specific bore geometry shape • See Table **2-1** for fluidic drag
Cheng and Polak, 2007	-	• Additional complexity • Fluidic drag is independent of the crossing characteristics
Duyvestyn, 2009	Deals only with fluidic drag	• Drilling fluid flows in one direction at once
Slavin et al., 2011	-	• Applicable only to three-segment bores
Slavin and Najafi, 2013	-	• Applicable only to three-segment bores
Faghih et al., 2015	Deals only with fluidic drag	• The slurry flows only in one direction over the installation course

3- Chapter 3: General Method for Pullback Force Estimation for Polyethylene Pipes in Horizontal Directional Drilling[1]

3-1- Introduction

Horizontal directional drilling (HDD) is a trenchless technology for pipe installation under obstacles which results in a minimal ground disruption comparing to the traditional cut-and-cover method (Najafi and Gokhale 2005). A typical HDD_ project involves three steps. During the first step, a small-diameter bore is drilled along a pre-designed bore path using a steerable and tractable drill bit. Afterwards, the bore is reamed to a diameter typically 50 percent greater than the intended pipe diameter through one or multiple reaming passes. In the last (third) step, the pipe string is pulled back into the reamed hole. The first HDD installation took place in 1971 for crossing Pajaro River near Watsonville, California, and since then, the number of completed HDD projects has been increasing steadily (Sarireh et al. 2012). Recently, the total number of HDD rigs manufactured worldwide reached more than 30,000 units, 80 % of which were manufactured in the US (Carpenter 2011). The major advantages of this method over the traditional cut-and-cover method are the preservation of the ground surface in crossing sensitive areas, such as wetlands or natural habitats, and having lower construction costs, considering the social costs of a project. Additionally, HDD also proves to be a feasible solution for installations in congested areas.

Forces developed in the pipe during the installation (pullback) operation often govern the pipe design. Therefore, various methods for the evaluation of pullback forces have been developed in the HDD literature (Huey et al. 1996; Baumert et al. 2005; Polak and Chu 2005; Cheng and Polak 2007a; ASTM F1962 2011; Rabiei et al. 2015). Among these methods, the Pipeline Research Council International (PRCI), and ASTM F1962, *Standard Guide for Use of Maxi-Horizontal Directional Drilling for Placement of Polyethylene Pipe or Conduit Under Obstacles, Including River Crossings*, are the most accepted ones in the design of HDD installations. In the PRCI method, which was originally developed for steel pipes, the in-bore pipe is considered as a series of straight and curved segments, and the incremental tensile force along each individual

[1] This chapter has been published in the ASCE Journal of Pipeline Systems Engineering and Practice.

segment is calculated using the provided equations (Huey et al. 1996). Finally, the pullback force is determined by summing the tensile force change of all segments along the pipe. The ASTM (2011) method proposes a set of equations for pullback force determination, including the Capstan effect. The ASTM method considers that the bore profile to be made up of two curved and one intermediate horizontally straight segments, and that the pipe entry and exit points are level, as shown in Figure 3-1. These restraining assumptions make the application of this method to actual HDD installations difficult; therefore, some recent HDD studies have attempted to generalize the existing ASTM equations (Slavin et al. 2011; Slavin and Najafi 2013).

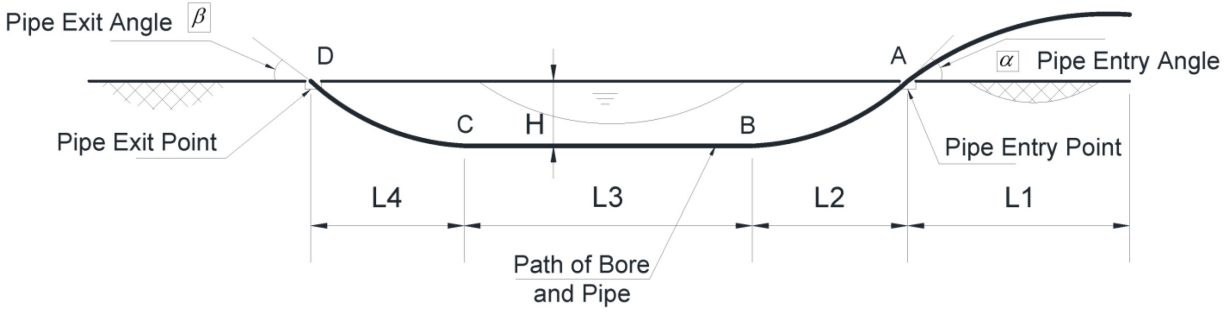

Figure 3-1- Typical HDD installation bore geometry in ASTM F1962

Slavin et al. (2011) extended the ASTM equations for situations where the pipeline entry and exit points are not level, considering the straight intermediate segment of the bore profile to be horizontal. In their proposed equations, the effects of possible anti-buoyancy measures (i.e., ballasting the pipe by filling it with water) and partial slurry drainage from the borehole were considered. Based on the analysis of a sample installation, they concluded that pulling the pipe upgrade was less risky than pulling down grade when anti-buoyancy techniques were not employed. However, in cases with liquid-filled pipes, downgrade installation was preferable. Later, the equations were extended to include cases where the intermediate pipe segment was positioned at a grade equal to the ground surface (Slavin and Najafi 2013). This demonstrated that for a pipe filled with water, the pullback forces for an upgrade or downgrade installation were greater than that of a similar level grade installation (Slavin and Najafi 2013).

Although the aforementioned studies attempted to modify the existing ASTM equations for application to a wider range of problems, the modified equations still present limitations, such as

assuming the entire bore path consists of only two curved and one straight segments. Therefore, developing a general method applicable to all bore path compositions is necessary. This paper proposes a general method for PE pipe pullback force determination based on a modified Capstan equation. Assuming the pipe to have a curvature only in a vertical plane, the proposed method is applicable to all HDD installations regardless of bore geometry, partial slurry drainage from the bore, and change in soil condition along the profile. The following sections include a review of the PRCI and ASTM methods for pullback force estimation, a description of the proposed method, two example applications of the proposed method, and a comparison of the ASTM and proposed methods estimated pullback forces. The latter illustrates the magnitude of error produced by the ASTM method for an installation with the typical ASTM bore path geometry.

3-2- Current Practice for Pullback Force Estimation

3-2-1- PRCI Method

The PRCI method is based on research conducted by Huey et al. (1996) for the American Gas Association (AGA). The method assumes that the pullback force at the pipeline entry point is always zero (the aboveground pipeline's contribution is assumed insignificant) and that it gradually increases along the pipe as the leading end approaches the exit point. The increase in tension along a straight pipe segment is given as:

$$\Delta T_s = \left| frict_s \right| + F_{fluid} \pm w_b \times L_s \times Sin(\theta_s) \tag{3.1}$$

where $frict_s$ (N) is the frictional force between the pipe and borehole surface; F_{fluid} (N) is the shear force acting on the pipe's outer surface due to the pipe interaction with surrounding in-bore slurry; w_b (N/m) is the unit effective (buoyant) weight of the pipe; L_s (m) is the length of segment; and θ_s (rad) is the angle of the pipe/borehole axis with respect to the horizontal. Representing a curved pipe segment as a three-point beam undergoing large deflections, with the maximum center deflection of $h = R(1 - \cos(\alpha / 2))$ where α (rad) is the included angle of curved segment, the PRCI method provides the following equation for tensile force change along a curved pipe segment:

$$\Delta T_c = 2\left|frict_c\right| + F_{fluid} \pm w_b \times L_c \times Sin(\theta_c) \tag{3.2}$$

where $frict_c$ (N) is the frictional force developed between pipe and borehole surface evaluated using an iterative procedure (Huey et al. 1996); L_c (m) is the length of the pipe's curved segment; and θ_c (rad) is the angle of line bisecting the pipe segment with respect to the horizontal. The PRCI procedure proposes the following equation for the estimation of fluidic drag force:

$$F_{fluid} = \pi \times D_p \times L \times \mu_{mud} \tag{3.3}$$

where D_p (m) is the pipe's outer diameter; L (m) is the length of the pipe segment; and μ_{mud} (Pa) is the fluidic drag coefficient with the recommended value of 350 Pa (0.05 psi). Based on analysis of two actual HDD installations pullback data, a more recent study (Puckett 2003) recommends using a reduced fluidic drag coefficient of 172 Pa (0.025 psi). The final equation for the pullback force required to pull the entire pipeline into the bore is:

$$T_{Pullback} = \sum \Delta T_s + \sum \Delta T_c \tag{3.4}$$

3-2-2- ASTM Method

ASTM F1962 (2011) assumes that pipe entry and exit points are at the same elevation and that the intermediate straight segment of the profile (segment B-C) is horizontal, as shown in Figure 3-1. During pipe installation, it is assumed that the pullback force peaks when the pipe leading end reaches one of the transition points (A, B, C, or D); therefore, four equations are proposed for estimating the corresponding non-fluidic components of pullback force as follows:

$$\begin{aligned}
T_A &= \exp(\nu_a \alpha)(\nu_a w_a (L_1 + L_2 + L_3 + L_4)) \\
T_B &= \exp(\nu_a \alpha)(T_A + \nu_b \left|w_b\right| L_2 + w_b H - \nu_a w_a L_2 \exp(\nu_a \alpha)) \\
T_C &= T_B + \nu_b \left|w_b\right| L_3 - \exp(\nu_b \alpha)(\nu_a w_a L_3 \exp(\nu_a \alpha)) \\
T_D &= \exp(\nu_b \beta)(\mathrm{T}_C + \nu_b \left|w_b\right| L_4 - w_b H - \exp(\nu_a \alpha)(\nu_a w_a L_4 \exp(\nu_a \alpha)))
\end{aligned} \tag{3.5}$$

where ν_a and ν_b are the in-bore and out-bore coefficients of friction, respectively; w_a and w_b (N/m) are the in-bore and out-bore unit effective (buoyant) weight of the pipe, respectively; L_1 to L_4 (m) are the projected lengths of different pipe segments, as shown in Figure 3-1; and H

(m) is the depth of installation. For estimating the fluidic drag component of the pullback force, the following equation is provided:

$$\Delta T = \Delta P \frac{\pi}{8}(D_b^2 - D_p{}^2) \tag{3.6}$$

where ΔP (Pa) is the hydrokinetic pressure estimated to be 70 kPa (10 psi), and D_b (m) is the borehole diameter. This force increment must be added to the forces obtained from Eq. (5a)-(5d) to calculate the pullback forces at corresponding points along the borehole. To derive these equations, ASTM F1962 addresses the pullback force evaluation problem for curved segments of a borehole differently than the PRCI method. ASTM calculations are based on the Capstan or Belt Friction equation. The Capstan equation was originally developed to estimate the magnitude of force required to pull a flexible, weightless rope wrapped around a cylinder. For convenience, the exponential amplification factor of the Capstan equation is applied to the pipe at the ends of the curved segments, points B and D in Figure 3-1 rather than at the curves entry points. The error magnitude produced by this presumably conservative assumption is examined in the last section of this paper through a parametric study of an HDD installation with a typical ASTM bore geometry.

3-3- Proposed Method

The central concept of the proposed method is based on accurate consideration of the pipe buoyant weight while adapting the basic Capstan equation to PE pipe negotiating a curve. The resulting equation can be implemented to estimate tensile force change along pipe curved segments. When dealing with straight segments and evaluating the total pullback force, the PRCI equations can be applied.

Figure 3-2 (a) illustrates a curved pipe segment in a vertical plane, subjected to tensile forces at each end, with a curve beginning and finish angle of θ_1 and θ_2, respectively. Generally, the tensile force at the finish (T_2) is determined based on the force at the beginning (T_1). Figure 3-2(b) shows the forces applied on an infinitesimal element of the pipe. Here, $dw = R\,d\theta\,w_b$ is the net buoyant weight of the element, assuming the positive direction for the weight to be upward. By writing the equilibrium of the forces along the x and y axis, the following equations are obtained:

$$dT\cos(\frac{d\theta}{2}) = v_b\, dN + w_b R\, d\theta\cos\theta$$
$$dN = (2T + dT)\sin\frac{d\theta}{2} + w_b R\, d\theta\sin\theta \tag{3.7}$$

After combining the above equations and taking the limit $d\theta \to 0$, the following differential equation is obtained:

$$\frac{dT}{d\theta} = Tv_b + v_b w_b R\sin\theta + w_b R\cos\theta \tag{3.8}$$

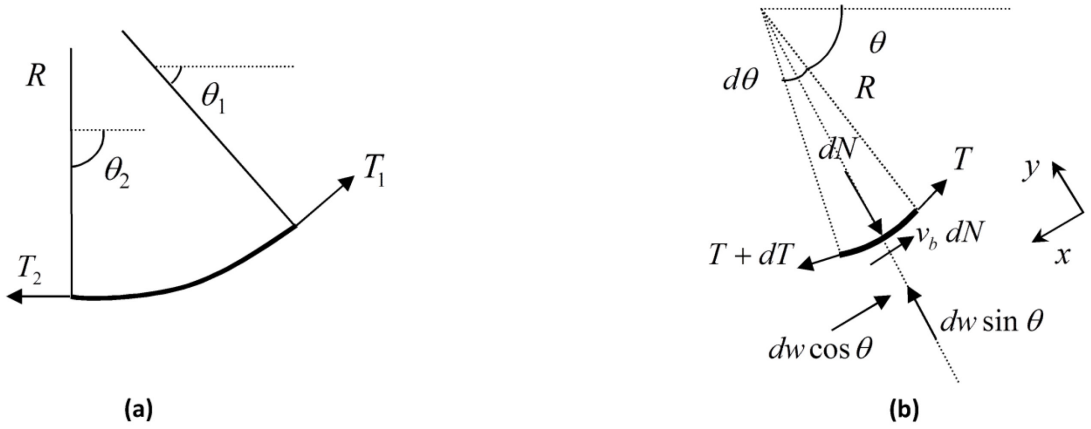

Figure 3-2- (a) Curved PE pipe segment negotiating a curve; (b) free body diagram of an infinitesimal element of the pipe

Having solved this differential equation, the final equation for the tensile force developed within the pipe can be written as:

$$T(\theta) = Ae^{v_b\theta} - \frac{v_b^2 R w_b\sin\theta}{v_b^2+1} + \frac{R w_b\sin\theta}{v_b^2+1} - \frac{2v_b R w_b\cos\theta}{v_b^2+1} \qquad \theta_1 < \theta < \theta_2 \tag{3.9}$$

By knowing the value of tensile force at the beginning point of the segment, $T(\theta_1) = T_1$, the unknown constant A is determined, and $T_2 = T(\theta_2)$ can then be calculated. It should be noted that this equation is derived for and limited to PE pipes, where, regardless of ballasting the pipe, $w_b > 0$, and the pipe is pushed against the bore crown. Both the proposed method and ASTM method do not consider pipe stiffness effects in pullback force evaluation, which agrees with recent findings (Slavin and Najafi 2012). The fluidic drag component of the pullback force is not

considered in Eq. (9), and therefore must be added using the ASTM/PRCI recommended procedure or other methods such as that proposed by Baumert et al. (2005).

Unlike the ASTM equations, the proposed equation is not recursive. Therefore, to determine the pullback force at each desired pipe leading end location, the pullback force calculations need to be performed separately all the way from the pipe entry point down to the location of the pipe leading end. Alternatively, similar to the PRCI method, it is possible to assume that the pullback force reaches its maximum when the pipe emerges from the ground and, as a result, carry out the calculations only once.

3-4- Results Analysis

3-4-1- Validation and Comparison

To verify the proposed method's ability to reasonably estimate the pullback force, forces observed on site during the installation of a 323 m. (1060-ft.) long 0.51 m. (20-in.) OD 9 DR HDPE pipeline in the Poole Slough Watermain Project (Duyvestyn 2006; Duyvestyn 2009) are compared with those estimated using the ASTM, PRCI, and the proposed methods. The project's pilot bore was reamed to a final diameter of 0.77 m (30-in), and the product pipe was partially filled with 148.30 N/m of ballast to reduce the pullback force required for the placement of the pipe in the bore. Similar to a majority of HDD installations, this project's pullback forces were recorded at the rig and not at the pipe leading end. Therefore, to obtain the pullback forces at the pipe leading end location, the contribution of the drill pipe and reaming assembly needs to be deducted from the forces recorded at the rig location. To do so, a higher value than the standard out-bore friction coefficient is considered, which is determined by equating the rig pullback force at initiation of installation with the force required to pull the entire product pipe length on the ground surface. This calculation results in an out-bore coefficient of friction of $v_b = 0.32$. Following the ASTM recommendation, the in-bore coefficient of friction is considered to be $v_a = 0.3$ and the average density of returning slurry is 1240 kg / m^3, which was determined on the project site. These values are used for estimating the pullback forces in all three discussed methods, including the proposed one. The bore profile of the project is shown in Figure 3-3 (Duyvestyn 2006; Duyvestyn 2009). To estimate the pullback force changes at a high resolution, the bore path is discretized into 28 segments. To use the ASTM equations for this project, the

typical ASTM profile, including two curved and one straight segments, is fitted to the original bore profile inFigure 3-3.

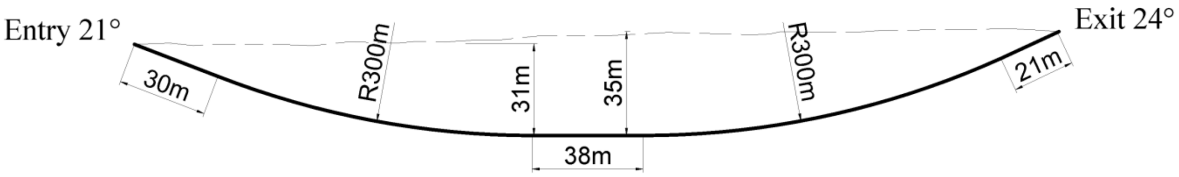

Figure 3-3- Poole Slough Watermain Project bore geometry (Duyvestyn 2009)

Figure 3-4 shows the estimated and measured pullback forces at different points along the project's bore. As the figure indicates, the proposed method estimates the pullback force variations over the installation course more accurately. Among the three implemented methods, only the proposed one has been able to capture the force decreasing trend over the second half of the installation, where the buoyant weight of the pipe assists with the installation. This is due to the fact that the proposed method, comparing to the ASTM, considers the bore geometry more realistically, and as a result is better able to capture the changes in pullback force observed through the installation. The difference between the peak measured and estimated pullback forces recorded at L=173.25 m is 3.2 percent. Conversely, the PRCI values increase until the end of installation due to the assumption that pullback force peaks when the pipe emerges from the ground. The PRCI's estimated peak force is 90.4 percent more than the observed value. This high difference shows the extreme conservatism of the PRCI method for this special installation (Slavin and Scholl 2014). Using the reduced fluidic drag coefficient of 172 Pa, the difference drops to 39.3 percent. For this specific installation, both the ASTM and proposed methods resulted in similar pullback forces, which is due to the fact that the bore profile shape (Figure 3-3) is very similar to the ASTM typical bore (Figure 3-1).

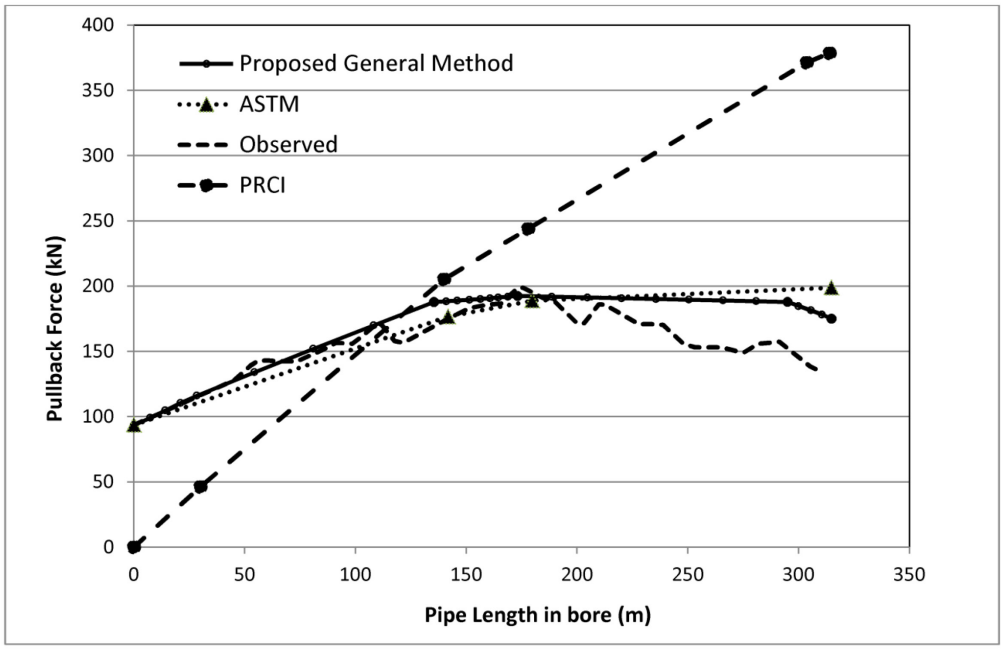

Figure 3-4- Measured and estimated pullback forces

Figure 3-5 shows the bore profile of a theoretical 300m. (1000-ft.) long 1.38 m. (54-in.) OD 17 DR HDPE pipe, as well as the fitted ASTM bore profile. Unlike the previous actual installation, in this case, the bore profile significantly deviates from the ASTM typical bore, as the bore curved segment lies between two inclined straight segments. The density of returning slurry is assumed to be 1200 kg/m^3 and the coefficients of friction are $v_a = 0.5$ and $v_b = 0.3$. Figure 3-6 demonstrates the pullback forces estimated using two different methods. The new proposed method estimates the peak pullback force to be 1756.3 kN and observed at L_1= 185.6 m, while the ASTM estimation of maximum force is 33% greater and occurs at the end of installation. Comparing to the previous example, this substantial difference between two methods results can be attributed to the large deviation of bore profile shape from that of the ASTM and having large out-bore coefficient of friction.

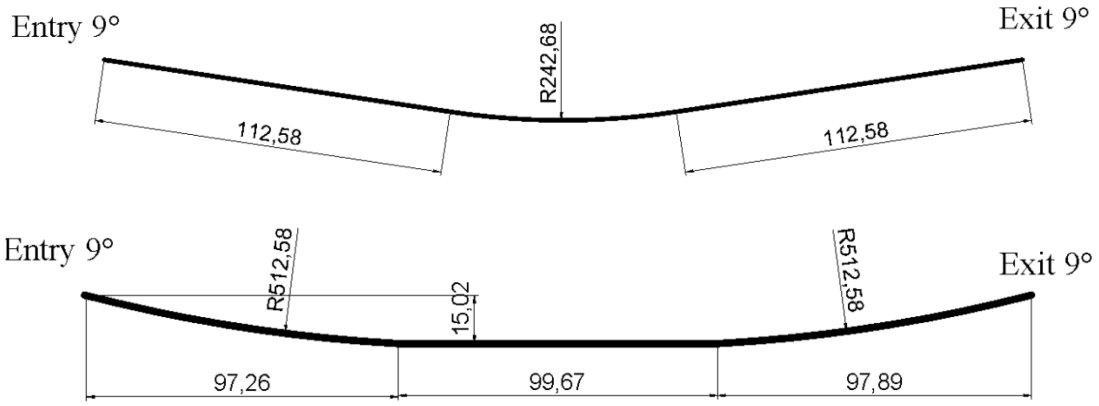

Figure 3-5- (a) Bore geometry of the theoretical 300-m-long installation; (b) ASTM fitted bore geometry

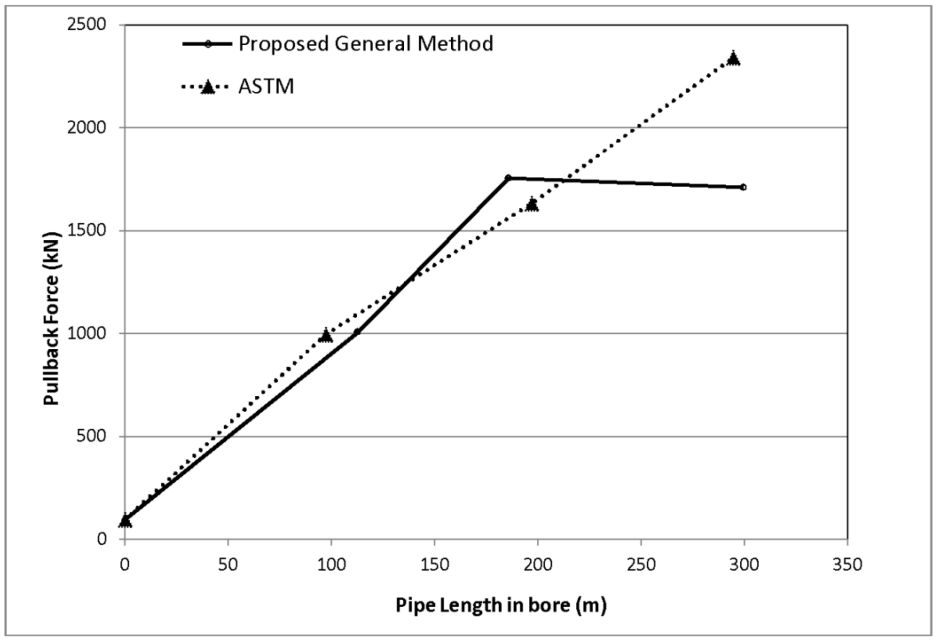

Figure 3-6- Estimated pullback forces

3-4-2- Comparison of the ASTM and Proposed Methods Estimated Pullback Forces

It is beneficial to investigate and understand the error resulting from use of the ASTM equations for pullback force estimation. This error is rooted in the assumptions made while adapting the basic Capstan equation to the HDD (Slavin and Petroff 2010) and is different from the discrepancy often observed between measured pullback forces and the ASTM estimated forces. For this purpose, the pullback force required to place a 750 m. long, 0.62 m. (24-in.) OD PE pipe within a bore of typical ASTM bore geometry is considered, and the error is reported in three-dimensional graphs for ease of interpretation. The error is calculated as follows:

$$Error\,(\%) = 100 \times \frac{T_{ASTM} - T_P}{T_P} \tag{3.10}$$

where T_{ASTM} and T_P are the pullback forces obtained using ASTM equations and the proposed method, respectively. The reference value and range of change for the different parameters are presented in Table 3-1. Figure 3-7 shows the effect of mud specific gravity and depth of installation on the pullback force error. To create these graphs, mud specific gravity and depth of installation are changed within the ranges specified in Table 1 while other parameters are kept fixed at the reference values. Since the pullback force magnitude at transition point D is affected by the value of pullback force at transition point B, two different graphs are presented for pullback force T_D in Figure 3-7. One graph, Figure 3-7(b), ignores the error from segment A-B, while the other, Figure 3-7(c), considers the total accumulated error. From Figure 3-7(a) and (b), it can be observed that the error increases as the installation depth increases. This behavior is due to curved segment length increasing as a result of depth increase, which results in greater errors in the ASTM's approach. As expected, the T_B error is also greater than the corresponding T_D error, as indicated in Figure 3-7(b). The error is due to the orientation of pullback force components in the downward curved segment of the pipeline, in comparison to the upward segment, where both the frictional and buoyant forces resist pipe advancement. Figure 3-7(c) shows that the accumulated error of the pullback force at point D, where the pullback often reaches maximum, is less than 3 percent and is primarily due to error from segments A-B.

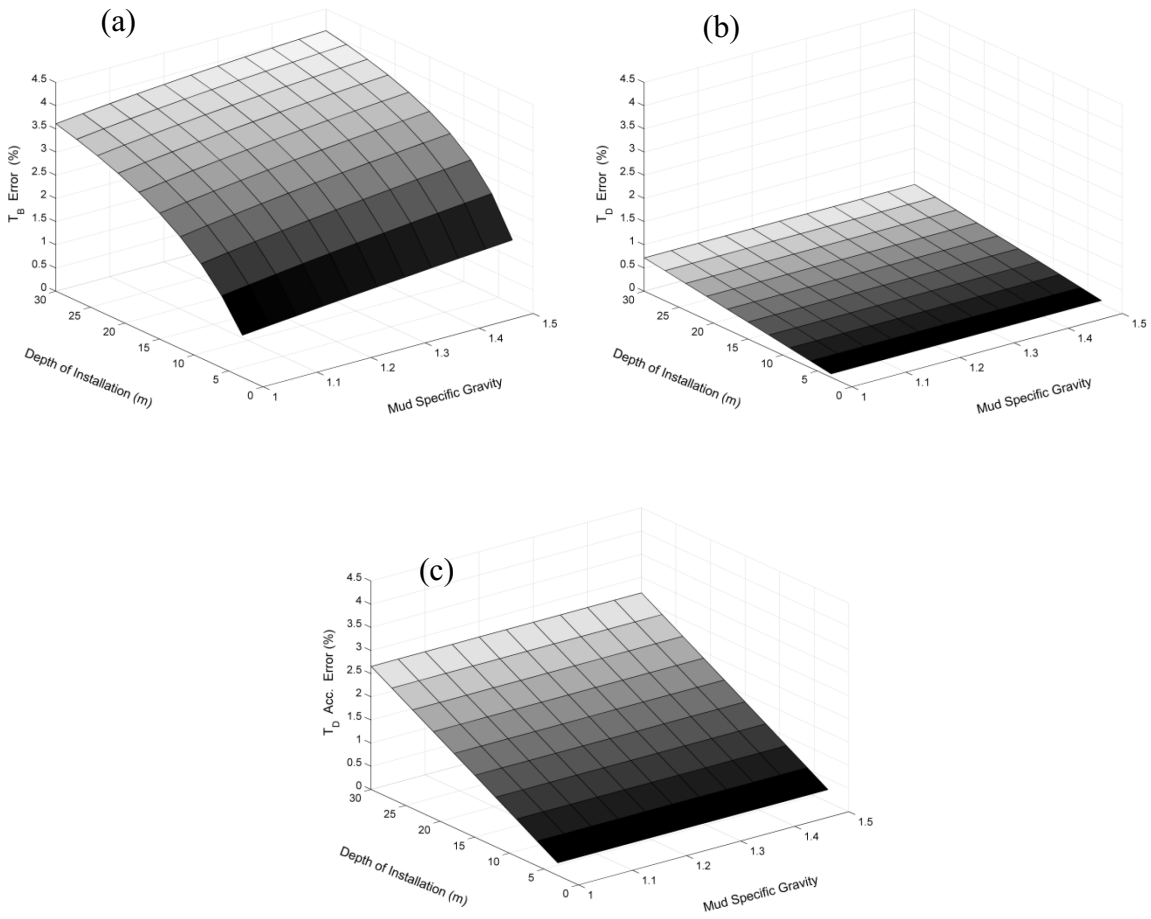

Figure 3-7- Pullback force error versus mud gravity and depth of installation at (a) Point B; (b) Point D excluding the accumulated error; (c) Point D including the accumulated error

Table 3-1. Installation parameters

Parameter	Reference	Range
Depth of installation (H)	15 m	3-30 m
Mud specific gravity	1.2	1-1.5
Out-bore friction coefficient (v_a)	0.1	0.1-0.8
In-bore friction coefficient (v_b)	0.3	0.1-0.8
Pressure drop ΔP	70 kPa	-
Pipe dimension ratio (DR)	11	-
Pipe entry angle (α)	18°	-
Pipe exit angle (β)	15°	-
L_1	30 m	-

Figure 3-8 illustrates how the error is affected by in-bore and out-bore coefficients of friction. While the T_D error only responds to in-bore condition changes, T_B is affected by both in- and out-bore coefficients. This is because a large portion of the pipe's length remains outside of the bore when the pipe head is at point B, making ground surface friction significant in the calculation of T_B as the pipe is pulled along the ground surface or on rollers. However, when the leading end of the pipe approaches point D, the portion of the pipe outside of the bore is less than 10 percent, making the ground surface friction less significant. Similarly, the accumulated maximum error of pullback force T_D is 3.2 percent, compared to the 9.6 percent error for T_B.

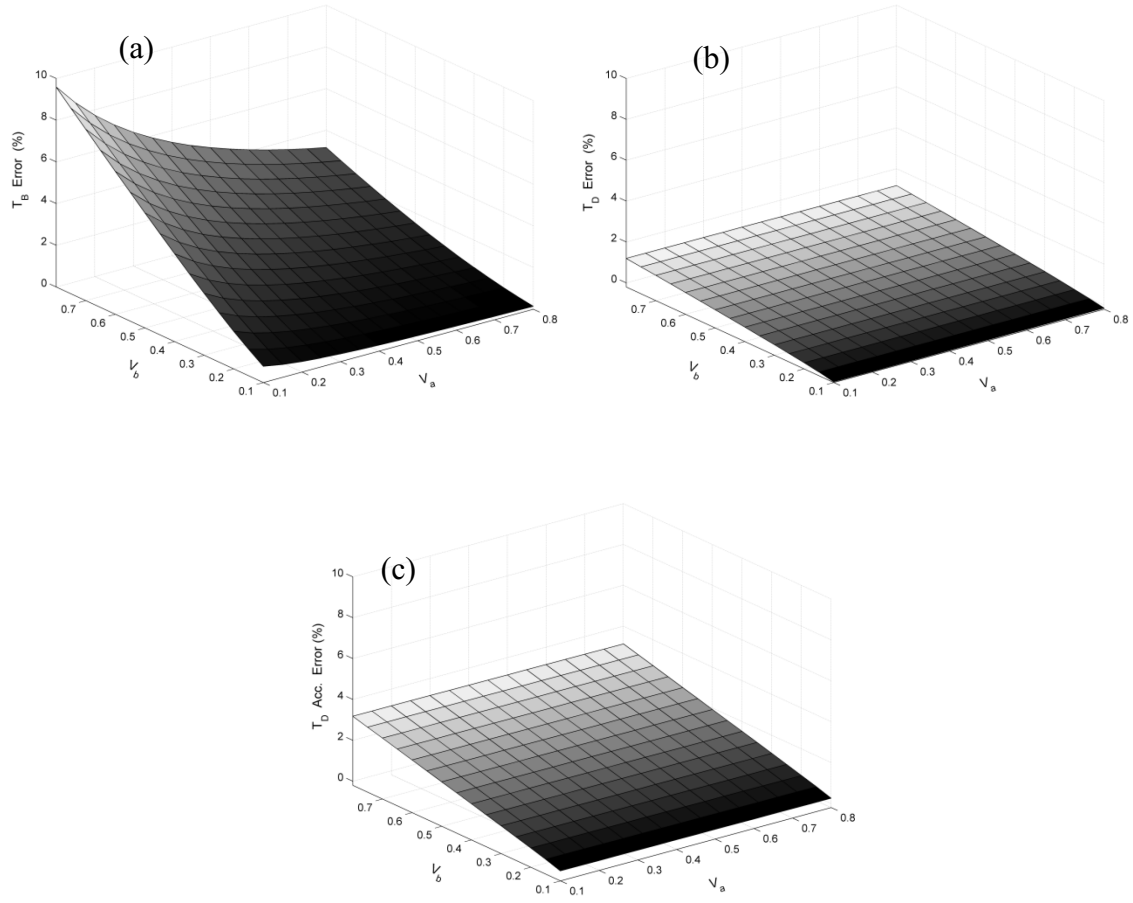

Figure 3-8- Pullback force error versus in-bore and out-bore coefficient of friction at (a) Point B; (b) Point D excluding the accumulated error; (c) Point D including the accumulated error

3-5- Conclusions

This paper has proposed and verified a general method, applicable to all HDD projects regardless of bore profile geometry, for pullback force determination in PE pipe based on adaption of the Capstan basic equation and more detailed consideration of pipe buoyant weight effects. The method assumes that each bore path curved segment lie in a vertical plane and does not consider compound curves. Pullback forces of an actual HDD installation were compared to forces calculated using the proposed method as well as the commonly used ASTM and PRCI methods. Results of the comparison indicated that the proposed method introduces less error than the ASTM method, both of which appear to give more accurate results than the PRCI method, based on at least one actual installation. For the investigated theoretical HDD project, the maximum error incurred through the use of the ASTM equations relative to that of the proposed method was 9.6 percent, largely due to error in pullback force determination for the downward curved segment. It was also determined that, at the end of installation, the pullback force error was sensitive to installation depth and the in-bore coefficient of friction. As an extension to the method presented in this paper, a new method for pullback force calculation can be derived for situations where the pipe has curvature in both vertical and horizontal planes.

4- Chapter 4: New Method for Predicting Pullback Force for Pipes Installed via Horizontal Directional Drilling (HDD)[2]

4-1- Introduction

Horizontal Directional Drilling (HDD) is becoming an increasingly common trenchless technology for underground pipe installation in places where minimum ground disruption is required (Najafi and Gokhale 2005). An HDD project typically includes three steps: 1) a steerable and tractable drill bit creates a pilot borehole; 2) the pilot hole is enlarged to a diameter greater than that of the intended pipe; 3) the product pipe is pulled into the enlarged borehole. Since its first successful application in crossing the Pajaro river near Watsonville, California in 1971, the HDD industry has steadily grown with more than 30,000 units of HDD rigs manufactured worldwide (Sarireh et al. 2012). It has several advantages over the traditional cut-and-cover method, including the preservation of ground surface in crossing sensitive areas, such as wetlands or natural habitats. Additionally, HDD also proves to be a feasible solution for installations in congested areas.

For a majority of HDD installations, the forces developed through the pipe over pullback operations govern the pipe design. Various methods are suggested in the literature for pullback force evaluation (Baumert and Allouche 2002; Cheng and Polak 2007b). Among these methods, the Pipeline Research Council International (PRCI), and ASTM F1962, Standard Guide for Use of Maxi-Horizontal Directional Drilling for Placement of Polyethylene Pipe or Conduit Under Obstacles, Including River Crossings, are most commonly referenced in the design of HDD installations. In PRCI, which was originally developed for steel pipes, the in-bore pipe is first broken into straight and curved segments and then the tensile force change along each individual segment is calculated by using the provided equations (Huey et al. 1996). Finally, the pullback force is calculated by summing the tensile force change of all segments along the pipe. As the stiffness of Polyethylene (PE) pipes is relatively low, the ASTM (2011) proposes a set of equations for pullback force determination based on the basic Capstan equation (Nelson 2009). The ASTM method assumes that the bore profile consists of a one horizontal straight and two

[2] This chapter has been published in the proceeding of NASTT's 2015 No-Dig Show held in Denver, Colorado.

curved segments and that the pipe entry and exit points are level. This paper proposes a new method for evaluating pullback force that is applicable to both HDPE and steel pipe installations and doesn't have the restraints of ASTM F1962 method.

4-2- Proposed Method

The proposed method begins similarly to those outlined by ASTM F1962 and PRCI, discretizing the bore pipe into straight and curved segments. Then, the tensile force increment along each segment developed through the pipe during its installation is evaluated via a set of proposed equations. Finally, the total pullback force at the location of the pulling head is determined by summing the force increments along the pipeline. While a common equation is implemented for straight segments, the proposed method is original in the way that the contribution of curved segments to the pullback force is evaluated. In the following sections the equations required to calculate the frictional drag component of the tensile force change along straight and curved segments are presented. Then, the fluidic drag component is discussed and pullback forces of two example HDD installations are investigated for illustration purposes.

4-3- Straight Segments

A typical straight pipe segment under applied forces, excluding the fluidic drag, is shown in Figure 4-1. Resulting from static equilibrium, the tensile force increment along a straight segment is given as

$$\Delta T_s = \left| frict_s \right| \pm w_b \times L_s \times Sin(\theta_s) \tag{4.1}$$

where $frict_s = v_b w_b L_s Cos\theta_s$ (N) is the frictional force between the pipe and bore surface, w_b (N/m) is the buoyant unit weight of the pipe, L_s (m) is the length of segment, and θ_s (rad) is the angle of the pipe/bore axis with respect to the horizontal.

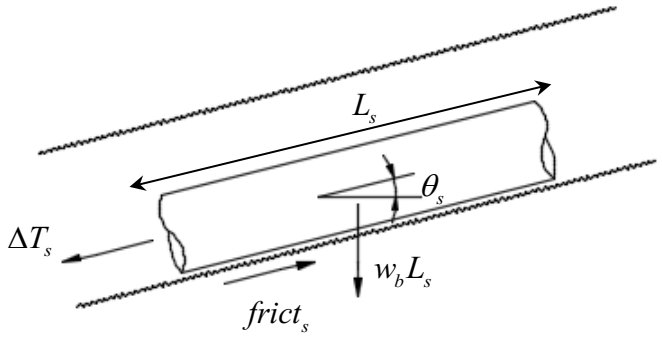

Figure 4-1- A typical straight pipe segment under forces contributing to frictional drag

4-4- Curved Segments

The tensile force change along a curved pipe segment is a product of three different components: pipe buoyant weight, pipe bending stiffness, and force direction change. In the following section, each of these components and the corresponding procedure for determining their values is discussed.

4-4-1- Pipe Buoyant Weight

Figure 4-2 shows a curved pipe segment under forces originating from pipe buoyant weight. This component represents the effect of pipe buoyant weight on the tensile force change. Knowing the curved pipe segment length, L_c (m), the contribution of pipe weight in tensile force change along the segment, ΔT_w, can be evaluated as:

$$\Delta T_w = v_b L_c w_b \sin\varphi \pm L_c w_b \cos\varphi \qquad (4.2)$$

where v_b is the in-bore coefficient of friction and φ is the angle between the radial line passing through the segment mid-point and the horizontal. In this equation, the second term's sign is positive when the segment is inserted into the ground, and negative for when it is pulled upward.

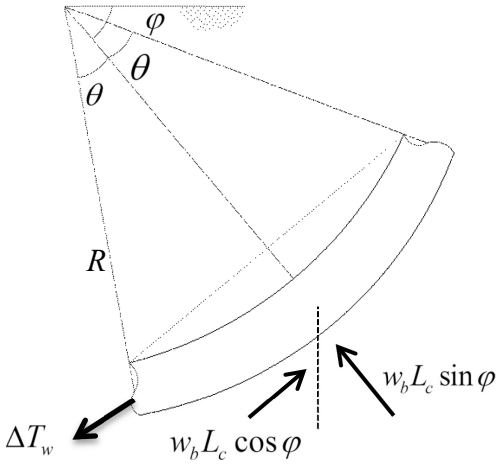

Figure 4-2- A typical curved pipe segment under forces originating from pipe buoyant weight

4-4-2- Pipe Bending Stiffness

Pipe bending stiffness reflects the excess frictional force developed between the pipe surface and the bore wall due to the effort required to fit a straight pipe segment into a curved bore. Resulting from geometry of bores in typical HDD projects, the curved pipe segments often undergo large deflections. Therefore, adapting theories based on small deflection assumptions may lead to pullback force overestimation.

Figure 4-3a shows a cantilever beam under a concentrated load, F (N), applied at the tip of the beam. The beam length is L_b (m) and assumed to be undergoing large deflections. The relation between concentrated load and maximum slope at the tip, φ_0, is given as:

$$L_b = \sqrt{\frac{EI}{2F}} \int_0^{\varphi_0} \frac{1}{\sqrt{\sin\varphi_0 \cos\varphi - \cos\varphi_0 \sin\varphi}} d\varphi \tag{4.3}$$

where EI (N.m^2) is the pipe bending stiffness (Beléndez et al. 2002). Typically, the beam flexural properties are known; therefore, by knowing the value of either the concentrated load or the beam maximum slope, the above equation can be solved for the unknown parameter. Additionally, the beam reaction force at the support in the vertical direction is the y component of the tip load, $F\cos\varphi_0$. Equation (4.3) may be rearranged as:

$$F = \frac{EI}{L_b^2}\frac{X^2}{2} \tag{4.4}$$

where X is the value of the integral in equation (4.4) which is tabulated in Table 4-1. Figure 4-3b shows a curved weightless pipe segment under forces developed between the pipe and the bore wall due to pipe stiffness. In this figure, each half of the curved pipe segment can be assumed to behave as a cantilever; therefore, the pipe mid-span reaction is $2N = 2 \times F\cos\varphi_0$. Also, by knowing the cantilevers' maximum slope from the bore geometry, which is $\varphi_0 = \theta$, the reaction forces at the pipe ends can be determined using equation (4.4). Finally, the tensile force increase due to pipe bending stiffness is given as:

$$\Delta T_s = 2Fv_b(1+\cos\varphi_0) \tag{4.5}$$

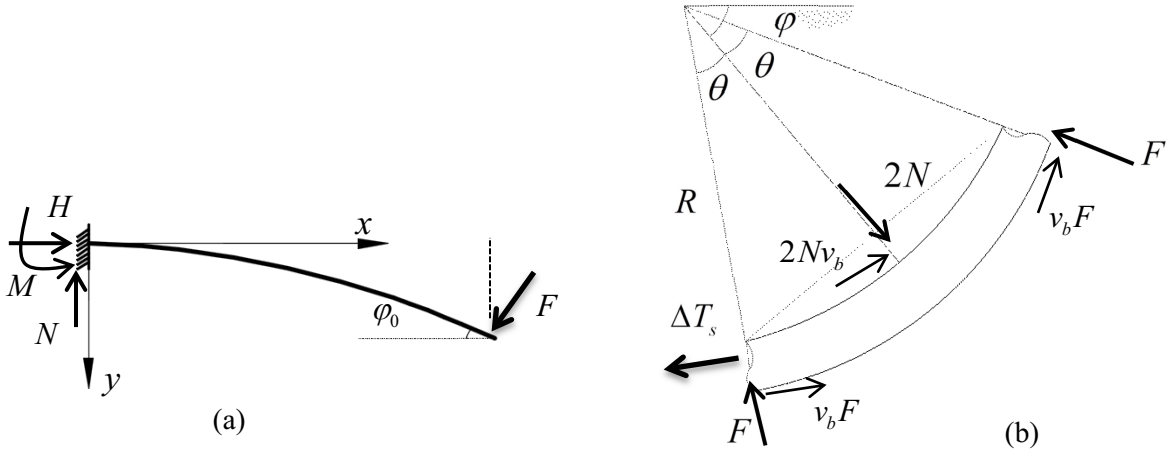

Figure 4-3- (a) Cantilever beam under concentrated load at the tip; (b) A typical curved pipe segment under forces originating from pipe bending stiffness

4-4-3- Tensile Force Direction Change

This component accounts for the frictional force increase due to tensile force direction change between the ends of a pipe segment negotiating a curved bore. Figure 4-4 shows a weightless pipe segment with zero bending stiffness subjected to tensile forces at the ends with a reaction force in the middle. In Figure 4-4, $T' = T$ and the curve reaction force, N', can be calculated by writing the equation of force equilibrium along the bisector as:

$$N' = 2T\sin\theta \tag{4.6}$$

where T (N) is the unknown total tensile force at the end of a curve. Therefore, the magnitude of frictional force amplification due to tensile force direction change is:

$$\Delta T_d = 2v_b T \sin\theta \tag{4.7}$$

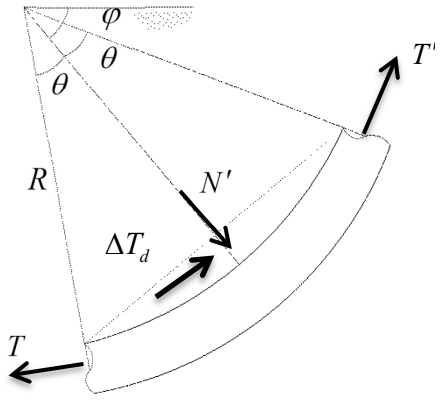

Figure 4-4- A typical curved pipe segment under forces originating from tensile force direction change along a curve

Once all components values have been determined, the total frictional drag increment along a curved segment can be calculated as:

$$\Delta T_c = \Delta T_w + \Delta T_s + \Delta T_d \tag{4.8}$$

This equation can be rewritten in the form of pipe end force as:

$$T = \frac{\Delta T_w + \Delta T_s + T_1}{1 - 2v_b \sin\theta} \tag{4.9}$$

where T_1 is the pipe pull force at the opposite end. Unlike PRCI, this equation requires no iterative process to determine the curved pipe segment end force, making it more suitable for practical application.

4-4-4- Fluidic Drag

ASTM F1962 proposes the following equation to estimate the fluidic drag due to viscous slurry stream on the product pipe's outer surface along the in-bore length of a pipe:

$$T_f = \Delta P \frac{\pi}{8}(D_b^2 - D_p{}^2) \tag{4.10}$$

where ΔP (Pa) is the hydrokinetic pressure estimated to be 70,000 Pa (ASTM F1962 2011), and D_b (m) and D_p (m) are the bore and pipe diameters, respectively. For steel pipes, the PRCI proposes the following equation to calculate fluidic drag:

$$T_f = 12L\pi D_p \mu_{mud} \tag{4.11}$$

where L (m) is the in-bore length of pipe, and μ_{mud} (Pa) is the fluidic drag coefficient with the recommended value of 350 Pa (Huey et al. 1996).

To determine the pullback force, the frictional drag increments along the pipeline from all straight and curved segments are summed and added to the fluidic drag as follows:

$$T_{pullback} = T_f + \sum(\Delta T_w + \Delta T_s + \Delta T_d) \tag{4.12}$$

4-5- Discussion of the Sample Installations

This section illustrates the application of the proposed method in two theoretical HDPE and steel pipe HDD installations. The obtained results are compared to ASTM F1962 and PRCI for HDPE pipe for steel pipe, respectively.

The bore geometry and installation parameters for the HDPE pipe are presented in Figure 4-5 and Table 4-2. The maximum pullback force at the pipe exit point is 389.0 and 381.4 kN as predicted by the proposed and ASTM F1962 methods (Figure 4-6). The fluidic drag is estimated to be 12.6 kN, which amounts to approximately 3 percent of the peak pullback force. The contribution of stiffness component to pullback force is nearly zero. This is due to HDPE pipes low bending stiffness and large radius of curvature of bends in typical HDD installations, resulting in low EI / L_b^2 ratios in Equation (4.4). Figure 4-6 indicates similarity between the predictions of both methods: it demonstrates that the proposed method can also be employed for the pullback force prediction of HDPE pipe installations. However, the proposed method

possesses an advantage over ASTM F1962, as it can be implemented regardless of the bore geometry, such as ground surface grade or number of segments composing the bore path.

For the steel pipe installation, the bore geometry and installation parameters are presented in Figure 4-7 and Table 4-3, respectively. In this installation, the fluidic drag, which evolves with installation progress, reaches its maximum value (163.0 kN) at the moment the pipe emerges from the ground. Contrary to HDPE installation, this value amounts to a significant portion of the maximum pullback force (about 43 percent), which is predicted to be 285.9 and 293.0 kN by the proposed and PRCI methods (Figure 4-8). This difference between ASTM F1962 and PRCI procedures in pipe-drilling fluid interaction clearly indicates the need of a more in-depth investigation of the fluidic drag problem.

The insignificant contribution of stiffness component to pullback force may be neglected for both HDPE and steel installations thus simplifying Equation (4.9).

$$T = \frac{\Delta T_w + T_1}{1 - 2v_b \sin\theta} \tag{4.13}$$

This equation can be implemented for pullback force change evaluation resulting from pipe-bore surface friction around bore curved segments in typical HDD installations.

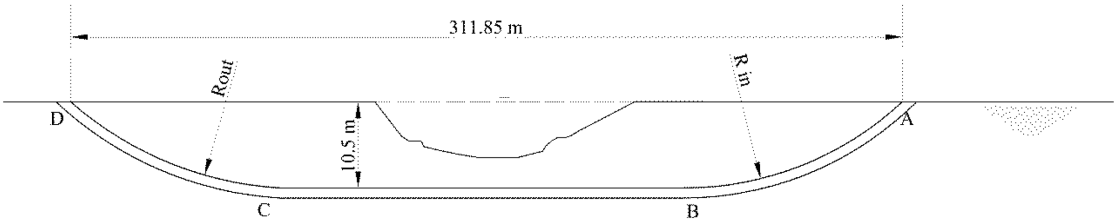

Figure 4-5- Bore geometry of HDPE pipe installation

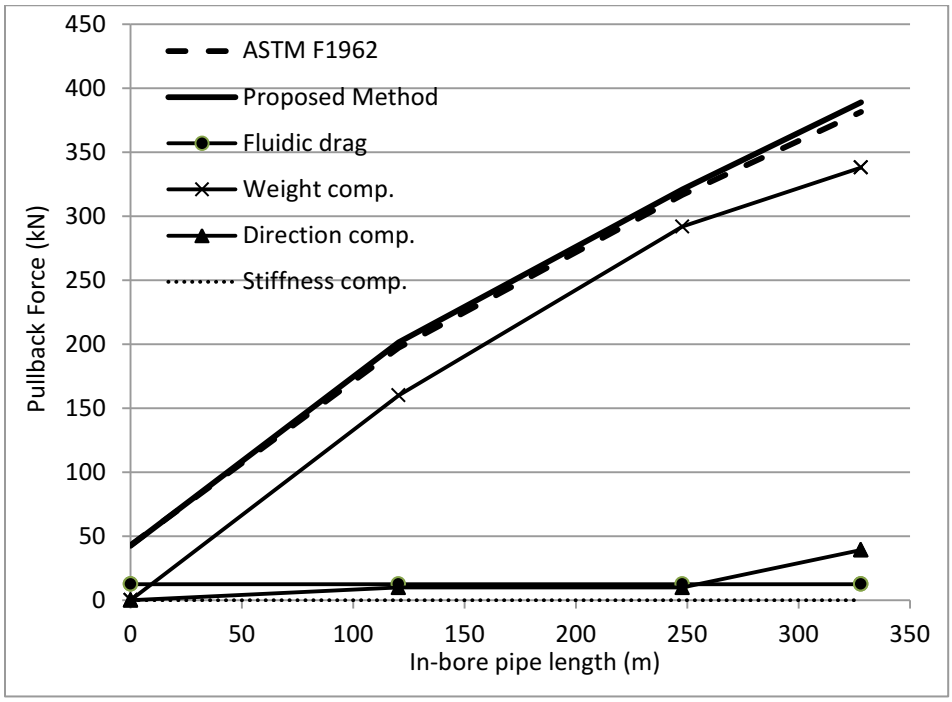

Figure 4-6- Predicted pullback forces by the proposed and ASTM F1962 methods for HDPE pipe installation

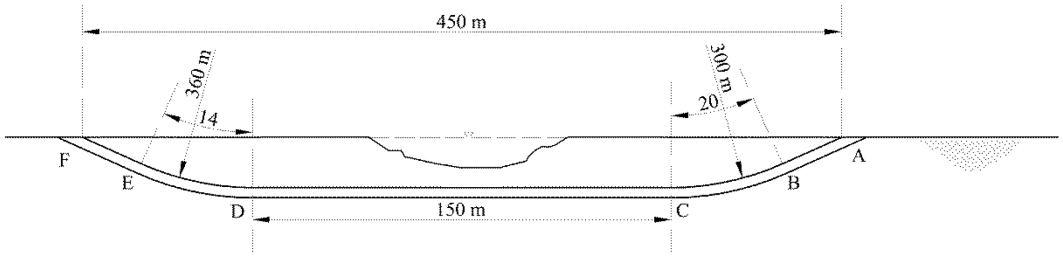

Figure 4-7- Bore geometry of steel pipe installation

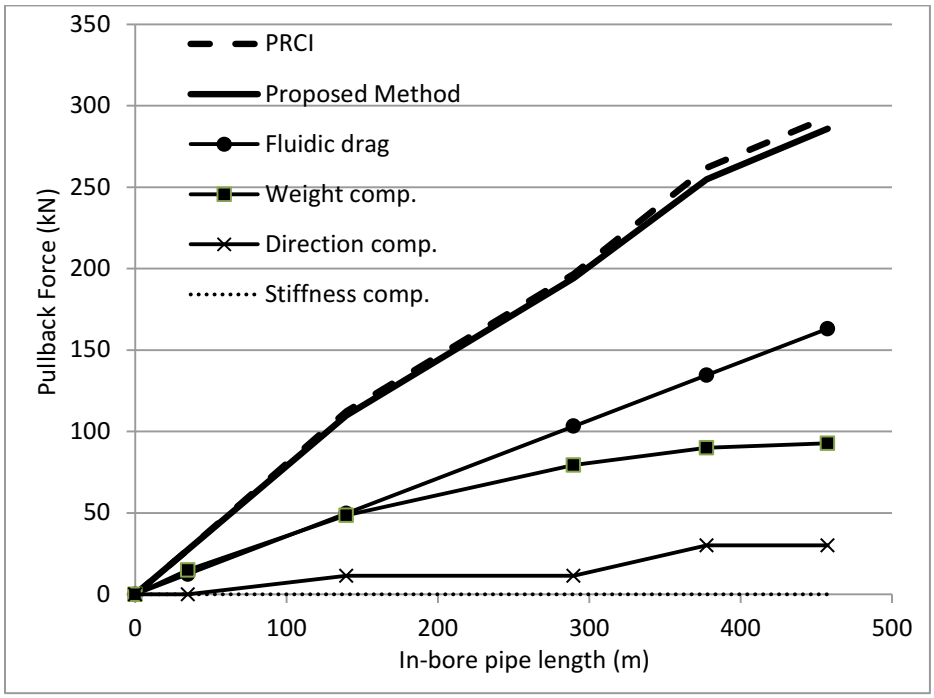

Figure 4-8- Predicted pullback forces by the proposed and PRCI methods for steel pipe installation

Table 4-1- X Value for different tip angles

$\varphi_0 = \theta$ (deg)	4	4.5	5	5.5	6	6.5	7	7.5	8	8.5	9	9.5	10
X	0.91	0.96	1.02	1.06	1.11	1.16	1.20	1.24	1.28	1.32	1.36	1.40	1.44

Table 4-2- HDPE pipe installation parameters

Parameter	**Value**
Unit weight of water	9.8 (kN/m^3)
HDPE specific gravity	0.95
Mud specific gravity	1.5
Product pipe diameter, D_p	0.61 (m)
Bore diameter, D_b	0.91 (m)
Pipe wall thickness, t	0.055 (m)
Out-bore friction coefficient, v_a	0.1
In-bore friction coefficient, v_b	0.3
HDPE modulus, E_{HDPE}	3011 (kN/m^2)

Table 4-3- Steel pipe installation parameters

Parameter	**Value**
Unit weight of water	9.8 (kN/m^3)
Steel specific gravity	7.85
Mud specific gravity	1.44
Product pipe diameter, D_p	0.32385 (m)
Pipe wall thickness, t	0.006 (m)
Out-bore friction coefficient, v_a	0.1
In-bore friction coefficient, v_b	0.3
Steel modulus, E_s	1.39e+6 (kN/m^2)

4-6- Conclusions

A new method for predicting pullback forces of pipe installed via HDD was presented, and its implementation was illustrated through two theoretical installations. For curved pipe segments, the pullback force amplification due to frictional drag is assumed to be a product of pipe buoyant weight, pipe stiffness, and tensile force direction change, and equations for estimating each of these components provided. For typical installations, it is shown that pipe stiffness component contribution is insignificant and can be ignored. The results matched well with the ASTM and PRCI based on theoretical cases; however, the proposed model will require field validation.

5- Chapter 5: Estimation of Hydrokinetic Pressure and Fluidic Drag Changes during Pipe Installations via HDD Based on Identifying Slurry Flow Pattern Change within Borehole [3]

5-1- Introduction

Since its establishment, Horizontal Directional Drilling (HDD) has been regarded as an innovative trenchless method by both industry and academic professionals (Najafi and Gokhale 2005). HDD is an ideal technique to navigate pipe placement through urban centres, environmentally sensitive areas, traffic-heavy streets and harbours, and other high-risk regions because it causes minimal disturbances to the surrounding area. As a result, the costs associated with HDD are lower than the costs associated with the traditional method of open cut excavation (Willoughby 2004). A standard HDD project will include three stages: (1) drilling the pilot bore, (2) widening the pilot bore so it is large enough to accommodate the product pipe, and (3) pulling the product pipe into the widened bore.

Although the trenchless industry has seen a surge in the number of HDD projects, pipes are still designed cautiously because professionals are unsure of how the installed pipe will interact with the soil and slurry medium during the pipe installation stage (Baumert et al. 2005). Design references like ASTM F1962 (2011) and Pipeline Research Council International (PRCI) (Huey et al. 1996) are vitally important to HDD design, yet they often ignore characteristics that are exclusive to HDD because the trenchless industry does not have enough relevant investigations to use as a resource. Consequentially, HDD design references must depend on investigations undertaken by other industries, such as oil well drilling and utility cable installation. Estimating hydrokinetic pressure and fluidic drag during the pipe placement stage is an area that greatly needs studying, and thus it is the focus of this paper. Hydrokinetic pressure is the minimum in-bore pressure, in addition to hydrostatic pressure, that must be sustained during pullback operations in order to exhaust the slurry from the bore to the surface at an optimum flow rate.

[3] A version of this chapter has been submitted to the ASCE Journal of Pipeline Systems Engineering and Practice.

Maintaining hydrokinetic pressure and drilling fluid circulation during installation operation aids in preserving bore stability, lubricating the bore wall, and transferring residual cuttings from reaming or swabbing stage. Fluidic drag, on the other hand, is the force created on pipe leading head during installation due to slurry interaction with the in-bore portion of the pipe.

A ground-mounted rig pumps drilling fluid down the drill string during oil well drilling operations. Following expulsion from the nozzle, the blend of fluid and cuttings runs back from the well bottom to the ground surface, flowing through the annular space between the drill string and the well. With regard to the slurry flow pattern, this process is similar to the pilot bore drilling stage, where the total slurry volume within annular space flows in a reverse direction compared to the pipe movement throughout the operation. In pullback stage, the entire bore length has already been reamed to its final diameter, so depending on the location of the product pipe leading head, the slurry exits to the ground surface through the product pipe and/or the drill rod annuli. In the same way, lightweight utility cable installation via the blown-cable technique (Slavin 2009), which is the basis of current ASTM F1962 fluidic drag evaluation (Slavin and Petroff 2010), observes annular flow in a singular direction during installation.

In order to estimate the fluidic drag, ASTM F1962 suggests using equation (5.1), which was originally used to calculate the drag force applied on a utility cable's outer surface (Slavin 2009; Slavin and Petroff 2010):

$$F = \Delta P \frac{\pi (R^2 - R_P^2)}{2} \tag{5.1}$$

where $R\,(\mathrm{m})$ and $R_P\,(\mathrm{m})$ are the bore and pipe radii, respectively, and $\Delta P\,(\mathrm{Pa})$ is the hydrokinetic pressure. ASTM F1962 assumes the hydrokinetic pressure (ΔP) to be 70 kPa, unquestionably. Equation (5.1) provides no data on drag change as the installation develops, and the slurry rheology is considered in the pressure implicitly. PRCI provides no value for the hydrokinetic pressure, but it suggests that fluidic drag can be calculated by multiplying the pipe's outer surface area in contact with the slurry by a fluidic drag coefficient:

$$F = 2\pi R_P L_1 \mu_{mud} \tag{5.2}$$

where $L_1\,(\mathrm{m})$ is the in-bore length of the product pipe, and $\mu_{mud}\,(\mathrm{Pa})$ is the fluidic drag coefficient with a value of 350 Pa taken from the Dutch standard NEN 3650, *Requirements for Pipeline Systems* (NEN 2007). Unlike ASTM, PRCI accounts for installation development in its calculated drag value, but it disregards the influence of slurry rheology and size of the annulus.

Although many advances have been made in the field of HDD, designs can still be perfected. For instance, Baumert et al. (Baumert et al. 2005) made several suggestions on how to enhance existing practices by examining current hydrokinetic pressure evaluation techniques during the HDD installation stage. Assuming the slurry to be characterized as a Bingham Plastic fluid, they deduced that pressure drop modeling could be made using slot flow approximation, with a few adjustments to increase precision. These adjustments included establishing a factor to incorporate pipe eccentricity and employing low shear rate to estimate drilling fluid rheological parameters. The oil well industry provided the original source for the modified equations used for pressure drop estimation in this study (N.L. Baroid 1998), and the authors implemented them without making any adjustment to account for different flow pattern observed in during HDD pipe installation.

In an attempt to model the fluidic drag component of the pullback force more realistically, Duyvestyn (2009) also implemented the slot flow approximation but considered slurry flow direction change during the pullback (pipe installation) stage. He assumed that in an installation, with the pipe leading head between the pipe entry and crossover points, the total slurry volume flows to the surface through annular space between the product pipe and bore. Then, once the crossover point has been reached, the slurry flow direction switches, and the slurry moves in front of the product pipe toward the rig. To determine the crossover point location, the hydrokinetic pressure required for exhausting the slurry via product pipe and drill rod annuli were calculated in terms of in-bore pipe length. After equating these pressures and solving for the in-bore pipe length, the crossover point was calculated. The major shortcoming of this study was ignoring the fact that in a typical installation, the slurry returns to the surface through both the product pipe and drill rod annular spaces over a considerable length. Furthermore, the pullback rate effects were not considered.

Supposing the drilling fluid to be characterized as a non-Newtonian Power-law fluid, a more recent study by Faghih et al. (2015b) proposed using the solution of general annular flow

problem for determining the fluidic drag. Similar to the previous studies (Polak and Lasheen 2001; Baumert et al. 2005), this study also assumes that the whole drilling fluid volume flows to the ground through the space between pipe and borehole and against the pipe pull direction.

This paper proposes a new method for predicting hydrokinetic pressure and fluidic drag changes during pullback operation. The method is based on identifying two different stages of slurry flow pattern along the bore and solving the governing set of coupled equations for desired pipe pulling head locations within each stage. The method assumes the slurry to be characterized as a non-Newtonian Power-law fluid, and it considers the effects of a variety of parameters: annulus size, installation progress, pipe pullback rate, and slurry rheology. This, compared to the existing methods, makes the new method a promising tool for modeling slurry-product pipe interaction in HDD pipe placement operations.

5-2- Identification of Slurry Flow Pattern during Pipe Installation

Slurry flow within the product pipe-drill rod-bore system, shown in Figure 5-1a, during pullback operations is analogous to the motion of fluid through two parallel tubes with a common inlet and outlet, as illustrated in Figure 5-1b, where the inlet is associated with the location of slurry discharge from the drill string into the bore and the outlet represents the ground surface in either side of the crossing. The gauge pressure at the inlet is equal to the sum of hydrokinetic and hydrostatic pressures while this value is zero at the outlet. Also, Q_1 and Q_2 are the volume rates of slurry returning to the ground surface through the product pipe annulus and drill rod annulus, respectively. In this analogy, the tubes' permeability (k_1 and k_2) change as installation progresses due to product pipe leading head movement within the bore. Additionally, the total flow rate (Q_t) is distributed between the tubes based on their relative permeability.

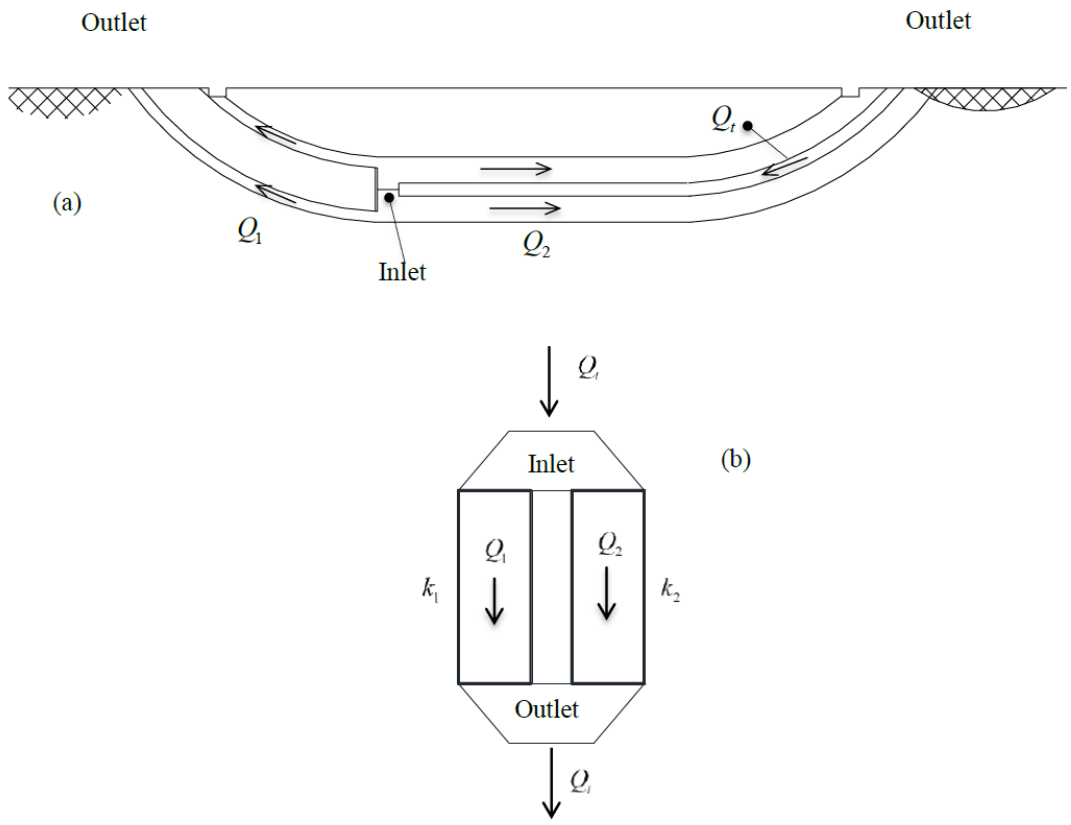

Figure 5-1- Parallel tubes analogy

In general, from a drilling fluid flow point of view, a typical HDD installation undergoes two different stages during the pullback operation, as illustrated in Figure 5-2. During Stage 1, the drilling fluid flows primarily to the ground surface through the product pipe-bore annulus (pipe annulus) since the resistance is significantly less in this direction compared to the drill rod-bore annulus (rod annulus). Furthermore, the velocity peaks somewhere between the pipe surface and bore wall in the pipe annulus, while the velocity increases from zero at the bore wall to a maximum at the drill rod's surface in the rod annulus. As the product pipe's leading end moves away from the entry point, the pumping pressure required to maintain a constant slurry flow rate becomes greater, resulting from an increase in the product pipe in-bore length (L_1). This increase of pressure terminates somewhere within Stage 1 and, thereafter, the pressure starts dropping until the pipe emerges from the ground.

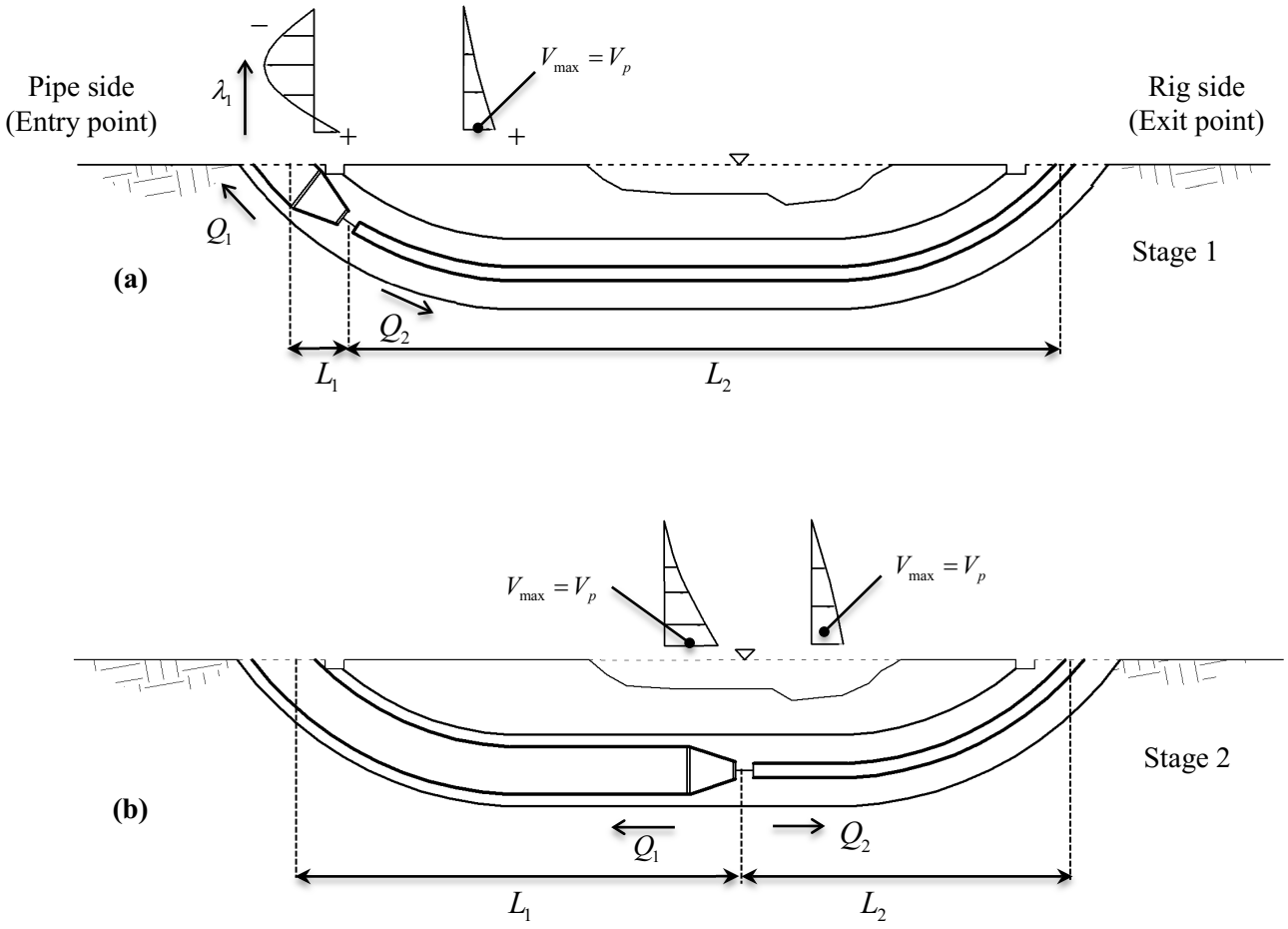

Figure 5-2- Different stages of drilling fluid flow during a typical HDD pipe installation operation

In Stage 1, as the pressure starts dropping, the absolute peak velocity location (λ_1 in Figure 5-2a) moves upward across the pipe annulus and toward the bore wall. This leads to the outer region of the velocity profile, associated with layers of slurry moving toward the pipe entry point, to shrink in size as the inner region grows. At a specific point along the bore marked as the end of Stage 1/start of Stage 2, the pressure has already dropped to an extent that the peak velocity reaches the bore wall and all slurry layers within the pipe annulus move in the same direction as the pipe pull. This breakdown of the bore length into two segments allows a smooth change in flow pattern during pipe placement process, an aspect that was ignored by previous studies (Slavin and Petroff 2010; Duyvestyn 2009).

In the next section, the equations governing slurry flow in each of the two above-discussed stages will be derived. It is assumed that both product pipe and drill rod annuli are concentric over pullback operation and the slurry flows in a laminar regime. Furthermore, the effects of drill pipe rotation, reamer presence in the bore, and annuli entrances on slurry flow are ignored.

5-3- Hydrokinetic Pressure and Fluidic Drag Calculation

To determine the fluidic drag and hydrokinetic pressure history during an installation, equations governing fluid motion should be developed for each stage of slurry flow and then solved for desired pipe leading head locations. To do so, equations must first be defined for the flow rate and velocity of a Power-law fluid flowing laminarly through a concentric annulus. In the fluid mechanics literature, two sets of equations are available for annular flow rate and velocity evaluation depending on whether the velocity gradient changes signs within the annulus. These equations are presented in the following subsections.

5-3-1- Annular Flow Rate and Velocity Equations

- **Case I (with velocity gradient sign change)**

Figure 5-3 shows a schematic representation of the velocity and shear stress profiles when the velocity gradient sign change occurs within the annulus. After dividing the velocity profiles into two inner $(\sigma \le \xi \le \lambda)$ and outer $(\lambda \le \xi \le 1)$ regions, the velocity in each region can be evaluated as (Chhabra and Richardson 2011):

$$V_{zi}(\xi) = R(P'\frac{R}{2m})^s \int_{\sigma}^{\xi} (\frac{\lambda^2}{x} - x)^s dx + V_p \qquad \sigma \le \xi \le \lambda \tag{5.3}$$

$$V_{zo}(\xi) = R(P'\frac{R}{2m})^s \int_{\xi}^{1} (x - \frac{\lambda^2}{x})^s dx \qquad \lambda \le \xi \le 1 \tag{5.4}$$

where $P' = \Delta P / L$ (Pa/m) is the pressure drop per unit length along the annulus, $R\,(\mathrm{m})$ is the bore diameter, $m\,(\mathrm{pa.s}^n)$ is Power-law consistency index, $s = 1/n$ is the reciprocal of the Power-law behaviour index, σ is the normalized radius of the annulus' inner bounding surface, and λ is the normalized location of the surface where the maximum velocity occurs. Furthermore, the subscripts "i" and "o" denote the inner $(\sigma_1 < \xi < \lambda_1)$ and outer $(\lambda_1 < \xi < 1)$

regions, respectively. Through implementing these two equations and a procedure similar to Hanks and Larsen's (1979) for annular flow rate evaluation, the flow rate equation of a Power-law fluid flowing through a concentric annulus when the inner surface is moving at the rate of V_p is obtained as:

$$Q = \pi R^3 \left\{ -\frac{2(1+s)}{3+s}\frac{V_p \lambda^2}{R} + (\frac{P'R}{2m})^s \frac{1}{3+s}[(1-\lambda^2)^{1+s} - \sigma^{1-s}(\lambda^2-\sigma^2)^{1+s}] \right\} + \pi R^2 V_P(\lambda^2-\sigma^2) \quad (5.5)$$

- **Case II (no velocity gradient sign change)**

A schematic representation of the shear and velocity profiles when the velocity profile has no maximum or minimum in the annular region is shown in Figure 5-4. For this case, the equations proposed by Malik and Shenoy (Malik and Shenoy 1991) can be implemented for annular flow rate and velocity estimation. After adjusting for the velocity and pressure sign, theses equations can be written as:

$$V_z(\xi) = V_p \int_{\xi}^{1} (\Lambda'(\mathrm{x} - \lambda^2/x))^s dx \quad (5.6)$$

$$Q = 2\pi R^2 V_p (0.5[(\frac{n-1}{3n+1})\lambda^2 - k^2] + \frac{n}{2(3n+1)\Lambda'}\{[\Lambda'(1-\lambda^2)]^{1+s} - k^{1-s}[\Lambda'(k^2-\lambda^2)]^{1+s}\}) \quad (5.7)$$

Where $\Lambda' = [\mathrm{sgn}(V_p)^{1-n}\Delta PR/(2mL)](R/V_p)^n$ is the dimensionless pressure gradient, which may be positive or negative depending on the direction of pipe pull with respect to z in

Figure 5-4. In this equation, unlike equation (5.5), λ is a constant with no physical interpretation (Malik and Shenoy 1991).

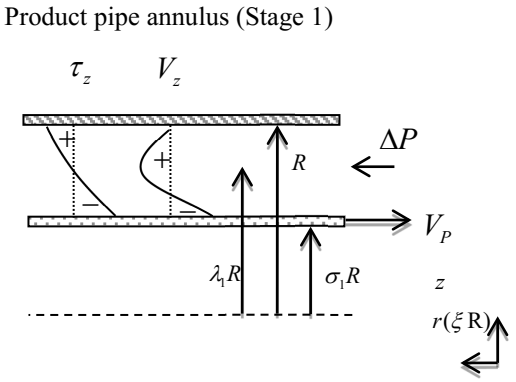

Figure 5-3- Schematic representation of velocity and shear stress profiles in a concentric annulus with velocity gradient sign change

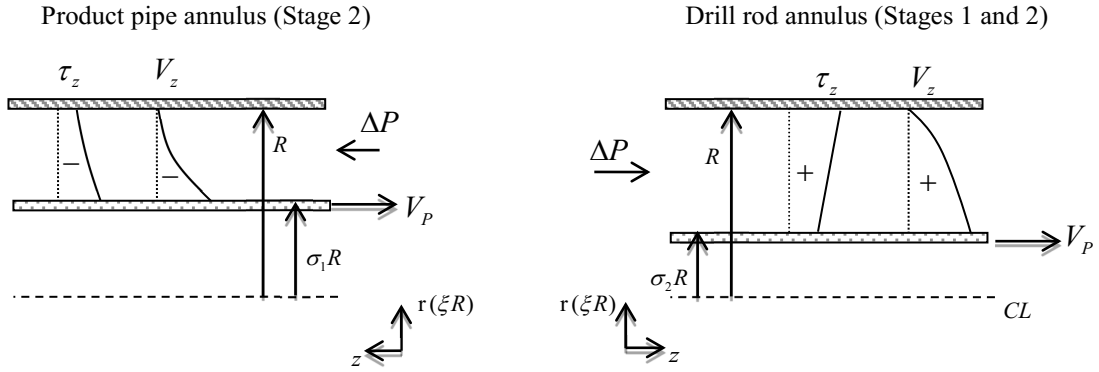

Figure 5-4- Schematic representation of velocity and shear stress profiles in a concentric annulus with no velocity gradient sign change

5-3-2- Governing Equations of Slurry Flow

Table 5-1 summarizes sets of coupled equations governing slurry flow within the product pipe-drill rod-bore system in each flow stage. The unknown parameters in each stage are $\lambda_1, \lambda_2, \Delta P$. In each set, the first two equations correspond to velocity profile boundary conditions in product pipe and drill rod annuli, respectively. The third equation is simply the continuity equation. Also, $Q_{dis}\,(\mathrm{m}^3/\mathrm{s})$ is the volume of slurry displaced by product pipe advancement into the bore per unit time with the value of $\pi R^2(\sigma_1^{\,2} - \sigma_2^{\,2}) \times \mathrm{V}_p$. After determining the unknown parameters for a desired pipe leading end location, the associated shear

stress developed on the product pipe's outer surface and resulting fluidic drag can be evaluated as (Chhabra and Richardson 2011):

$$\tau_z = (\frac{\Delta P}{L_1})\frac{R}{2}(\sigma_1 - \frac{\lambda_1^{\,2}}{\sigma_1}) \tag{5.8}$$

$$F = 2\pi\sigma_1 R \times L_1 \times \tau_z \tag{5.9}$$

To identify the location of boundary between stages one and two, the set of equations in Table 5-1 governing the first stage may be solved for the unknown in-bore pipe length, L_1, after setting $\lambda_1 = 1$ in the first equation. Having identified the boundary, each stage can now be divided into as many segments as needed to predict hydrokinetic pressure and drag force changes at a desired resolution.

Table 5-1- Coupled sets of equations governing slurry flow over each flow stage

Stage	Coupled equations
1	$V_{zi}(\xi = \lambda_1) = V_{zo}(\xi = \lambda_1)$ $V_z(\xi = \sigma_2) = V_p$ $Q_{pump} + Q_{dis} = Q_1 + Q_2$
2	$V_z(\xi = \sigma_1) = -V_p$ $V_z(\xi = \sigma_2) = V_p$ $Q_{pump} + Q_{dis} = Q_1 + Q_2$

All the presented equations have been coded using the MATLAB programming language, so hydrokinetic pressure and drag force changes can be simulated during a typical HDD pullback process. The code retrieves bore geometric parameters, Power-law model indices, slurry flow rate, and pipe pullback rate as input, and provides the user with hydrokinetic pressure and fluidic drag force changes versus pipe in-bore length.

The next section presents and discusses simulation results for two actual HDD installations obtained via the MATLAB code, which has been developed based on the proposed two-stage method.

5-4- Example Installations and Discussion

To verify the new proposed method, the pullback data for two actual HDD installations have been collected and compared against estimated pullback forces. Each job involved the installation of a large diameter steel pipe; the projects' contractor, The Crossing Company (TCC), employed the American Augers DD-440 heavy rig with the maximum thrust/pullback capacity of 1,900 kN for pulling the pipe string through the reamed hole. No anti-buoyancy technique was implemented during the installations. Table 5-2 summarizes the major parameters of each installation.

Table 5-2- Installations parameters

Parameter	Case 1	Case 2
Crossing length, m	998	604
Pipe O.D. , m	0.508 (20")	0.914 (36")
Pipe wall thickness, m	0.112	0.204
Borehole Dia., m	0.762	1.219
Drill rod O.D., m	0.140	0.140
Mud pump flow rate, m^3 / min	1.50	1.80
Pullback rate, m/min	7.32	7.32

5-4-1- Case 1

The bore profile of the first example crossing is depicted in Fig. 5. After taking samples of the returning drilling fluid and testing them using a standard six-speed viscometer on the project site, the Power-law rheological model was fitted to the test data, following the specified procedure in the American Petroleum Institute (API) 13D (2011). The calculated Power-Law model parameters are $n = 0.18$ and $m = 6.78\,Pa.Sec^n$.

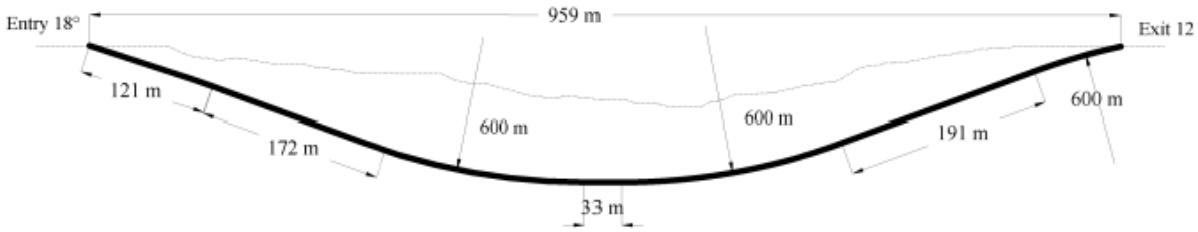

Figure 5-5- Case 1 bore profile

The boundary between the two stages is determined to be at L_1=325.33 m, which means slurry flows to the ground surface in front of the pipe and toward the pipe exit point over about two thirds of the bore length. This happens because the rod annulus is wider than the pipe annulus, causing the slurry to return to the surface over a significant length of the bore through the passage with less resistance to slurry flow, the rod annulus. Figure 5-6 shows the predicted flow rate changes moving through product pipe and drill pipe annuli, Q_1 and Q_2, respectively. At the initiation of pullback operations, all slurry reaches the ground surface through the pipe annulus as it offers the least resistance to flow passage. As operations continue, the flow rate within the pipe annulus (Q_1) drops and reaches zero at *L*=178.93 m. Thereafter, Q_1 becomes negative, indicating a change in slurry flow direction within the pipe annulus. In spite of change in Q_1 and Q_2 values, the total flow rate (solid line) remains constant due to the assumption that no fluid loss occurs during installation.

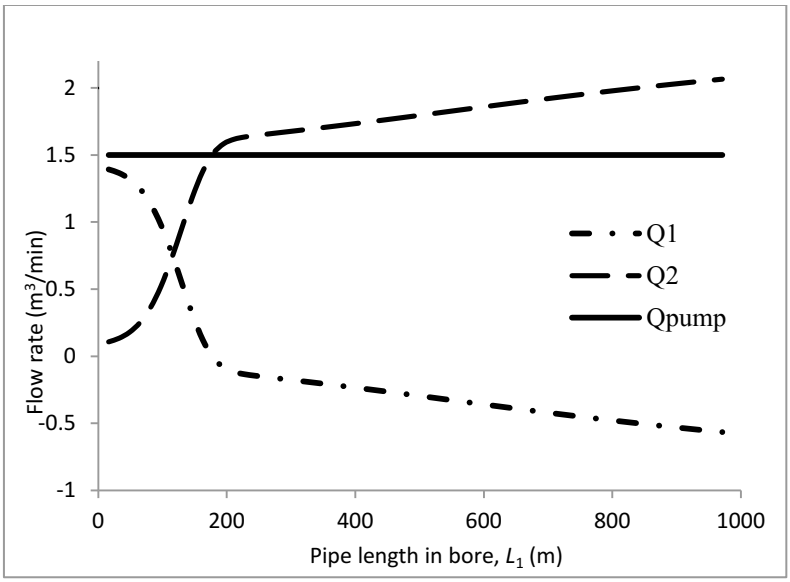

Figure 5-6- Estimated flow rates within pipe and rod annuli for Case 1

Figure 5-7 illustrates the fluidic drag and hydrokinetic pressure changes in one graph. The maximum predicted pressure and drag force in this figure are $\Delta P = 23.5 k\text{Pa}$ and $F = 12.68 k\text{N}$, respectively. It is should be noted that this pressure is about one third of the ASTM F1962 recommended value, 70 kPa. Overestimation increases with PRCI as it approximates the drag to be 549 kN, which is about 43 times larger than the two-stage method's prediction. This figure also illustrates how the fluidic drag is related to pressure change. Clearly, in contrast to the ASTM's assumption in equation (5.1), the fluidic drag is independent from hydrokinetic pressure value. The pressure is zero when the operation starts and peaks at L=227.7 m, and thereafter it keeps dropping until the end of installation, while the drag steadily increases through the pipe installation course.

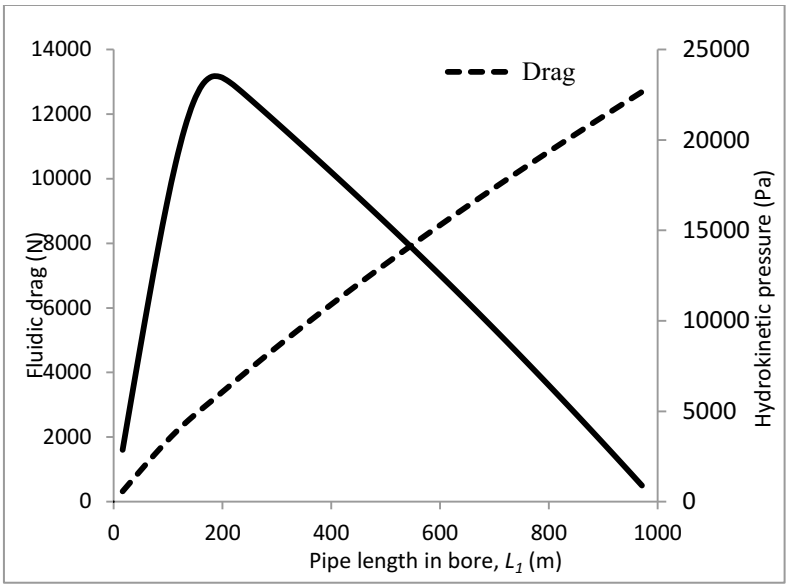

Figure 5-7- Hydrokinetic pressure and fluidic drag change for Case 1

By evaluating the pullback forces recorded at the rig location against those attained from the PRCI method, as shown in Figure 5-8, the proposed method can be substantiated. The proposed method and the PRCI method are very similar; each approach uses comparable equations for calculating frictional drag and weight components of the pullback force (Huey et al. 1996), as defined in PRCI, but the way in which they calculate fluidic drag is dissimilar.

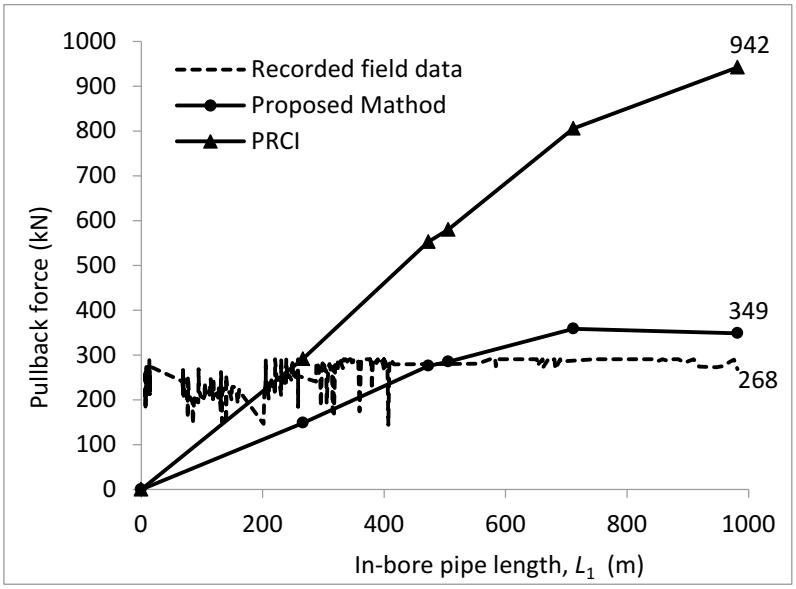

Figure 5-8- Estimated and recorded pullback forces for Case 1

Overall, the proposed method's approach proves to be a much closer match to the field measurements than that of the PRCI method, particularly during the second segment of the installation. The fluidic drag in the proposed method comprises just around 5% of the total pullback force, whereas in the PRCI method, fluidic drag is approximately double the recorded terminal pullback force. The large fluidic drag coefficient in equation (5.2), meant for determining the fluidic drag component, is what causes the PRCI method to miscalculate the pullback force. To refine the proposed method's pullback force estimation over the early stages of installation, the contribution of the out-bore portion of the pipe, pulled along the ground surface, can be considered.

5-4-2- Case 2

This installation involves traversing a pond and the 44-m wide Baseline Road in Edmonton, Alberta, Canada. The bore, with the profile provided in Figure 5-9, was drilled through layers of clay till, sandstone, and clay shale. After taking samples from the returning drilling fluid and testing them, the drilling fluid was identified as a Power-law fluid with $n = 0.17$ and $m = 8.14\, Pa.Sec^n$.

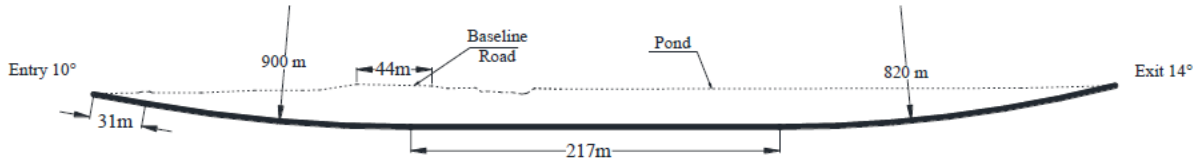

Figure 5-9- Case 2 bore profile

Figure 5-10 shows the estimated flow rates moving within pipe and rod annuli during the pipe installation operation. The boundary between two stages is determined to be at L_1= 135.49 m. Similar to Case 1, Q_1 drops sharply as the installation proceeds and the total volume of drilling fluid being circulated in the bore, $Q_1 + Q_2 = 1.8\ m^3/\min$, remains constant through the pipe pullback operation. $\Delta P = 23.5\, k\text{Pa}$.

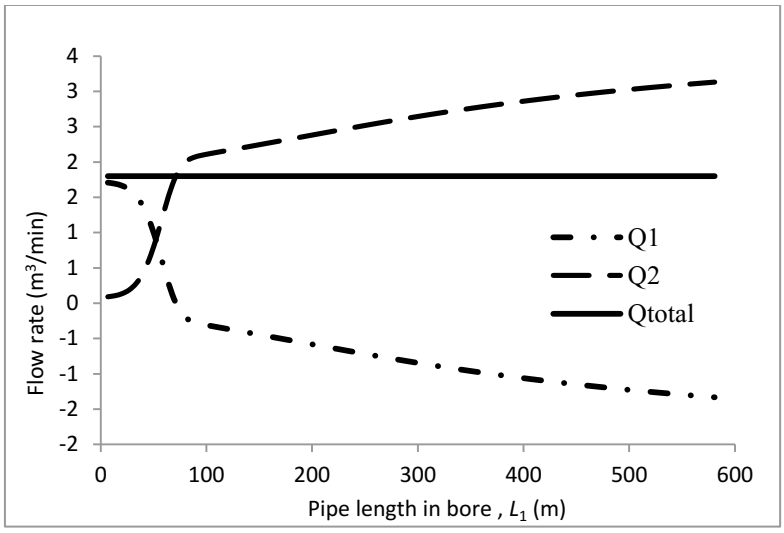

Figure 5-10- Estimated flow rates within pipe and rod annuli for Case 2

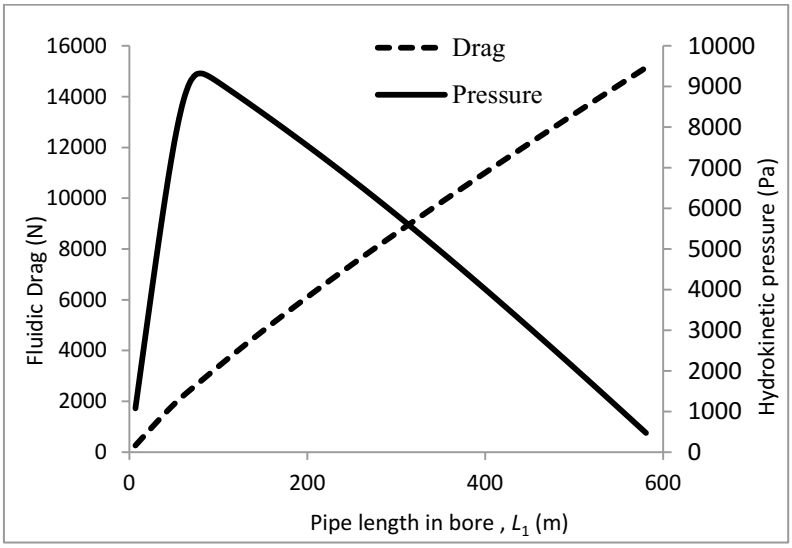

Figure 5-11- Hydrokinetic pressure and fluidic drag change for Case 2

Compared to Case 1, this installation is about 400 m shorter and has a bore that is 0.40 m larger. As a result, considering the small difference between Case 1 and Case 2 mud pump flow rates, less effort is required to circulate the drilling fluid through the system, as shown in Figure 5-11. The fluidic drag increases in a linear fashion from the initiation of the pullback and reaches its maximum, 15.15 kN, when the pipe emerges from the ground. The estimated maximum hydrokinetic pressure is 9.32 kPa, 60% less than the corresponding value for Case 2, when L_1=81.30 m.

The recorded pullback forces and the estimated ones, using the proposed and PRCI methods, are presented in Figure 5-12. The estimated end pullback force by the proposed method, 486 kN, is just 7.43% smaller than the recorded value, whereas this value rises to 85% for the PRCI method. This clearly shows the ability of the new proposed method in estimating the pullback forces is more promising than the PRCI.

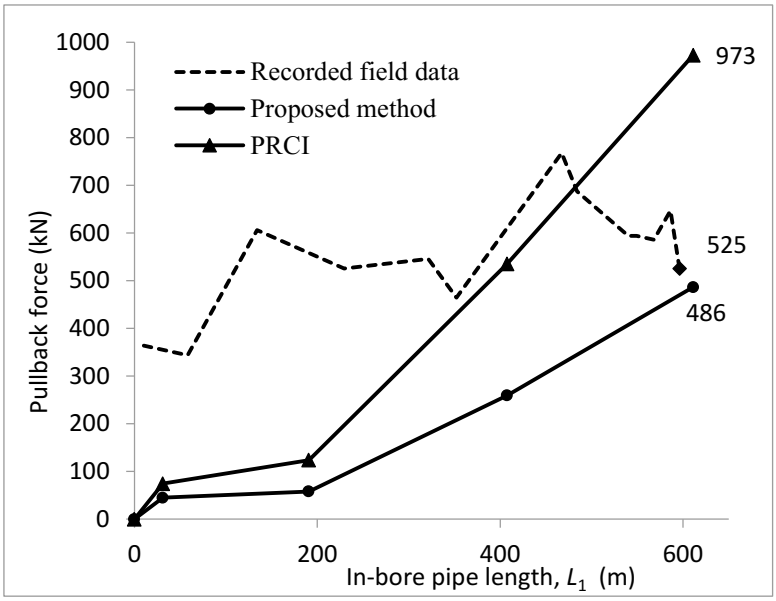

Figure 5-12- Estimated and recorded pullback forces for Case 2

5-5- Conclusions

This paper proposes a new method for evaluating the hydrokinetic pressure and fluidic drag changes during pullback operation in HDD pipe installation projects, assuming the slurry is a Power-law fluid. The method is based on identifying two different stages of slurry flow pattern along the bore-hole and solving the governing sets of coupled equations for desired pipe pulling head locations at each stage. For verification of the proposed method, the pullback data of two actual HDD projects are compared against forces estimated using the proposed and PRCI methods. The differences between recorded and proposed method estimated pullback forces are 30% and 7%, for installations Case 1 and Case 2, respectively. While using the PRCI method, these values rise to 238% and 85%. This over conservatism of the PRCI method is due to overestimating the contribution of the fluidic drag component of pullback force, which can be avoided by implementing the new proposed method.

In contrary to ASTM F 1962 recommendation, it has been observed that the fluidic drag is independent from the hydrokinetic pressure and varies linearly with in-bore pipe length. At the initiation of the pullback, the drag is zero and it reaches the maximum at the moment the pipe emerges from the ground surface on the opposite end of the bore. Also, for the two presented actual installations, the maximum estimated hydrokinetic pressures are less than the 70 kPa recommended value by ASTM.

6- Chapter 6: Fluidic Drag Estimation in Horizontal Directional Drilling using Finite Volume Method [4]

6-1- Introduction

As one of the fastest growing trenchless techniques for pipe installation, Horizontal Directional Drilling (HDD) has gained attention from both industry and academia over the past few decades (Najafi and Gokhale 2005). This growth in popularity can be attributed to HDD's ability to provide a practical solution to factors such as costs associated with traffic disturbance in congested urban areas and strict environmental regulations regarding utility placement across rivers and wetlands (Willoughby 2004). The technique causes minimal damage to the surrounding environment and disruption to ground surface traffic, making it a promising solution for pipe placement in high risk areas. An HDD project typically includes three main phases: first, a steerable and tractable driller creates a pilot bore; second, the pilot hole is enlarged to a diameter greater than the product pipe; and third, the product pipe is pulled into the enlarged bore (Najafi and Gokhale 2005).

In spite of HDD's growth in popularity, the interaction of the installed pipe with the surrounding soil and slurry medium during pipe installation phase is not well understood, leading to conservative pipe design (Baumert et al. 2005). Due to a lack of relevant investigations, current HDD design references rely on studies completed in other industries, like oil well directional drilling and utility cable installation industries (Slavin and Petroff 2010) Subsequently, in design references such as ASTM F1962 (2011) and Pipeline Research Council International (PRCI) (Huey et al. 1996), unique HDD characteristics are sometimes ignored. One area requiring investigation is evaluation of hydrokinetic pressure and fluidic drag during the pipe placement phase, which is the focus of this study. Hydrokinetic pressure is the minimum in-bore pressure at the location of drilling fluid discharge from drill string into the bore in addition to the hydrostatic pressure. This incremental pressure must be maintained during pullback operations to exhaust the slurry from the bore to the surface at a desired flow rate. This helps maintain bore stability, lubricate the bore wall, and transport residual cuttings created in the reaming or swabbing phase. Fluidic drag is the incremental force developed on pipe leading end

[4] A version of this chapter has been accepted for publication in the Journal of Pipeline Engineering.

during installation due to slurry interaction with the in-bore portion of the pipe. Similar to the frictional drag component of the pullback force, this component also resists pipe installation.

In oil well drilling operations, the drilling fluid is pumped from the ground-mounted rig down into the drill string. After being discharged from the nozzle and getting mixed with cuttings, the resulting slurry flows back from the well bottom to the ground surface through the annular space between the drill string and the well. In terms of the slurry flow pattern, this process resembles the pilot bore drilling phase, where the total slurry volume within annular space flows in a direction opposite to the pipe movement throughout the operation. During the pullback phase, however, since the total bore length has already been reamed to its final diameter, the slurry exits to the ground surface through the product pipe and/or drill rod annuli depending on the product pipe leading head location. Similarly, lightweight utility cable installation via the blown-cable technique (Slavin 2009), which is the basis of current ASTM F1962 fluidic drag evaluation (Slavin and Petroff 2010), observes annular flow in a singular direction during installation.

Adopting the equation used to determine drag force exerted on a utility cable's outer surface, the ASTM F1962 recommends using the following simple equation for estimating the fluidic drag (ASTM F1962 2011):

$$F = \Delta P \frac{\pi(r_b^{\,2} - r_P^2)}{2} \tag{6.1}$$

where r_b (m) and r_P (m) are the radii of the bore and pipe, respectively, and ΔP (Pa) is the hydrokinetic pressure. The ASTM F1962 estimates the hydrokinetic pressure (ΔP) to be 70 kPa without any qualification. This equation does not provide any information on drag change with installation progress, and the effects of slurry rheology are also implicitly considered in the pressure value. PRCI does not provide an estimate for the hydrokinetic pressure. However, it proposes determining the fluidic drag by multiplying the pipe's outer surface area in contact with the slurry by a fluidic drag coefficient as follows:

$$F = 2\pi r_P L_1 \mu_{mud} \tag{6.2}$$

where, L_1 (m) is the in-bore length of the product pipe and μ_{mud} (Pa) is the fluidic drag coefficient with a value of 350 Pa adopted from the Dutch standard NEN 3650, Requirements for Pipeline Systems (NEN 2007). Contrary to the ASTM F1962, the estimated drag by PRCI

evolves with installation progress; however, the effects of slurry rheology and annulus size are ignored.

To estimate the fluidic drag component of pullback force, Polak and Lasheen (2001) implemented the solution of Navier-Stokes' equation (Constantin and Foias 1988) in cylindrical coordinate for flow of incompressible Newtonian fluids. In the proposed solution, the pipe pullback rate and the annulus geometry were considered. The main shortcoming of their work is the assumption that the entire drilling fluid volume returns to the surface through the space between pipe and borehole wall in the opposite direction of pipe pull; this is applicable to oil well drilling operations, but not HDD.

Baumert et al. (2005) reviewed existing methods for hydrokinetic pressure evaluation during the HDD installation phase and provided recommendations to improve the current design practice. Supposing the slurry to behave as a Bingham Plastic fluid, they concluded that slot flow approximation could be adopted for pressure drop modeling; however, some improvements, such as introducing a factor for pipe eccentricity inclusion and using low shear rate mud rheological parameters, were suggested to improve accuracy. The adopted equations for pressure drop estimation in this study were originally from the oil well drilling industry (N.L. Baroid 1998), and the authors implemented them without making any adjustment to account for different flow patterns observed in HDD pipe installation.

In an attempt to model the fluidic drag component of the pullback force more realistically, Dyvestyn (2009) also implemented the slot flow approximation but considered slurry flow direction change during the pullback (pipe installation) phase. He assumed that in an installation, with the pipe leading head between the pipe entry and crossover points, the total slurry volume flows to the surface through annular space between the product pipe and bore. Then, once the crossover point has been reached, the slurry flow direction switches, and the slurry moves in front of the product pipe toward the rig. To determine the crossover point location, the hydrokinetic pressure required for exhausting the slurry via product pipe and drill rod annuli were calculated in terms of in-bore pipe length. After equating these pressures and solving for the in-bore pipe length, the crossover point was calculated. The major shortcoming of this study was ignoring the fact that, in a typical installation, over a considerable length the slurry returns to

the surface through the both product pipe and drill rod annular spaces. Furthermore, the pullback rate effects were not considered.

This paper introduces a new method for determining the fluidic drag based on using Finite Volume Method (FVM) for solving the governing partial differential equation of fluid motion in an eccentric annulus. This method, unlike the ASTM and PRCI methods, considers the effect of different parameters, including the geometry of product pipe and drill rod annuli, pullback rate, pipe eccentricity, and slurry rheology, making it a promising tool for accurate pipe-slurry interaction modeling. The new method enables the HDD designers to simulate and follow the hydrokinetic pressure and fluidic drag changes with installation progress. Furthermore, it equips the HDD contractors and field crew with a tool to estimate the gradual pattern change of drilling fluid return to the surface with installation progress, which is an important feature of the new method from the drilling fluid circulation management point of view.

6-2- Proposed Method

During the pullback phase of a typical HDD operation, the amount of drilling fluid pumped from the ground-mounted rig down into the bore through the drilling rod is known and often maintained during the installation course. In contrast, the distribution of this flow rate between the two drilling fluid return passages, namely pipe annulus and rod annulus as shown in Figure 6-1, is not known and needs to be determined. The proposed method for estimating the hydrokinetic pressure and fluidic drag in this paper is based on solving the continuity equation of drilling fluid flowing within the borehole. To estimate the volume of drilling fluid flowing within either pipe annulus or rod annulus, the problem of fluid motion within an eccentric annulus first needs to be solved. In the next section of the paper, a numerical method for solving the problem of eccentric annular flow is presented. Then, based on applying this numerical method to pipe and drill rod annuli, a procedure for estimating fluidic drag and hydrokinetic pressure changes with installation progress will be introduced.

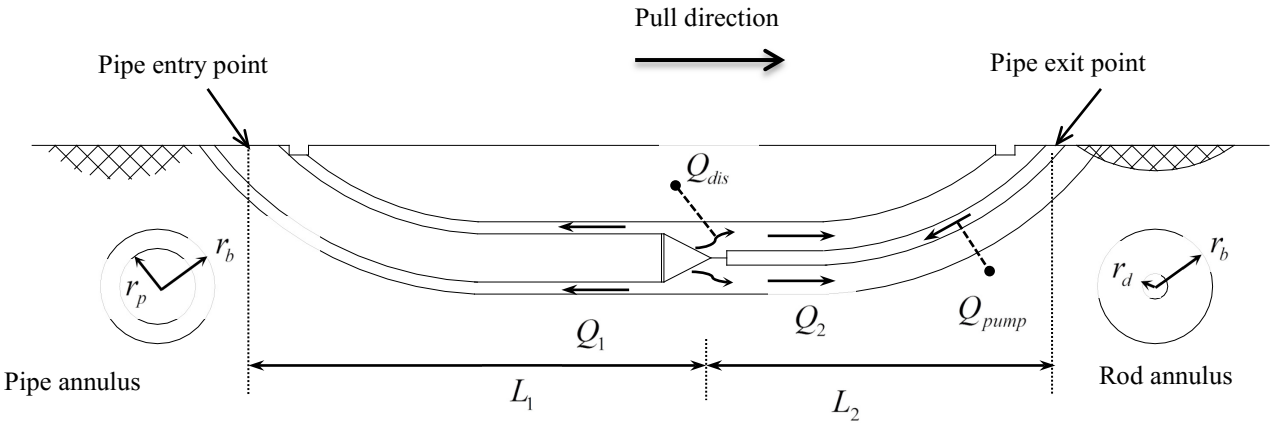

Figure 6-1- A schematic of drilling fluid flow pattern within a bore during HDD pullback operation

6-2-1- Eccentric Annular Flow

For a steady, laminar flow of an incompressible fluid through an eccentric annulus, the governing partial differential equation of motion in bipolar coordinates is given by (Haciislamoglu 1989):

$$(\frac{a}{\psi})^2 \frac{\Delta P}{\Delta L} + \frac{\partial}{\partial \varepsilon}(\mu \frac{\partial v}{\partial \varepsilon}) + \frac{\partial}{\partial \eta}(\mu \frac{\partial v}{\partial \eta}) = 0 \tag{6.3}$$

where v (m/ sec) is the fluid annular velocity, ε and η (rad) are the polar coordinates as shown in Fig. 2, $\frac{\Delta P}{\Delta L}$(Pa/ m) is the pressure drop per unit length through the annulus, and μ(Pa .Sec) is the fluid viscosity. Also,

$$a = r_i \sinh \varepsilon_i = r_0 \sinh \varepsilon_0 \quad (\varepsilon_0 \le \varepsilon \le \varepsilon_i,\ 0 \le \eta \le 2\pi) \tag{6.4}$$

$$\psi = \cosh \varepsilon - \cos \eta \tag{6.5}$$

where r_i (m) and r_o (m) are the radii of the inner and outer cylindrical surfaces, respectively, and ε_i and ε_0 are the corresponding bipolar coordinates, which can be calculated from the following equations:

$$\varepsilon_i = \cosh^{-1}[\frac{(1+S) - e^2(1-S)}{aeS}] \tag{6.6}$$

$$\varepsilon_o = \cosh^{-1}[\frac{(1+S)-e^2(1-S)}{ae}] \tag{6.7}$$

where S is the radius ratio and e is the dimensionless eccentricity given by:

$$S = \frac{r_i}{r_o} \tag{6.8}$$

$$e = \frac{\delta}{r_o - r_i} \tag{6.9}$$

where $\delta\,(\mathrm{m})$ is the distance between the centers of the two circles bounding the annulus.

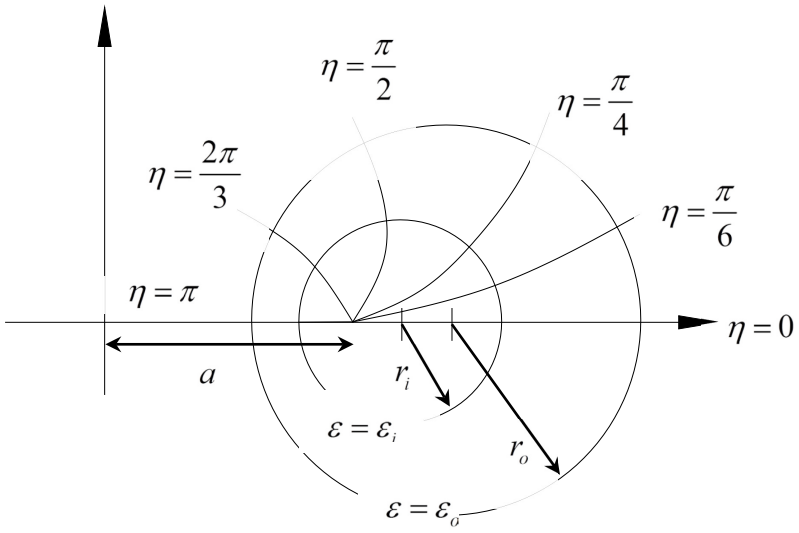

Figure 6-2- Eccentric annulus in bipolar coordinates

After dimensions analysis, equation (6.3) can be rewritten as:

$$(\frac{\sinh\varepsilon_o}{\psi})^2 f + \frac{\partial}{\partial\varepsilon}(\mu_D \frac{\partial V_D}{\partial\varepsilon}) + \frac{\partial}{\partial\eta}(\mu_D \frac{\partial V_D}{\partial\eta}) = 0 \tag{6.10}$$

where V_D is the dimensionless velocity and f is the dimensionless pressure drop gradient, and they are defined as:

$$V_D = \frac{v}{(\frac{K}{\rho r_o^n})^{\frac{1}{2-n}}} \tag{6.11}$$

$$f = \frac{\frac{\Delta P}{\Delta L}}{(\frac{K^2}{\rho^n r_o^{n+2}})^{\frac{1}{2-n}}} \tag{6.12}$$

where $K\,(\mathrm{Pa.Sec}^n)$ and n are the consistency and flow indices in the Herschel-Bulkley (H-B) rheological model defined as (Chhabra and Richardson 2011):

$$\tau = \tau_0 + K\gamma^n \tag{6.13}$$

In this equation, $\tau_0\,(\mathrm{Pa})$ is the fluid yield stress. For fluids with zero yield stress, the equation reduces to the conventional Power-law fluid model. The dimensionless viscosity (μ_D) is given by:

$$\mu_D = (\frac{\rho^{n-1} r_o^{2n-2}}{K})^{\frac{1}{2-n}} \mu \tag{6.13}$$

The partial differential equation of fluid motion, equation (6.10), must be solved to calculate the velocity distribution. For this purpose, the common Finite Volume Method (FVM) is implemented in this study (Haciislamoglu 1989). In this method, first the annulus is divided into a network of grids, and then the equation of motion is discretized by assuming a profile for velocity change across neighboring grid points. Afterwards, through an iterative procedure, the initial estimated annular velocity field is refined until the desired convergence is achieved. During the refinement process, the boundary conditions need to be satisfied as well, which are $v = 0$ at bore surface and $v = V_p$ at pipe surface.

Having calculated the dimensionless velocity distribution, the flow rate, $Q\,(\mathrm{m}^3/\mathrm{Sec})$, can be determined by numerically integrating the normalized velocity over the annular space as:

$$Q_D = \int_0^{2\pi} \int_{\varepsilon_0}^{\varepsilon_i} V_D (\frac{\sinh \varepsilon_0}{\psi})\, \partial\varepsilon\, \partial\eta \tag{6.15}$$

$$Q = r_0^2 (\frac{K}{\rho r_0^n})^{\frac{1}{2-n}} Q_D \tag{6.16}$$

where Q_D is the dimensionless flow rate. To determine the fluidic drag per unit length of the annulus ($F\,[\mathrm{N/m}]$), the shear stress developed on the pipe can be integrated as:

$$F_D = \int_0^{2\pi} \tau_D \partial\eta \left(\frac{\sinh \varepsilon_0}{\psi}\right) \tag{6.17}$$

$$F = \left(\frac{K^2}{\rho^n r_0^{4n-4}}\right)^{\frac{1}{2-n}} F_D \tag{6.18}$$

where $\tau_D = \gamma_D \, \mu_D$ is the normalized shear stress. The normalized shear rate (γ_D) is given by:

$$\gamma_D = \left| \psi \sqrt{\left(\frac{\partial V_D}{\partial \varepsilon}\right)^2 + \left(\frac{\partial V_D}{\partial \eta}\right)^2} \right| \tag{6.19}$$

Based on the above presented relations, a function called flow rate has been developed in MATLAB programming language. The flow rate function takes the annulus geometry, mud rheological parameters, and the pressure drop gradient as an input, then returns the estimated annular velocity and shear stress distribution, annular flow rate, and the fluidic drag as an output using FVM.

6-2-2- Continuity Equations Solution

During the pullback phase of an HDD installation, assuming the drilling fluid loss to be zero, the following continuity equation always holds:

$$Q_{pump} + Q_{dis} = Q_1 + Q_2 \tag{6.20}$$

where $Q_{pump}\,(\mathrm{m}^3/\mathrm{Sec})$ is the drilling fluid flow rate pumped from the rig into the bore and $Q_{dis} = \pi R^2 (\sigma_1^{\,2} - \sigma_2^{\,2}) \times \mathrm{V}_p \;\; (\mathrm{m}^3/\mathrm{Sec})$ is the volume of slurry displaced as a result of product pipe advancement into the bore per unit time. In the latter, $\mathrm{V}_p\,(\mathrm{m/Sec})$ is the pipe pullback rate. Also, $Q_1\,(\mathrm{m}^3/\mathrm{Sec})$ and $Q_2\,(\mathrm{m}^3/\mathrm{Sec})$ are the flow rates of the returning drilling fluid via pipe annulus and rod annulus, respectively. The drilling fluid flow pattern in an HDD pullback operation is schematically depicted in Figure 6-1.

To determine the fluidic drag and in-bore hydrokinetic pressure changes during a pullback operation, the continuity equation needs to be solved for desired pipe leading head locations (L_1) along the bore path. In a typical installation, the values of Q_{pump} and Q_{dis} are often known and kept fixed throughout, while the values of Q_1 and Q_2 need to be calculated. For this purpose, a

MATLAB code has been developed to solve the continuity equation. The code uses the flow rate function discussed in the previous section to estimate the annular flow rates moving within pipe and rod annuli, or Q_1 and Q_2 . Because these flow rates depend on the unknown in-bore hydrokinetic pressure drop gradient ($\Delta P/\Delta L$), implementing an iterative procedure to find a pressure gradient that satisfies equation (6.3) is inventible.

To simulate the drilling fluid's return pattern change with installation progress, first the MATLAB code divides the bore path into several segments and determines the Q_{dis}. The number of segments corresponds to the user's desired precision of fluidic drag and/or hydrokinetic pressure variations monitor. Afterwards, for every point on the segments' boundaries, representing a product pipe leading head location in the bore, the following steps are taken:

1- Guess the hydrokinetic pressure, ΔP.
2- Calculate the pressure drop gradient along the product pipe annulus, $\Delta P/L_1$, and drill rod annulus, $\Delta P/L_2$.
3- Call the flow rate function and determine Q_1 and Q_2.
4- Check for convergence by comparing the right and left sides of equation (6.20).
5- If necessary, adjust the hydrokinetic pressure and repeat from step 2 onward. Otherwise, proceed to step 6.
6- Save the calculated hydrokinetic pressure, fluidic drag, and Q_1 and Q_2.

For the initial guess of hydrokinetic pressure in step (1), simple solutions to the drilling fluid flow problem such as those based on slot representation of the annular spaces (Baumert et al. 2005; Duyvestyn 2009) may be used. Next section discusses the simulation results obtained from the code for two example installations. Then, effects of pipe eccentricity in the bore on the estimated hydrokinetic pressure and drag values are investigated.

6-3- Example Installations and Discussion

To verify the new proposed method, the pullback data of two actual HDD installations have been collected and compared against the method proposed in this paper, which is based on implementing FVM simulation for estimating the fluidic drag component of pullback force. Both projects involved installing large diameter steel pipes. The projects' contractor, The Crossing Company, employed the American Augers DD-440 heavy rig for pullback operation with the maximum thrust/pullback capacity of 1,900 kN. During the installations, no anti-buoyancy technique was implemented. Table 6-1 summarizes the major parameters of each installation.

Table 6-1- Installations parameters

Parameter	Case 1	Case 2
Crossing length, m	998	604
Pipe outer diameter, m	0.508 (20")	0.914 (36")
Pipe wall thickness, m	0.112	0.204
Borehole diameter, m	0.762	1.219
Drill rod outer diameter, m	0.140	0.140
Mud pump flow rate, m^3/min	1.50	1.80
Pullback rate, m/min	7.32	7.32

6-3-1- Case 1

The bore profile of the crossing is depicted in Figure 6-3. After taking samples of the returning drilling fluid and testing them using a standard six-speed viscometer on the site of the project, H-B and Power-law rheological models were fitted to the test data. The fitting was done following the recommended procedure in the American Petroleum Institute (API) 13D (2011). The viscometer data, as well as the two fitted rheological models, are shown in Figure 6-4. For

clarity and due to the importance of low shear rate data on estimated values, the low shear rate portion of data is plotted separately in Figure 6-4(b).

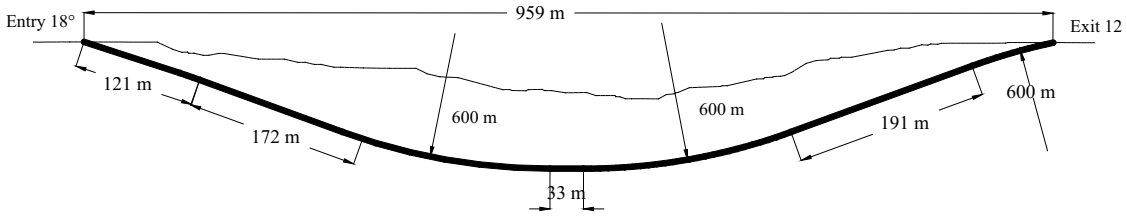

Figure 6-3- Case 1 bore profile

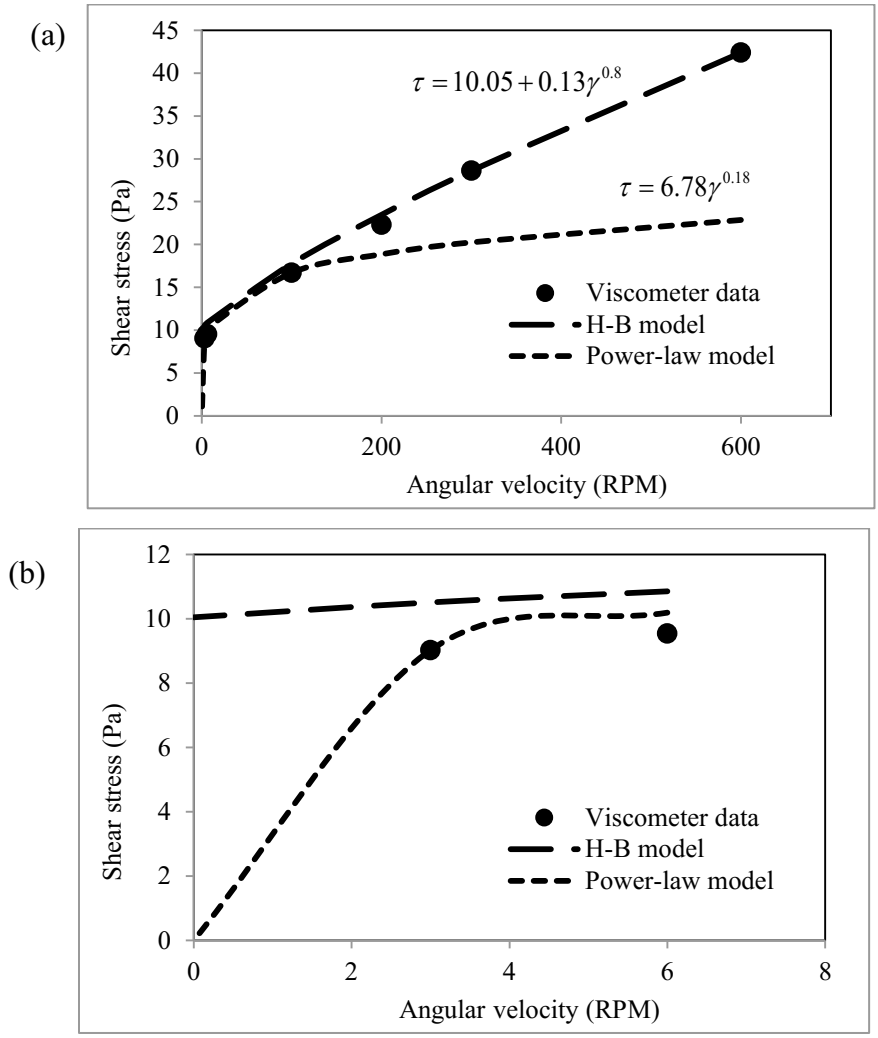

Figure 6-4- Viscometer test data and fitted rheological models: (a) full data range, (b) low shear rate range

As an example, the velocity, shear rate, and shear stress distributions in the pipe annulus when $L_1 = 50$ m are presented in Figure 6-5. In this figure, x and y are axes of a Cartesian coordinate system with the origin placed at the center of the annulus. Evidently, a large region in the middle of the annulus is moving at a uniform velocity of 5.40 m/min, dominating the velocity graph. This region is the unsheared plug of an H-B fluid (Chhabra and Richardson 2011), where the shear rate is zero, as shown in Figure 6-5(b). This large plateau formation is observed due to pumping a drilling fluid with a large yield stress at a relatively low flow rate ($1.50\ \mathrm{m}^3/\mathrm{min}$). The maximum estimated shear stress is 15.85 Pa and observed on the pipe's surface, where the shear rate is maximum (143.4 1/Sec).

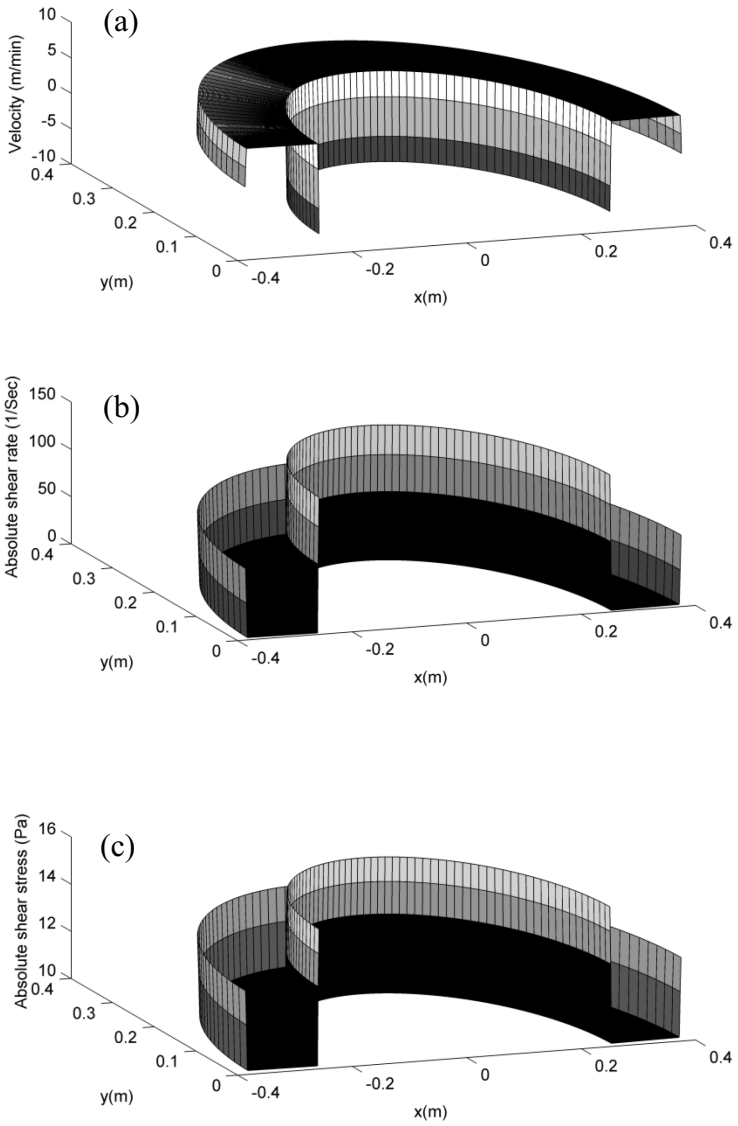

Figure 6-5- (a) Velocity, (b) absolute shear rate, and (c) absolute shear stress distributions in pipe annulus at L1=50 m for H-B fluid.

Figure 6-6 shows the simulation results for the case of Power-law fluid at the same location in the bore. The maximum estimated velcoity is 6.40 m/min, 18% higher than the H-B model estimation, and it decreases to -7.32 m/min at the pipe's surface. This drop in velocity happens at lower rates compared to the H-B model, which reults in smaller shear rates and shear stresses in Figure 6-6(b) and (c), respectively. The maximum estimated shear stress is 12.15 Pa, which is 23% less than the corresponing value in Figure 6-5(c).

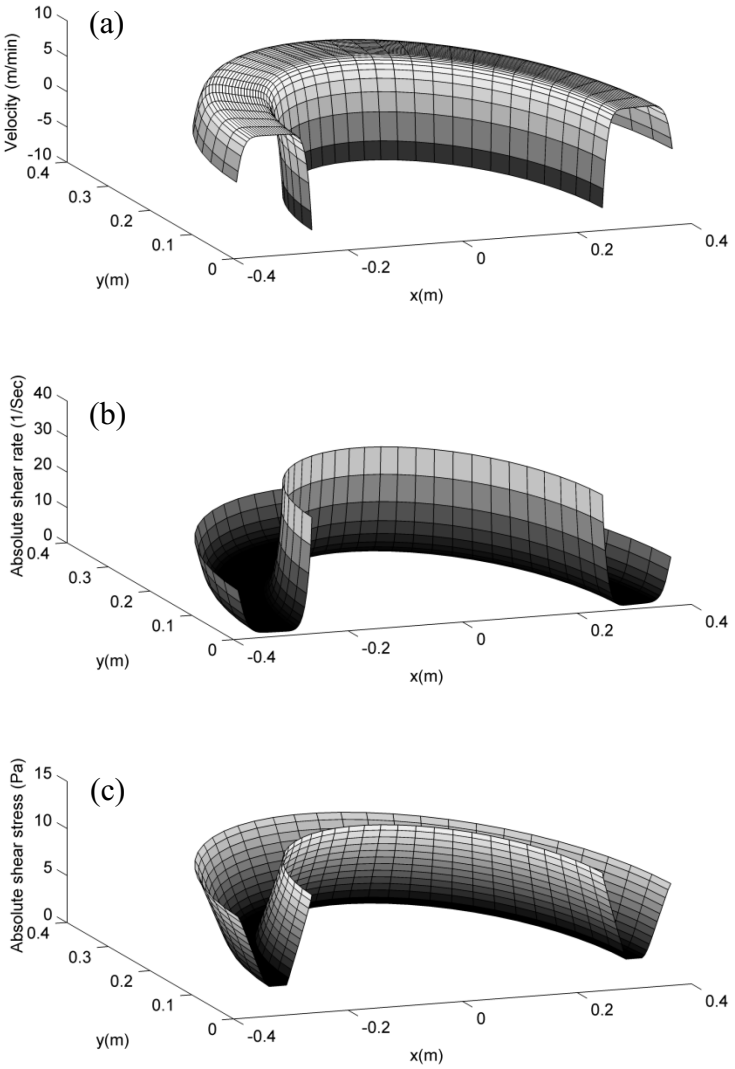

Figure 6-6- (a) Velocity, (b) absolute shear rate, and (c) absolute shear stress distributions in pipe annulus at L1=50 m for Power-law fluid.

The flow rate history of drilling fluid returning to the surface via product pipe and drill rod annuli is presented in Figure 6-7. While $Q_1 + Q_2$ remains constant and equal to $Q_{pump} + Q_{dis}$ over the installation course, Q_1 and Q_2 values are changing as a result of change in resistance to drilling fluid flow within the corresponding fluid return passages. During early stages of installation, the drill string in-bore end, where the drilling fluid discharges into the bore, is close to the pipe entry point (Figure 6-1). Therefore, it is easier for the fluid to exhaust via the pipe annulus rather than taking the longer rod annulus path. As the installation proceeds, the in-bore

length of pipe, or the resistance to drilling fluid return through pipe annulus, grows and Q_1 consequently drops. Concurrently, the resistance along the drill rod annulus is decreasing, causing an increase in Q_2. From a drilling fluid return management point of view, it is important to properly estimate the time of drilling fluid return termination ($Q_1 = 0$) through the pipe annulus so necessary measures can be taken ahead of collecting and recycling the drilling fluid. The Power-law model estimates this happens when L_1=200 m, while the H-B model estimates this happens 480 m farther into the bore at $L_1 = 680$ m. This demonstrates the importance proper drilling fluid rheological characterization has in estimating the drilling fluid flow pattern during the pipe installation process. At the end of the installation, the Power-law model estimated annular flow rate within the pipe annulus is $-0.53\ \mathrm{m^3/min}$, which is significantly larger than the H-B model's $-0.07\ \mathrm{m^3/min}$ estimation. This behaviour results from the fact that the tendency of fluids with large yield point–to-flow is less than corresponding Power-law fluids.

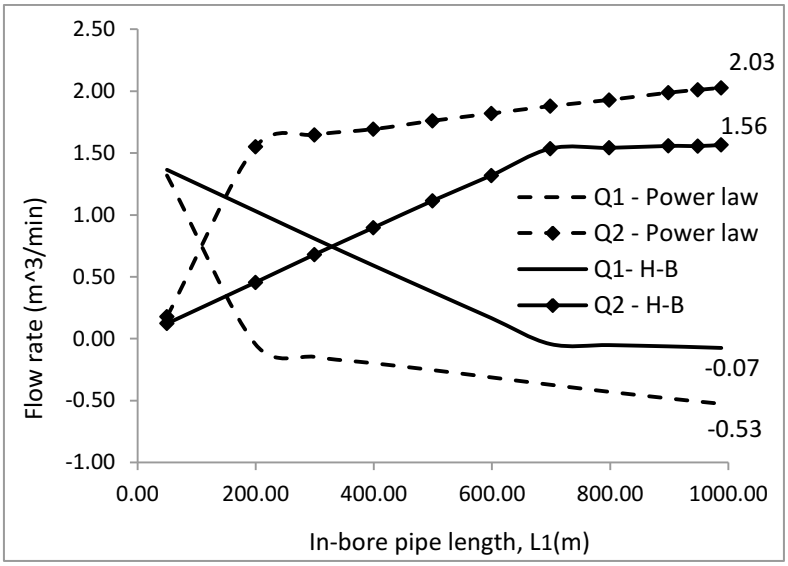

Figure 6-7- Estimated flow rate within pipe and rod annuli for Power-law and H-B fluid models.

Figure 6-8 depicts how the hydrokinetic pressure changes with installation progress. Both graphs follow the same pattern: the pressure increases with installation progress until it peaks at approximately $L_1 = 200\,\mathrm{m}$, and thereafter it drops steadily to zero as the pipe leading end reaches the bore opposite end. The maximum pressure estimated by the H-B model is $103.46\,\mathrm{kPa}$, which

is significantly larger than the Power-law model estimation. This pressure is 48% higher than the ASTM suggested value of 70 kPa, showing the standard's non-conservative approach in estimating the hydrokinetic pressure.

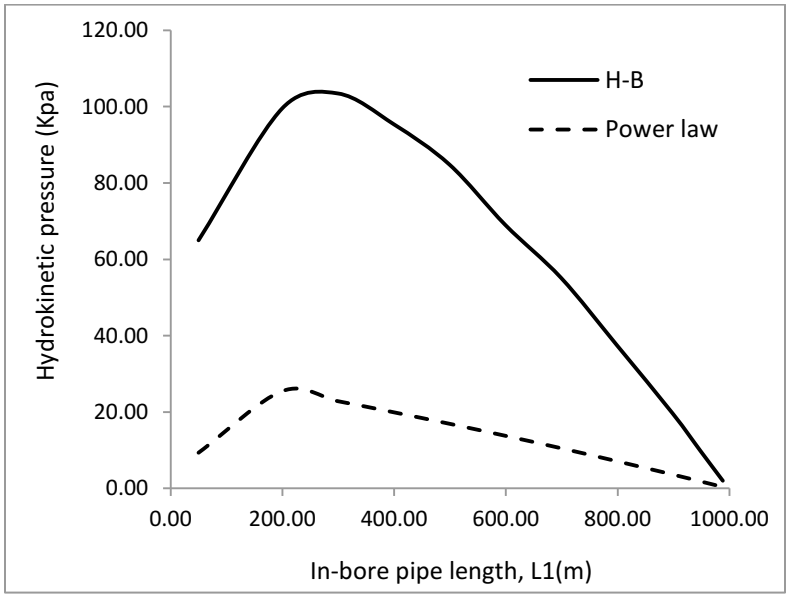

Figure 6-8- Estimated hydrokinetic pressure for Power-law and H-B fluid models.

Figure 6-9 demonstrates the fluidic drag changes versus installation progress. All methods suggest that the drag reaches its maximum when the pipe leading emerges from the ground, with the difference being that the PRCI estimations are notably larger. The maximum estimated drag by the FVM for both fluid models is less than 5% of PRCI estimation, showing the overly conservative approach of PRCI in estimating the fluidic drag, which is aligned with the findings of previous studies (Puckett 2003; Baumert et al. 2005). Using the ASTM recommended procedure (equation (6.1)), the drag is calculated as 9.42 kN, which is much closer to the FVM simulation results compared to the PRCI. In contrary to the PRCI and proposed methods, the ASTM considers the drag to be independent of the installation progress and, therefore, the estimated drag force is constant over the whole installation course.

To verify the new proposed method, the pullback forces recorded on the project site at the rig location are compared against those obtained from the PRCI method and FVM, as presented in Figure 6-10. The only difference between the PRCI and proposed methods is in the way each method calculates the fluidic drag, while for the frictional drag and weight components of the pullback force, both methods use similar equations as outlined in the PRCI (Huey et al. 1996).

To generate the proposed method graph in Figure 6-10, the HB model results are utilized for the fluidic drag component of pullback force.

Compared to the PRCI, it is evident that the proposed method estimation, especially over the second half of the installation, matches the field measurements better. The PRCI fluidic drag is about two times larger than the recorded terminal pullback force, while in the proposed method, the drag accounts for only about 6% of the total pullback force. This failure of PRCI in estimating the pullback force is associated with the large fluidic drag coefficient (μ_{mud} in equation (6.2)) utilized for calculating the fluidic drag component.

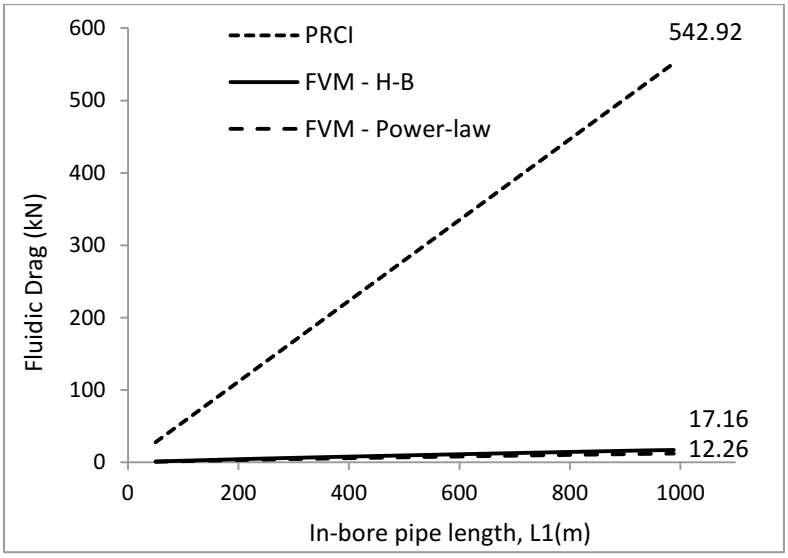

Figure 6-9- Estimated fluidic drag by FVM and PRCI method

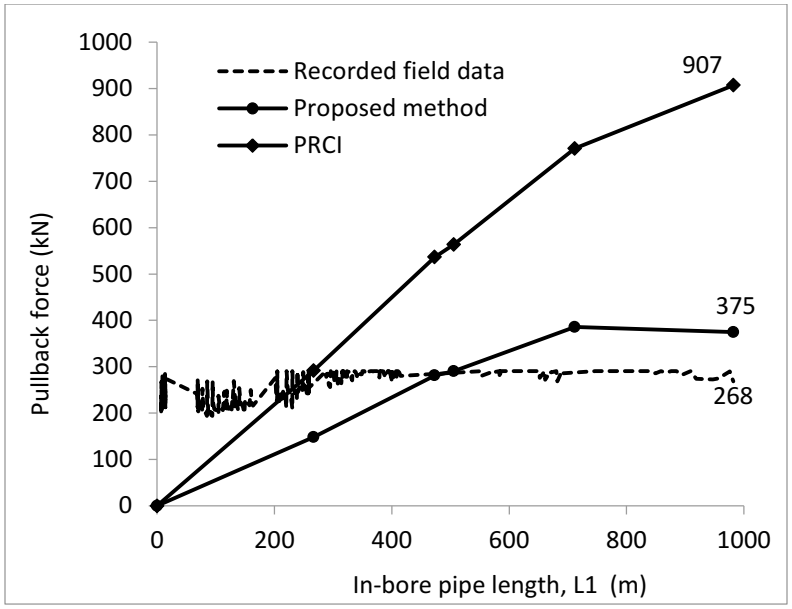

Figure 6-10- Estimated and recorded pullback forces

6-3-2- Case 2

This installation involves traversing a pond and the 44-m wide Baseline Road in Edmonton, Alberta, Canada. The bore, with the profile provided in Figure 6-11, was drilled through layers of clay till, sandstone, and clay shale. The viscometer test results as well as the fitted rheological models are presented in Figure 6-12.

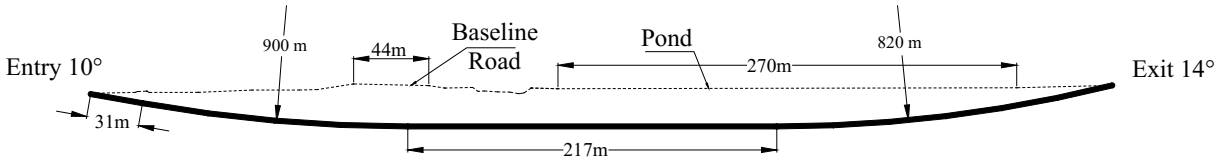

Figure 6-11- Case 2 bore profile

(a)

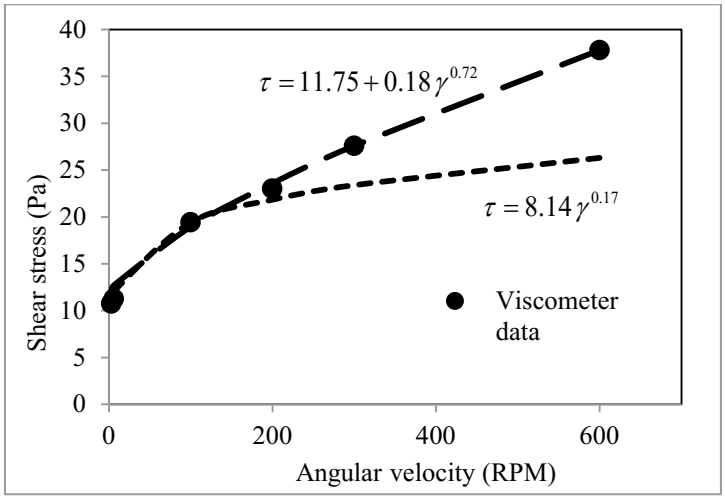

(b)

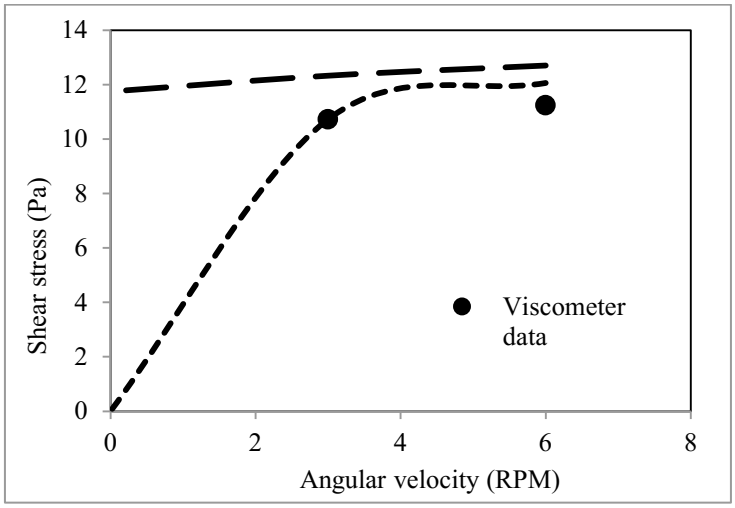

Figure 6-12- Viscometer test data and fitted rheological models: (a) full data range, (b) low shear rate range

Figure 6-13 and Figure 6-14 show the velocity, shear rate, and shear stress distributions within the pipe annulus when the pipe leading is close to emerging from the ground for the two studied fluid models. At this stage of installation, the in-bore end of the drill string is very close to the pipe exit point. Therefore, all of the drilling fluid volume injected from the drill string returns to the mud pit at the rig side. Within the pipe annulus, the fluid motion is mainly driven by the shear stress applied on the annulus inner boundary, pipe surface, due to pipe pullback. By moving from the pipe surface toward the bore wall, the surface area of the cylinder over which the force balancing the fluidic drag acts increases and, consequently, the shear stress drops, as shown in Figure 6-13(c) and Figure 6-14(c). For the H-B model, the shear stress on the pipe surface is 12.70 Pa and by moving only 2.64 cm toward the bore wall, this value decreases to 11.75 Pa, the H-B model yield stress. Therefore, a large region of annulus remains stuck to the borehole wall, unshared and unmoving.

By looking at the shear stress graphs for Case 1 and Case 2, it is clear that the majority of drilling fluid within the pipe annulus moves as an un-sheared plug, regardless of the amount of installation progress. Since the drilling fluids used in both crossings exhibited significant yield stress (Figure 6-4 (b) and Figure 6-12(b)), the H-B model, which accounts for yield stress, can estimate the drag and hydrokinetic pressure change more accurately.

It should be noted that the H-B fluid model (equation (6.13)) used in this paper has restriction limitation, which does not provide any information about the value of shear stress when $\gamma = 0$. Therefore, the shear stress change across the plug in Figure 6-5 and Figure 6-14 is undefined. However, this does not affect the estimated hydrokinetic pressure or shear stress on the pipe surface. Zaisha et al. (2012) recently addressed this issue by dividing the annulus cross-section into two shear and un-sheared regions, and then implementing a different set of equations for each region.

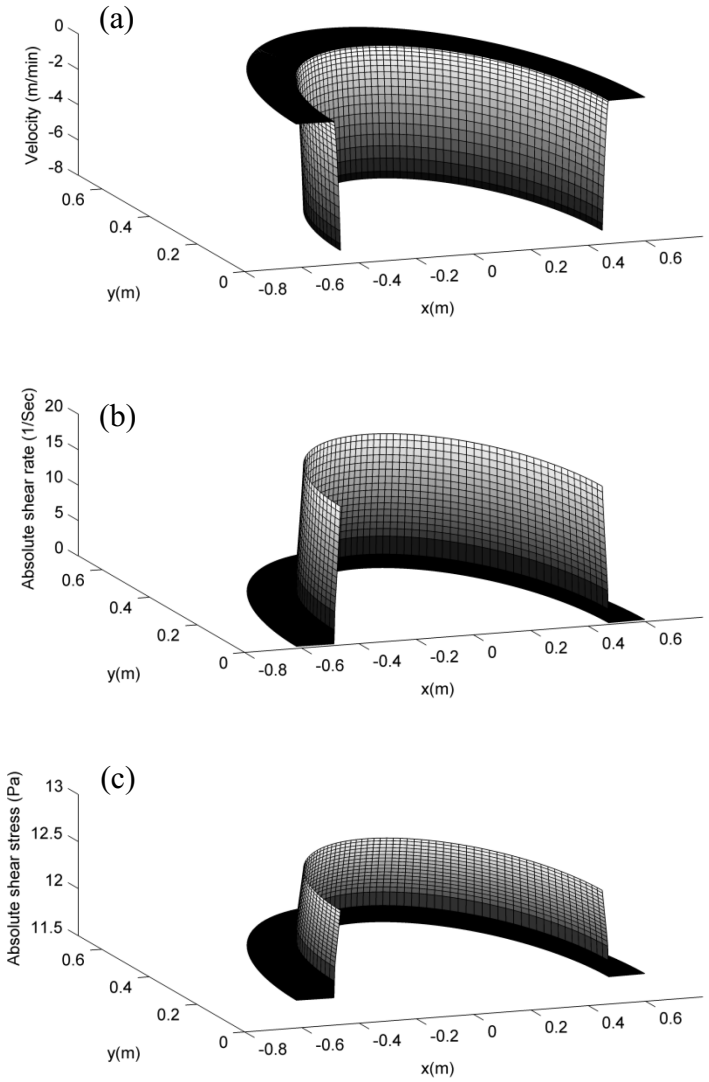

Figure 6-13- (a) Velocity, (b) absolute shear rate, and (c) absolute shear stress distributions in pipe annulus at $L_1 = 598\,\mathrm{m}$ for H-B fluid.

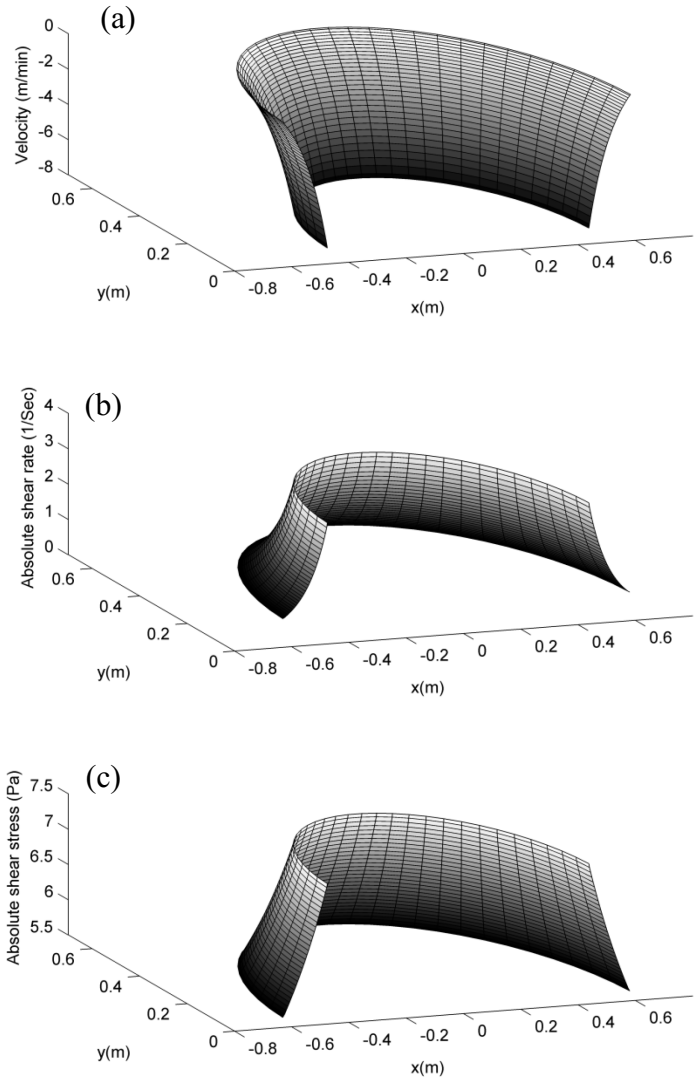

Figure 6-14- (a) Velocity, (b) absolute shear rate, and (c) absolute shear stress distributions in pipe annulus at $L_1 = 598\,\text{m}$ for H-B fluid.

Figure 6-15 shows the flow rate in pipe and drill rod annuli. The Power-law and H-B models estimate the drilling to stop returning to the pipe side when the pipe in bore length is 100 m and 400 m, respectively. Similar to Case 1 and due to exhibiting less viscosity at low shear rates, the estimated flow rate within the rod annulus at the end of installation is 55.10% less than the H-B model's estimation. The estimated maximum hydrokinetic pressure by the H-B and Power-law models is 61.35 kPa and 9.92 kPa, respectively. Unlike the previous installation, in this case, the ASTM suggested value for hydrokinetic pressure of 70 kPa is larger than the HB model

estimation. Compared to Case 1, Case 2 has a shorter borehole and a wider annulus, resulting in observing lower pressures in Figure 6-16. This dependency of the hydrokinetic pressure on the installation parameters is a feature of actual installations which can be captured by the FVM, and methods such as the ASTM that ignore this fact fail to do so.

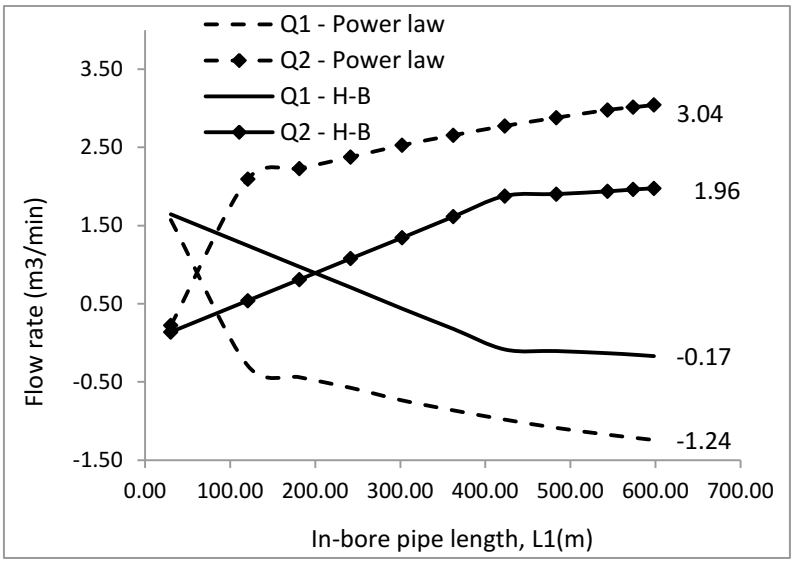

Figure 6-15- Estimated hydrokinetic pressure for Power-law and H-B fluid models.

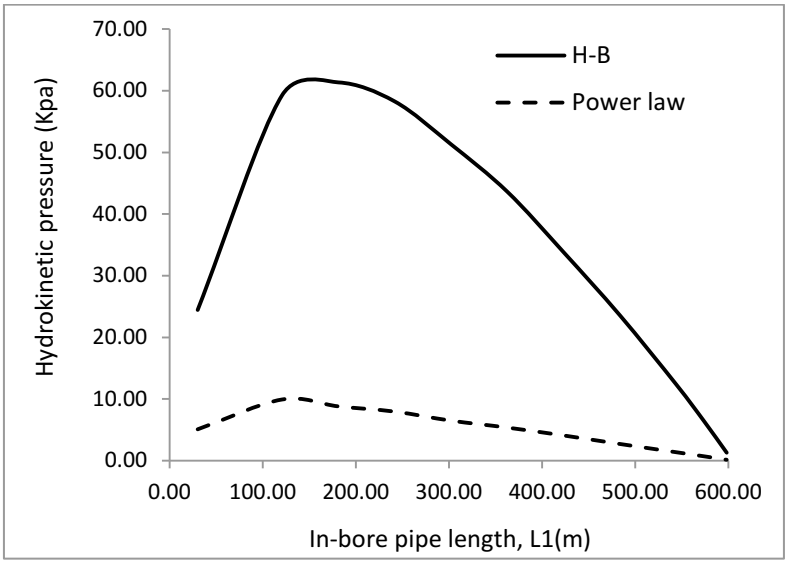

Figure 6-16- Estimated hydrokinetic pressure for Power-law and H-B fluid models.

The fluidic drag-in bore pipe length graph estimated by different methods is presented in Figure 6-17. The peak estimated drag by the Power-law and H-B models is only 3.50% and 2.45% of the PRCI estimation.

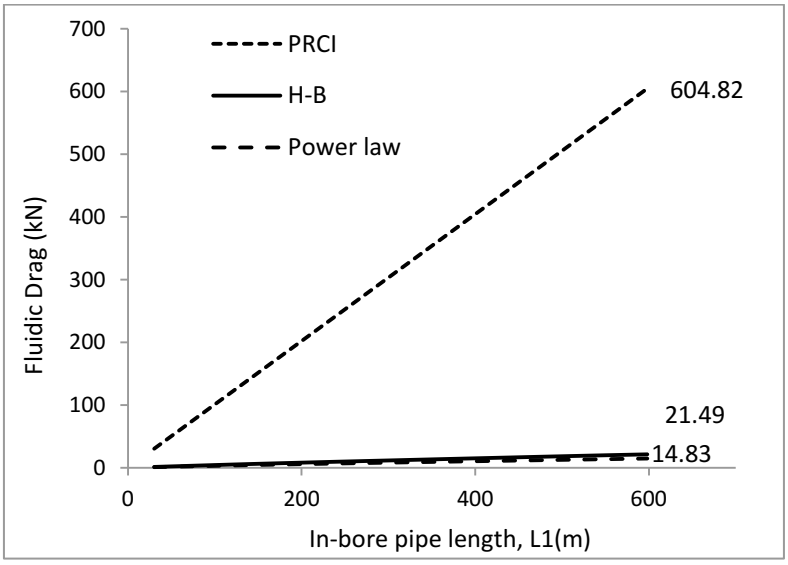

Figure 6-17- Estimated fluidic drag by FVM and PRCI method

The pullback forces recorded on the field, as well as the estimated forces by the PRCI method and the proposed method in this paper, are presented in Figure 6-18. While the end pullback force estimated by the proposed method is only 6% less than the recorded force, the PRCI estimation is 85% greater than the observed force on the field. This clearly proves the ability of FVM to accurately estimate the tensile force required for placing pipe in HDD. As a refinement to the proposed method, the contribution of the out-bore portion of the pipe into the pullback force can considered. By doing so, the location and magnitude of maximum pullback force can be estimated in a more promising way. A study conducted by Slavin (2010) revealed that for installations with a high exit angle and/or low in-bore coefficient of friction, it is probable that the pullback force peaks within the bore and not at the pipe exit point.

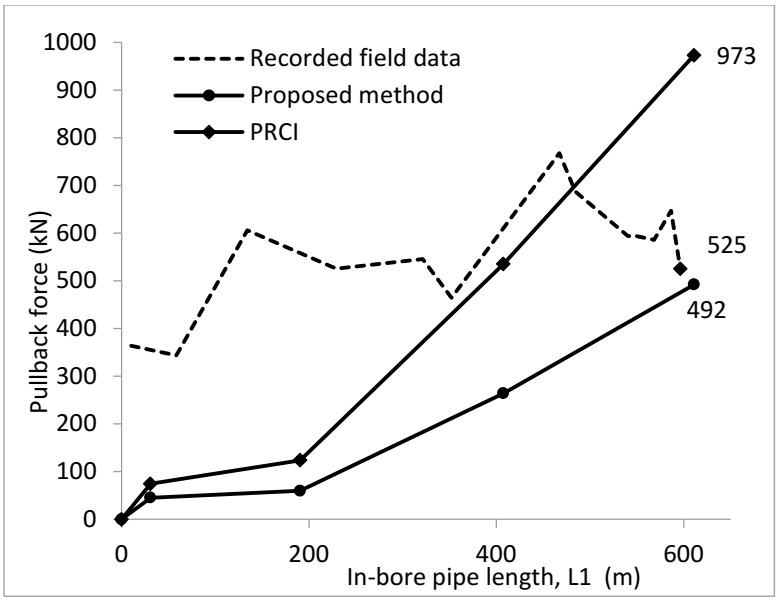

Figure 6-18- Estimated and recorded pullback forces

For rig sizing, the HDD designers typically recommend using a rig with higher pull force capacities than the maximum theoretically calculated pullback force to account for possible force increase. For Case 1 and Case 2 crossings, the employed rig pull capacity (1,900 kN) is about two times larger than the estimated forces by the PRCI, while for the proposed method, this number rises significantly to 5.07 and 3.86 for Case 1 and Case 2, respectively. Noting that the proposed method, unlike the PRCI, succeeded in estimating the actual pullback forces, these large numbers mean that the required rig for pulling the pipe string has been oversized by the jobs' designers, which could have been avoided by using the proposed method.

6-4- Eccentricity

In previous sections, it was assumed that both the product pipe and drill rod were placed eccentrically at the center of the borehole, and then the FVM simulations were carried out. This section addresses the effects of pipe eccentricity on the estimated fluidic drag for the two studied actual installations. For the installation of pipes with low bending stiffness, such as High Density Polyethylene (HDPE) pipes, the eccentricity, e in equation (6.9), is maximum and equals 1. This eccentricity is unchanged across the pipe segment within the bore since the pipe is highly flexible and easily deflects under its own buoyant weight to fit the bore shape. For pipes made of stiff materials, like steel, the pipe eccentricity is not constant; $e = \pm 1$ across the straight segments of the bore and $-1 < e < 1$ over the curved ones.

The FVM code does not take into account the eccentricity variation along the pipe segment within the bore and, therefore, the simulations have been performed supposing the eccentricity to be constant and equal to $e = 0, 0.25, 0.5, 0.75,$ and 0.95 across the bore. Figure 6-19 shows the fluidic drag changes versus installation progress for different eccentricities in installations Case 1. The pullback increases when the pipe leading end is at the pipe exit location is below 6.5% for both installations, indicating the insignificant effect of eccentricity on fluidic drag value. However, it should be noted that this difference is in fact smaller because of varying pipe eccentricity along the borehole's curved segments. From a pipe design point of view, since the fluidic drag itself makes up a small fraction of the total pullback force, ignoring the eccentricity effects is rational and not detrimental.

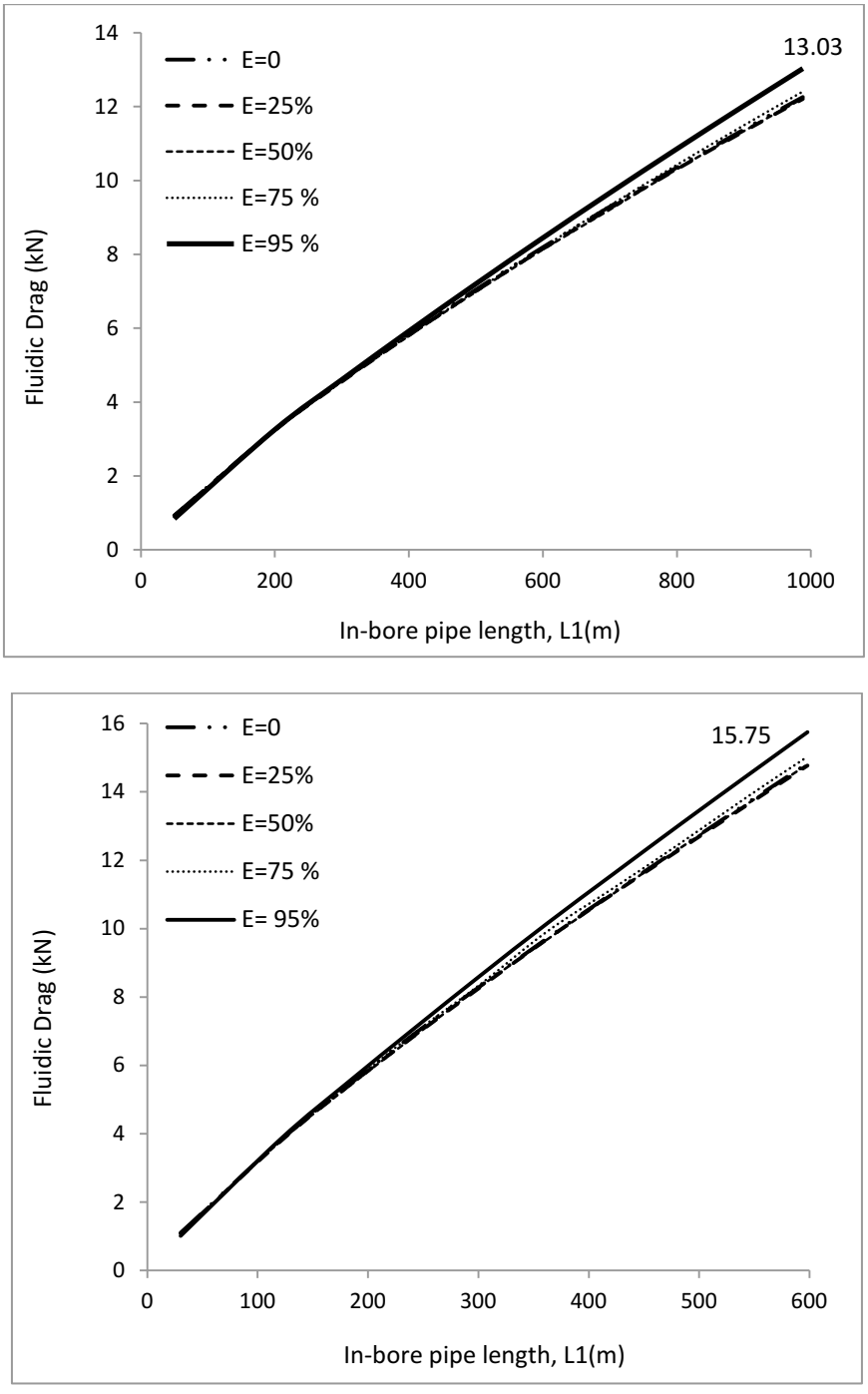

Figure 6-19- Fluidic drag changes with pipe eccentricity for installations Case 1 and Case 2

6-5- Conclusions

A new method for estimating the fluidic drag and hydrokinetic pressure changes during pipe installation using HDD has been introduced. The method takes into account a wide range of major factors, such as product pipe and drill rod eccentricities, and is applicable to muds characterized as H-B fluids. For solving the problem of eccentric annular flow, the FVM has been implemented to solve the fluid equation of motion numerically as a part of the procedure to determine drilling fluid's return pattern through a bore. The method has been applied to two actual example steel pipe HDD installations, and the simulation results are compared with those obtained from PRCI. The estimated pullback forces at the pipe exit location by the PRCI are 238% and 85% higher than actual measured values in the field for Case 1 and Case 2, respectively. While using the new proposed method, these values drop to 40% and 7%. This large deviation of estimated pull forces by PRCI is a result of overrating the fluidic drag component of pullback force that needs to be revised. Like the PRCI method, the FVM simulations reveal that the fluidic drag changes in a linear manner with installation progress, and it peaks when the pipe leading end is at the exit point.

Hydrokinetic pressure and fluidic drag are both dependent on the rheological model implemented to characterize the drilling fluid. During HDD pullback operations, since the flow rates are typically low ($1-2\ m^3/min$) and the annuli are wide, rheological models such as H-B that account for the fluid yield stress need to be implemented if the pumped drilling fluid is exhibiting a substantial yield stress. The fluidic drag and hydrokinetic pressure estimated by the Power-law model tend to be smaller than the corresponding values estimated by the H-B model. Furthermore, the effect of pipe eccentricity on the estimated fluidic drag is insignificant and can be ignored in HDD designs.

7- Chapter 7: Simple Methods for Fluidic Drag Estimation during Pipe Installation via HDD[5]

7-1- Introduction

With the number of large congested urban areas sharply increasing over the last several decades and the rising costs of normal vehicular traffic and business disruption, the demand for new construction methods with minimal impact on the surrounding environment has been growing within the underground utility installation industry. This need has been the main driving force behind the development of different trenchless (no-dig) techniques, where the underground utility lines are laid without creating a continuous trench on the ground surface. Originating from the oil well drilling industry, horizontal directional drilling (HDD) has been utilized for about four decades and is one of the most promising trenchless methods (Najafi and Gokhale 2005; Allouche et al. 2000). HDD is an ideal technique for pipe placement through urban areas, environmentally sensitive areas, traffic-heavy streets, and other high-risk regions (Sarireh et al. 2012; Willoughby 2004). To place a pipe using HDD, first a small diameter hole (pilot bore) is drilled along the planned path using a downhole assembly with steering and tracking capabilities. Over the second stage of installation, the hole is then widened, typically up to a dimeter 50 percent larger than the final product pipe size, by passing a reamer (hole opener) over one or multiple passes depending on the final bore size. Finally, the product pipe is pulled back into the enlarged hole. These three construction phases are often referred to as the pilot hole drilling, reaming, and pullback stages, respectively.

Pipes installed via HDD need to sustain loads imposed on them during installation and service periods. From a pipe design perspective, the installation loads often govern, so the majority of researchers have focused on identifying and quantifying the installation loads (Huey et al. 1996; Rabiei et al. 2016d; Rabiei et al. 2015). In spite of a notable surge in the number of HDD projects, pipes are still designed cautiously because professionals are unsure how the pipe will interact with the surrounding environment (soil and in-bore drilling fluid) during the pipe installation operation (Baumert et al. 2005). Current design references, such as ASTM F1962

[5] A version of this chapter will be submitted to the ASCE Journal of Pipeline Systems Engineering and Practice.

(2011) and Pipeline Research Council International (PRCI) (Huey et al. 1996), ignore some unique characteristics of HDD because of a lack of relevant investigations to use as a resource. As a result, the current design procedures depend on investigations undertaken by other industries, such as oil well drilling and utility cable installation (Slavin and Petroff 2010). Evaluating the fluidic drag during the pipe installation stage is an area that greatly needs investigation, and thus it is the focus of this paper. Fluidic drag is the incremental force created on the pipe's leading head during installation due to slurry interaction with the in-bore portion of the pipe.

To estimate the fluidic drag component of the pullback force, ASTM F1962 suggests using Equation (7.1), which was originally used to calculate the drag force applied on a utility cable's outer surface during installation via the cable blowing method (Slavin 2009; Slavin and Petroff 2010):

$$F_{fluid} = \Delta P \frac{\pi (R^2 - R_P^2)}{2} \tag{7.1}$$

where $R\,(\mathrm{m})$ and $R_P\,(\mathrm{m})$ are the bore and pipe radii, respectively, and $\Delta P\,(\mathrm{Pa})$ is the hydrokinetic pressure, which the standard suggests to be 70 kPa. Equation (7.1) provides no data on drag change as the installation develops, and the slurry rheology is considered in the pressure implicitly. PRCI provides no value for the hydrokinetic pressure, but it suggests an equation that accounts for the length of the pipe in contact with drilling fluid as:

$$F_{fluid} = 2\pi R_P L_p \mu_{mud} \tag{7.2}$$

where $L_p\,(\mathrm{m})$ is the in-bore length of the product pipe, and $\mu_{mud}\,(\mathrm{Pa})$ is the fluidic drag coefficient with a value of 350 Pa taken from the Dutch standard *NEN 3650, Requirements for Pipeline Systems* (NEN 2007). While each of these two procedures account for some aspects of pullback operations, both ASTM and PRCI ignore drilling fluid rheological characteristics and pipe placement rates (Rabiei et al. 2016b). A study by Baumert et al. (2005) found that the calculation of fluidic drag by either ASTM or PRCI can result in overly conservative forces by as much as 1–2 orders of magnitudes.

In an attempt to model the fluidic drag component of the pullback force more realistically, Duyvestyn (2009) implemented the slot flow approximation and considered slurry flow direction

change during the pullback stage. Duyvestyn assumed that in an installation with the pipe leading head between the pipe entry and crossover points, the total slurry volume flows to the surface through annular space between the product pipe and bore. Once the crossover point has been reached, the slurry flow direction switches, and the slurry moves in front of the product pipe toward the rig. To determine the crossover point location, the hydrokinetic pressure required for exhausting the slurry via product pipe and drill rod annuli were calculated in terms of in-bore pipe length. After equating these pressures and solving for the in-bore pipe length, the crossover point was calculated. The major shortcoming of this study was ignoring the fact that in a typical installation, the slurry returns to the surface through both the product pipe and drill rod annular spaces over a considerable length. Furthermore, this study did not consider the pullback rate effects.

Recently, Rabiei et al. (Rabiei et al. 2016a; Rabiei et al. 2016c) developed two methods for the fluidic drag estimation problem: one implements finite volume method (FVM) to solve the fluid equation of motion (Rabiei et al. 2016c), and the other is based on fluid flow pattern change identification during installation (Rabiei et al. 2016a). Compared to the existing methods, these new methods are more sophisticated in the sense that they both account for slurry rheology, annulus geometry, pullback rate, and drilling fluid flow direction change during installation. Aside from these advantages, however, they require high computational effort, making them inappropriate for practical applications. Hence, this paper suggests a set of new simple methods for fluidic drag evaluation, tailored to be implemented by HDD practitioners for quick drag evaluation while the accuracy of more refined methods is maintained.

7-2- Proposed Methods

The results of fluidic drag analysis by FVM and the two-stage method revealed that this force component of pullback force varies almost linearly with in-bore pipe length (Rabiei et al. 2016c; Rabiei et al. 2016a). This behaviour is observed during HDD pullback operations because: i) the amount of drilling fluid pumped down the hole is small since the bore is already clean, and ii) compared to the average drilling fluid annular velocity, the pipe is being pulled at high rates. Therefore, for the purpose of fluidic drag evaluation, this study suggests that drilling fluid circulation might be ignored and, as a result of that, the solution to the annular Couette flow (ACF) problem can be utilized. Also, a more simplified solution may be obtained by

approximating the annulus with a slot and using the solution to the planar Couette flow (PCF) problem. In the next section, both solutions are presented and discussed.

7-2-1- Annular Couette Flow

ACF is the laminar flow of a fluid contained between two concentric cylinders, one of which is moving with respect to the other one axially at a constant velocity, as shown in Figure 7-1. In this problem, after solving the fluid equation of motion in a cylindrical system, the shear stress on the outer surface of the inner cylinder (pipe) can be obtained as:

$$\tau_p = \frac{m}{R_p}\left(\frac{qV_p}{R^q(1-k^q)}\right)^n \tag{7.3}$$

where $R_p\,(\mathrm{m})$ and $R\,(\mathrm{m})$ are the radii of inner and outer pipes, $V_p\,(\mathrm{m/sec})$ is the inner pipe's pull velocity, $q = 1 - 1/n$, $k = R_p / R$, and $m\,(\mathrm{Pa.s\,c}^n)$ and n are consistency and behaviour indices in the Power-law rheological model, which are related as:

$$\tau = m\gamma^n \tag{7.4}$$

where $\gamma\,(1/\mathrm{sec})$ is the fluid shear rate. Knowing the shear stress at the pipe's surface from Equation (7.3), the drag force can be obtained by multiplying this value by the pipe's surface area in contact with drilling fluid as:

$$F_{fluid} = \frac{m}{R_p}\left(\frac{qV_p}{R^q(1-k^q)}\right)^n L_p A_p \tag{7.5}$$

where $A_p\,(\mathrm{m}^2)$ is the pipe's surface area in contact with drilling fluid per meter, and $L_p\,(\mathrm{m})$ is the in-bore pipe length.

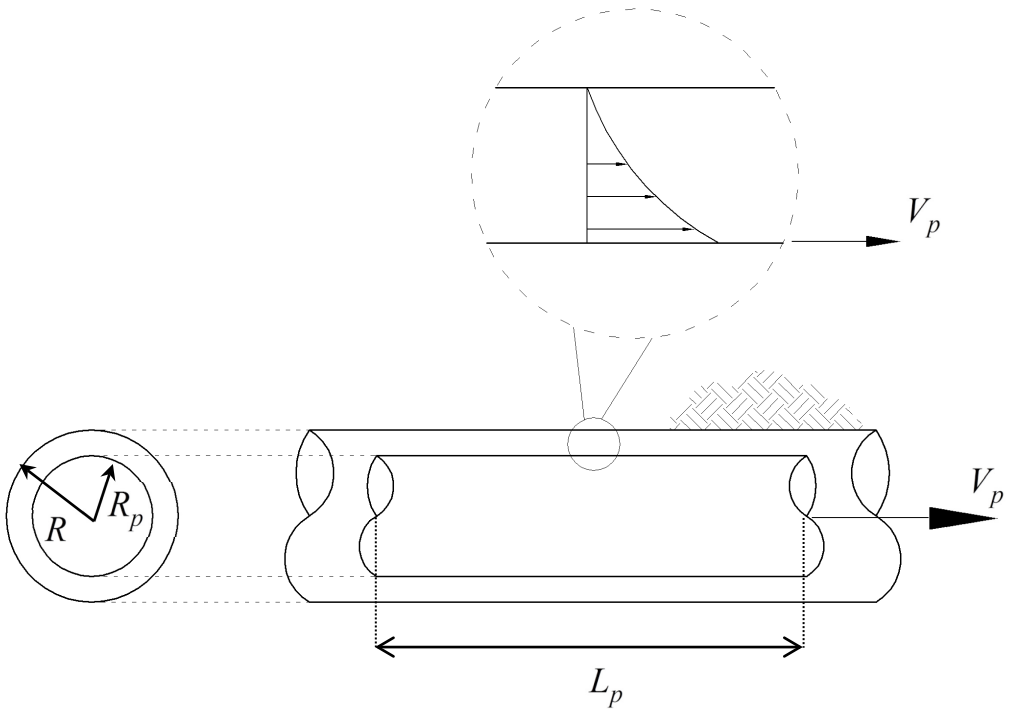

Figure 7-1- Schematic representation of Annular Couette Flow

For a Hershcel-Bulkley (H-B) fluid with the characteristics equation of:

$$\tau = \tau_0 + k\gamma^n \tag{7.6}$$

where $\tau_0\,(\mathrm{N/m^2})$, $k\,(Pa.Sec^n)$, and n are yield stress, consistency index, and behaviour index, respectively, the shear stress at the pipe's surface can be determined as follows:

$$\tau_p = \frac{c_1}{R_p} \tag{7.7}$$

where c_1 is an unknown constant satisfying the equation:

$$V_p = \int_\sigma^1 R\left(\frac{c_1}{R\xi k} - \frac{\tau_y}{k}\right)^{1/n} d\xi \tag{7.8}$$

where $\sigma = R_p / R$.

Therefore, the final equation for fluidic drag of an H-B fluid is:

$$F_{drag} = \frac{c_1}{R_p} L_p A_p \tag{7.9}$$

7-2-2- Planar Couette Flow

In the PCF method, the annulus is approximated by a slot with the same cross-sectional area, as shown in Figure 7-2. Then, the fluid equation of motion is solved for the slot, considering the slot's lower bounding surface to be moving at the pullback rate of V_p. In this problem, assuming the fluidic drag to be identified as a Power-law fluid, the fluidic drag can be determined as:

$$F_{fluid} = m(\frac{V}{R - R_p})^n L_p A_p \tag{7.10}$$

For H-B fluids, the drag equation has the following form:

$$F_{fluid} = (\tau_y + (\frac{V_p}{R - R_p})^n m) L_p A_p \tag{7.11}$$

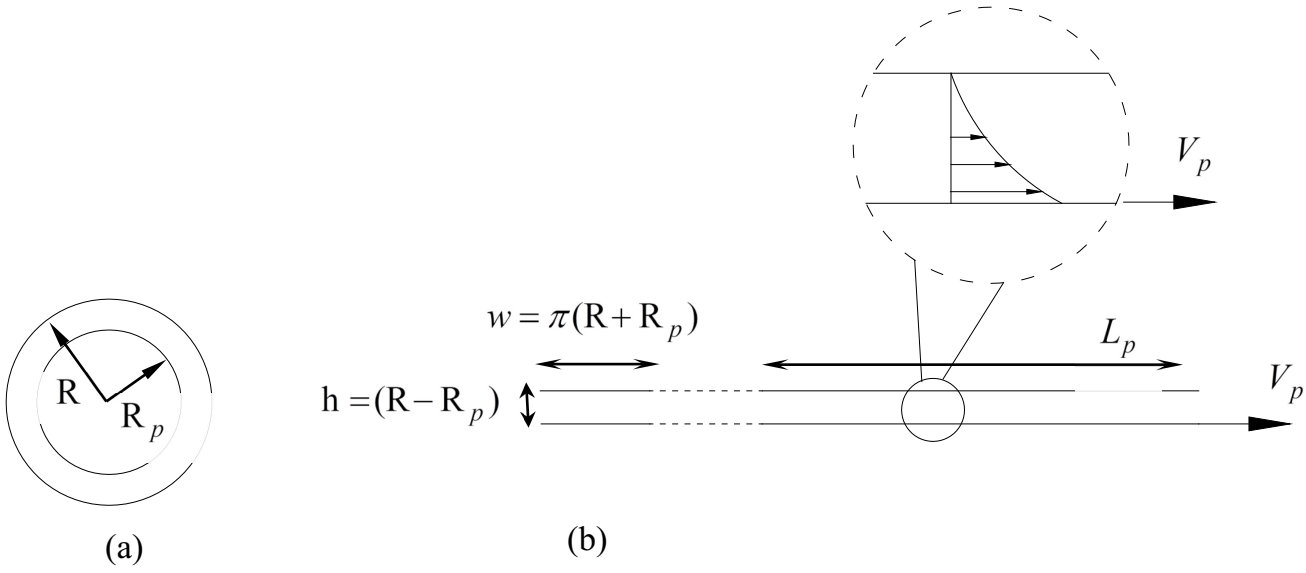

Figure 7-2- Representation of PCF: a) annulus geometry b) equivalent slot geometry

7-3- Case Studies

7-3-1- Overview of Field Installations

This section presents and discusses the fluidic drag values estimated by the simplified methods for two actual installations completed in Alberta, Canada. The authors have already verified the FVM and two-stage method (Rabiei et al. 2016a; Rabiei et al. 2016c) using the recorded pullback data of these two installations. Therefore, in order to verify the new proposed simplified methods in this study, the estimated fluidic drag values are compared against results obtained from the FVM and two-stage method. Table 7-1 summarizes the main parameters of the two studied installations.

The bore geometry for each crossing is presented in Figure 7-3. In order to characterize the returning drilling fluid in the field, samples were taken and tested using a standard six-speed viscometer. Then, H-B and Power-law rheological models were fitted to the test data following the recommended procedure in the American Petroleum Institute (API) 13D (2011). The viscometer data, as well as the fitted rheological models, is presented in Figure 7-4.

The Case 1 bore was drilled through medium to high clay-shale bedrock with sandstone interbeds beneath an 800-m wide river at the location of the crossing. Case 2 involved traversing a pond and the 44-m wide Baseline Road in Edmonton, Alberta, Canada. The pilot bore passed through layers of clay till, sandstone, and clay-shale.

Table 7-1- Main parameters of the two actual installations studied

Parameter	Case 1	Case 2
Crossing length, m	998	604
Pipe outer diameter, m	0.508	0.914
Pipe wall thickness, m	0.112	0.204
Borehole diameter, m	0.762	1.219
Drill rod outer diameter, m	0.140	0.140
Mud pump flow rate, m^3/min	1.50	1.80
Pullback rate, m/min	7.32	7.32
Recorded end pullback force,	268	525

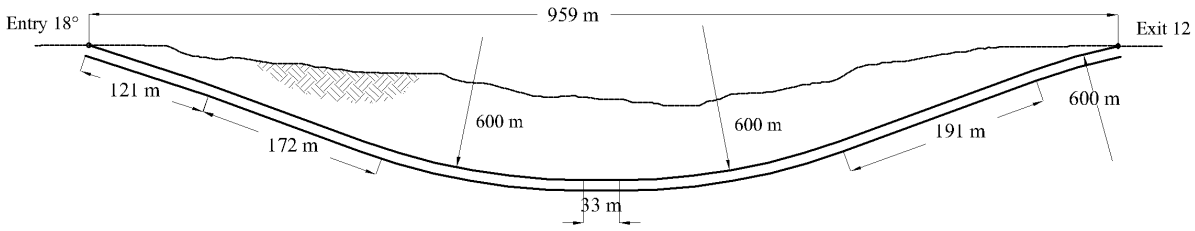

(a)

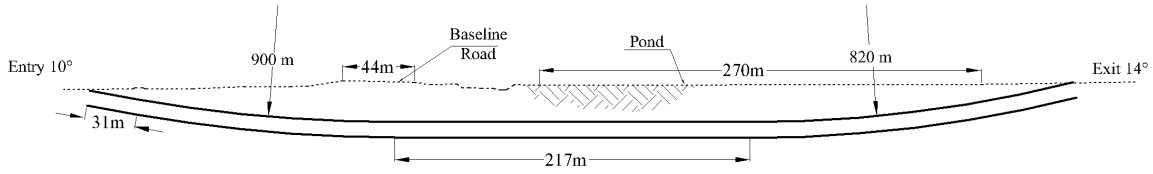

(b)

Figure 7-3- Bore profiles for Case 1 (a) and Case 2 (b)

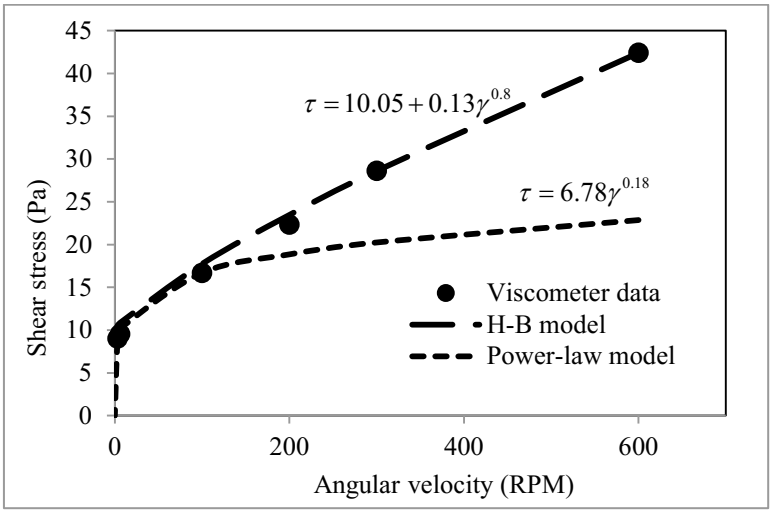

(a)

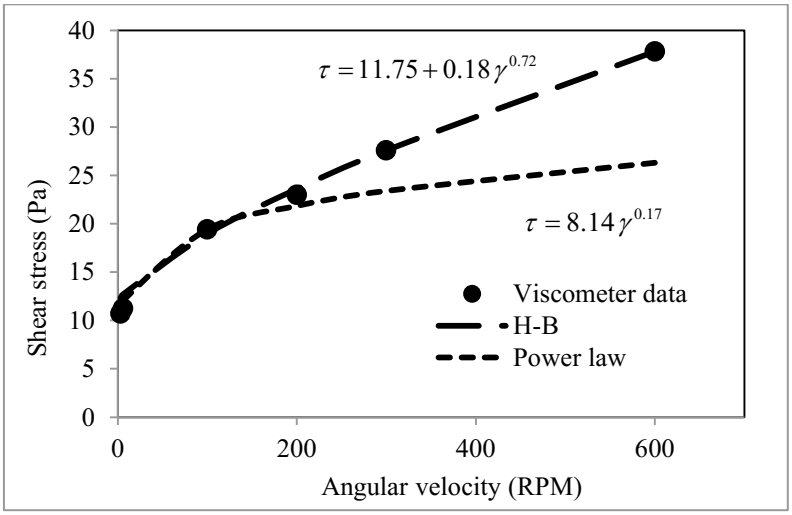

(b)

Figure 7-4- Viscometer test data and fitted rheological models for Case 1 (a) and Case 2 (b) (Rabiei et al. 2016c)

7-4- Discussion of Results

Figure 7-5 and Figure 7-6 show the estimated fluidic drag by different methods for Power-law and H-B fluids. Clearly, all of the proposed simple methods have exhibited the ability to regenerate the estimations of the more detailed two-stage method and FVM, although this ability deteriorates by introducing yield stress or switching from the Power-law to H-B model. The other observation that can be made from these graphs is that the drag changes linearly with the in-bore pipe length regardless of the implemented fluid rheological model. Unlike the ASTM, this behaviour is aligned with the PRCI's fluidic drag evaluation procedure, where the drag force is directly related to the length of pipe in contact with drilling fluid, L_p. The fluidic drag is larger for Case 2, which is due to installing a pipe with greater surface area through a more viscous drilling fluid.

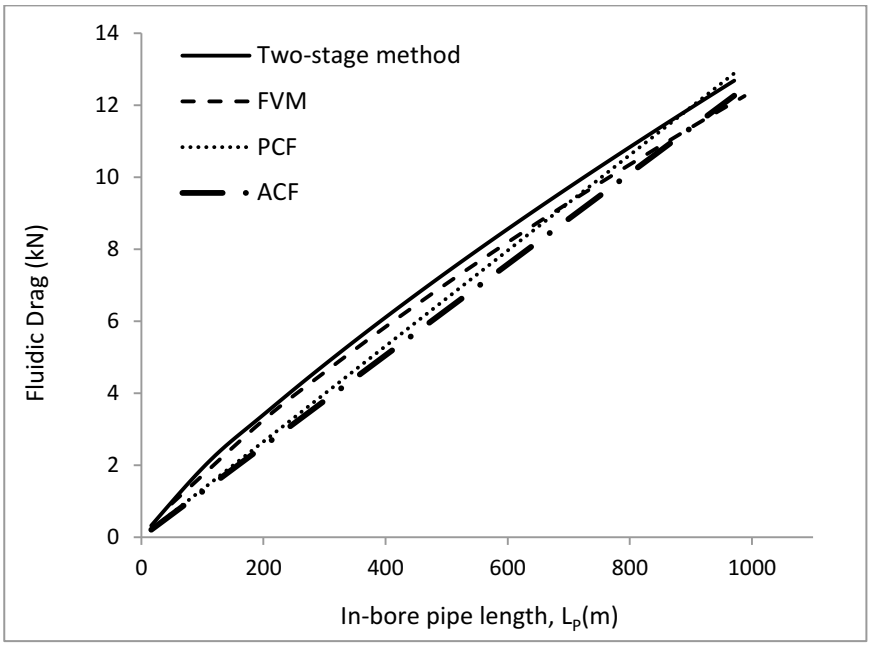

(a)

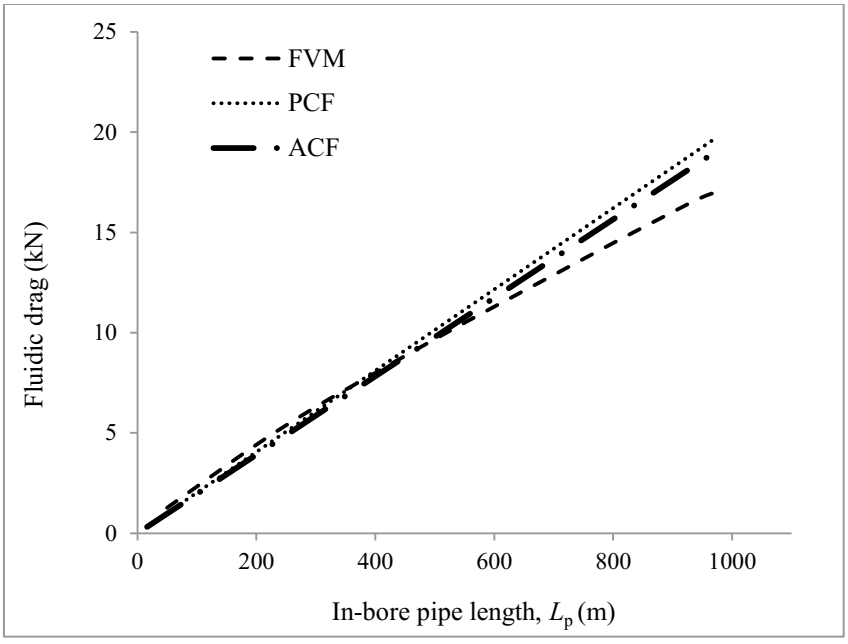

(b)

Figure 7-5-Estimated fluidic drag for Case 1 using a) Power-law fluid model, b) H-B fluid model

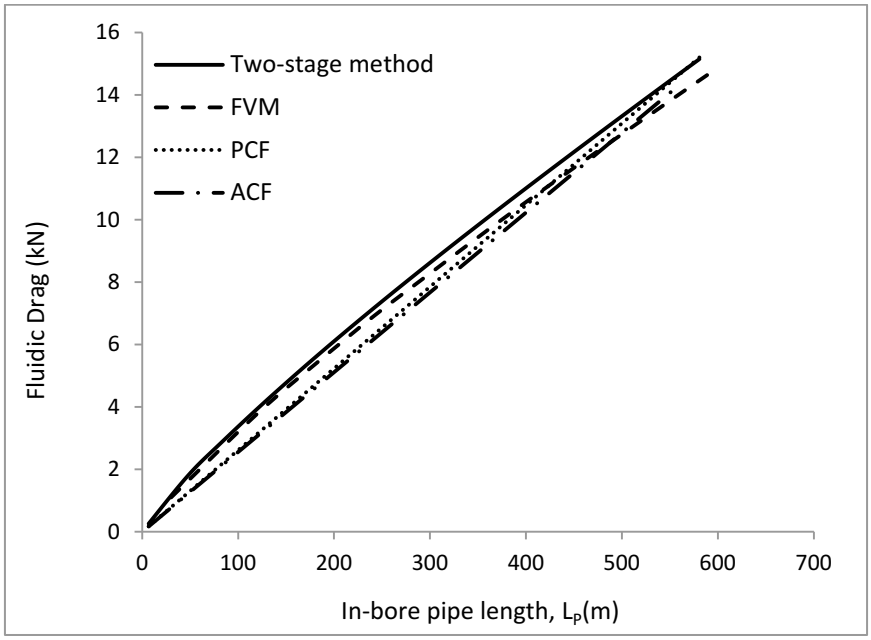

(a)

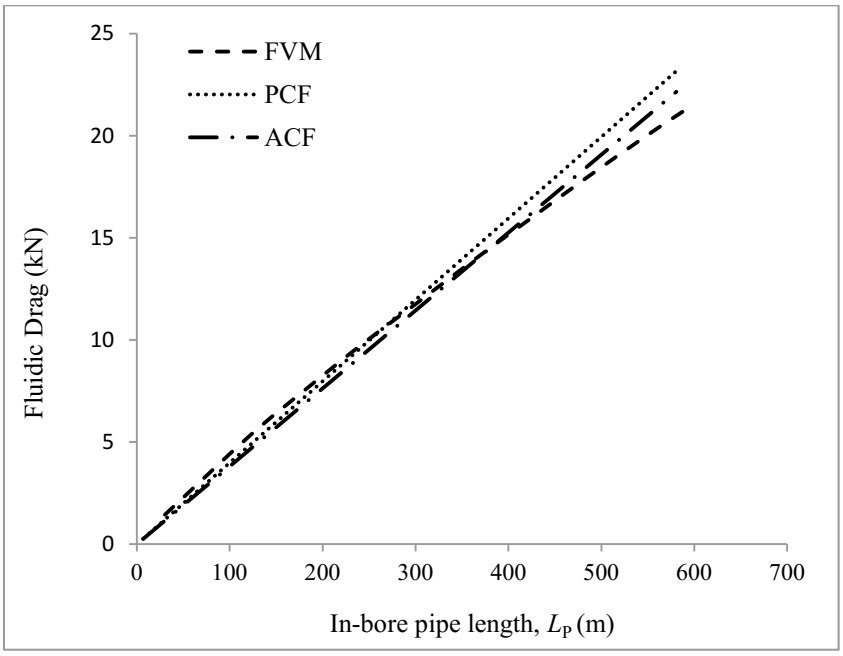

(b)

Figure 7-6 - Estimated fluidic drag for Case 2 using a) Power-law fluid model, b) H-B fluid model

Table 7-2 summarizes the maximum fluidic drag obtained by different methods. Regardless of the chosen model for drag calculation, the H-B fluid model always results in greater values for drag. For instance, when using the ACF solution in Case 1, the H-B model estimates an end drag of 19.00 kN, which is 54.9 percent higher than the corresponding value obtained by the Power-law model. These higher values are obtained because the drilling fluid used in this project exhibited a significant yield stress, as presented in Figure 7-4, and the drilling fluid was sheared at low rates during pullback operations. Furthermore, the forces obtained from the simple methods are all greater than the associated FVM forces, which is favorable from a pipe design point of view.

Table 7-2- Peak fluidic drag estimated by different methods

	Power-law (kN)				H-B (kN)		
	FV	Two-stage	PCF	ACF	FV	PCF	ACF
Case 1	12.26	12.69	12.89	12.27	17.16	19.68	19.00
Case 2	14.83	15.15	15.20	14.85	21.49	23.16	22.15

Table 7-3 presents the percentage difference of the estimated fluidic drag with respect to the FVM for different methods. The maximum percentage difference is 3.4, obtained using the PCF method in Case 1. This clearly demonstrates the proposed simple methods' ability to produce results similar to the more robust FVM.

Table 7-3- Percentage difference between the estimated drag by different methods and FVM

	Power-law			H-B	
	Two-stage	PCF	ACF	PCF	ACF
Case 1	0.86	1.25	0.02	3.42	2.54
Case 2	0.53	0.61	0.04	1.87	0.76

Overall, after analyzing the results for the two discussed installations, it is obvious that the proposed new simple methods are able to estimate fluidic drag accurately with less computational effort than the FVM and the two-stage method. The results suggest that the PRCI equation is to be used for fluidic drag estimation, but new fluidic drag coefficients need to be adopted from the equations presented in this paper. For drilling fluids with substantial yield

stress, it is recommended that the methods proposed for H-B fluids are used. From a pipe design perspective, the improvement achieved from using the ACF method instead of the PCF method is insignificant considering the small contribution of the fluidic drag to the total pullback force. As an example, the fluidic drag in Case 2 makes up less than five percent of the end pullback force of 268 kN.

It should be noted that all the suggested simple methods assume that the pipe is located at the center of the hole during pullback operations, which is contrary to what happens in actual installations. However, a recent numerical study by (Rabiei et al. 2016c) revealed that the impact of eccentricity on the predicted fluidic drag is insignificant and can be neglected.

7-5- Conclusions

This study has suggested a series of simple methods for estimating the fluidic drag component of pullback force during HDD pipe installation operations, which are applicable to both Power-law and H-B drilling fluids. To verify these methods, their estimations for two actual installations are compared against verified drag forces obtained from the more refined FVM and two-stage methods. The maximum obtained percentage differences between the estimated drag using the simplified methods and FVM are 3.4 and 1.9 for Cases 1 and 2, respectively. For drilling fluids with substantial yield stress, implementing methods that account for yield stress is suggested. It has been observed that the fluidic drag changes linearly with in-bore pipe length. Therefore, the current PRCI equation can be followed, but a new fluidic drag coefficient, as presented in this paper, must be used.

8- Chapter 8: Summary and Conclusions

8-1- Summary

Horizontal Directional Drilling (HDD) is a three-stage trenchless construction technology for pipe installation. The forces developed within the pipe during the installation phase, the terminal stage of an HDD construction, often govern pipe design; therefore, accurate estimation of these forces (pullback forces) is crucial for HDD project success.

This study identified existing gaps in the current HDD pullback force evaluation procedure and developed methods for dealing with them. The study mainly focuses on fluidic drag components evaluation, although some methods for non-fluidic drag have also been developed.

For non-fluidic drag determination of HDPE pipes, the method proposed by ASTM F 1962 (2011) has been extended. The extension makes the new method independent from the bore geometry and, therefore, results in a method applicable to a wider range of actual crossings. Also, a non-iterative model is proposed for tensile force amplification estimation along curved pipe segments. The model may be used for either steel pipe or HDPE pipe and implements the theory of beam with large deflections.

For fluidic drag evaluation, two numerical methods are proposed which involve satisfying the continuity equation within the bore. The first method, the two-stage method, is applicable to Power-law fluids and considers the product pipe and drill pipe to be placed at the bore centre during the installation course, whereas the second method, Finite Volume Method (FVM), accounts for eccentricity and is applicable to drilling fluids exhibiting yield point. A series of simple methods are also developed, so the HDD practitioners can use them for fast fluidic drag evaluation without significant loss of accuracy.

8-2- Conclusions

This study proposed a general method for pullback force estimation of HDPE pipes, which is a refined version of ASTM equations and, unlike the ASTM method, is not restrained by the bore geometry. For a theoretical installation with the ASTM's typical bore geometry, it has been demonstrated that the maximum error introduced through the use of the ASTM equations relative to that of the proposed general method is 9.6 percent, largely due to error in pullback force determination for the downward curved segment.

This study also proposed a numerical model for pullback force that is applicable to both steel and HDPE pipes. The model assume that the pullback force change across a curved pipe segment is a product of three components: pipe weight, pipe bending stiffness, and tensile force direction change between pipe ends. It has been demonstrated that the bending stiffness effect on pullback force amplification when a pipe segment negotiates a curved bore is insignificant and can be disregarded. This observation has led to a non-iterative equation for pullback force amplification calculation. The predicted forces by the new non-iterative model were well matched with the ASTM and PRCI methods' estimations for two HDPE pipe and steel pipe installations, respectively.

In this study, three different methods have been developed and verified for fluidic drag evaluation. For verification purposes, field data collected from several crossings completed in Alberta, Canada, have been used. Unlike the ASTM and PRCI methods, the newly developed methods account for a wide range of parameters affecting the fluidic drag value, such as drilling fluid rheological characteristics, annulus size, pullback velocity, etc. In general, the fluidic drag accounts for less than 10 percent of pullback force. This value changes depending on crossing specifications as well as the type of anti-buoyancy measures taken during pipe installation. The proposed methods enable the HDD contractors/practitioners to predict drilling fluid motion within bore and during pipe installation operation, so they can fine-tune their plans for drilling fluid collection and recovery. The proposed two-stage method and FVM in this study are the only existing methods in the HDD literature that allow for gradual change of drilling fluid flow direction from pipe annulus to drill rod annulus over installation course. Using these methods, the location of crossover point, where drilling fluid stops flowing toward pipe entry, can be

estimated. This data is very useful for managing the machinery required for collecting and transporting the drilling fluid to recovery site.

For fluidic drag, it has been demonstrated that PRCI is overly conservative, while the ASTM method leads to closer estimations. The fluidic drag tends to change linearly as the installation progresses; therefore, methods like the ASTM method that relate the fluidic drag directly to pressure fail to model the fluidic drag history accurately. This is more pronounced over the late stages of installations where, in spite of a hydrokinetic pressure drop, the drag increases due to an increase in pipe surface area in contact with drilling fluid. This linear change of drag can be captured properly by using the PRCI method along with a modified fluidic drag coefficient. The modified fluidic drag coefficient is attainable using one of the simplified fluidic drag estimation methods introduced in chapter 7 of the thesis. For the two actual installations studied, the maximum obtained percentage differences between the estimated drag using the simplified methods and FVM is 3.4 percent, showing the ability of these methods to generate results as promising as the more refined ones.

Regarding the eccentricity, the FVM results revealed that this factor's impact on estimated drag can be disregarded, especially from a pipe design perspective. As the eccentricity increases, so does the drag value. The maximum calculated increase in drag for eccentricity of E=0.95 is 6.5 percent.

8-3- Limitations and Future Works

This research study mainly focused on the interaction of drilling fluid with pipe during HDD installation operations and, for the first time, methods were suggested for estimating this effect on pullback force amplification based on the unique characteristics of HDD pullback force operations. The main limitation presently in this field is a lack of experimental work in directly measuring fluidic drag and hydrokinetic pressure to support the proposed models in a more adequate way. Currently, both ASTM F 1962 and PRCI disregard the effects of soil mechanical characteristics on pullback force, whereas the Dutch standard NEN 3650 accounts for it through the inclusion of a soil modulus of subgrade reaction into the pullback force estimation procedure.

The presented general equation in chapter 3, equation (3.9), is only applicable when the pipe is pushed against the bore crown, or $w_b > 0$. Therefore, it is not applicable when the pipe sits on the bore bottom, something which rarely happens during HDPE pipe installation. Also, this equation only accounts for pipe curvature in the vertical plane; as a result, developing a new equation when the pipe bends in both horizontal and vertical planes is necessary.

Like PRCI, the proposed non-iterative method for pullback force estimation of steel pipes is also based on the assumption that a curved pipe segment contacts the bore wall at only three discrete points: curved bore two ends and one pint in the middle. This major assumption needs to be investigated and verified by future theoretical/experiential studies and, in case of necessity, new methods should be developed.

In continuing the current investigation, a study on pipe-soil interaction during pipe installation operations via HDD can be conducted. The study may involve several tasks: a) creating different models using a numerical software package, like ABAQUS, to simulate pullback operation through different soil formations, b) developing a procedure to include soil characteristics into the pullback force estimation process, and c) comparing estimated pullback forces for several actual crossings completed in different soil types against values recorded in the field. Also, both the PRCI and ASTM F1962 methods assume the friction coefficient at the pipe-bore interface to be constant and independent of pipe material and soil type while estimating the pullback force. The accuracy of this substantial assumption can also be investigated and new friction coefficients can be developed for different pipe-soil type combinations.

In order to estimate pullback force change across a curved pipe segment, the PRCI method assumes the pipe behaves as a three-point beam with a distributed and mid-span point loads. This means that the pipe contacts the bore wall at only three points, regardless of path curvature and bore and pipe radii. At the other end of the spectrum, ASTM F1962 considers the pipe to be continuously in contact with the bore surface between the two curved bore ends since the HDPE bending rigidity is relatively low. However, for steel pipes, the actual deformed pipe shape is somewhere in between. A study that considers a more realistic shape for curved pipes needs to be conducted in order to develop a new method for pullback force change estimation along curved bores.

9- Chapter 9: Reference

Allouche, E. N., Ariaratnam, S. T., and Lueke, J. S. (2000). "Horizontal directional drilling: profile of an emerging industry." *Journal of Construction Engineering and Management,* 126(1), 68-76.

API 13D. (2011). *Recommended practice on the rheology and hydraulics of oil-well drilling fluids / issued by American Petroleum Institute Exploration and Production Department.* Washington, D.C. : American Petroleum Institute, .

ASCE. (2014). *Pipeline design for installation by horizontal directional drilling: ASCE manual of practice.* American Society of Civil Engineers, Reston, VA.

ASTM F1962. (2011). "Guide for Use of Maxi-Horizontal Directional Drilling for Placement of Polyethylene Pipe or Conduit Under Obstacles, Including River Crossings."

Baumert, M. E., and Allouche, E. N. (2002). "Methods for estimating pipe pullback loads for horizontal directional drilling (HDD) crossings." *Journal of Infrastructure Systems,* 8(1), 12-19.

Baumert, M. E., Allouche, E. N., and Moore, I. D. (2005). "Drilling fluid considerations in design of engineered horizontal directional drilling installations." *International Journal of Geomechanics,* 5(4), 339-349.

Baumert, M. E., Allouche, E. N., and Moore, I. D. (2004). "Experimental investigation of pull loads and borehole pressures during horizontal directional drilling installations." *Canadian Geotechnical Journal,* 41(4), 672-685.

Beléndez, T., Neipp, C., and Beléndez, A. (2002). "Large and small deflections of a cantilever beam." *European Journal of Physics,* 23(3), 371.

Carpenter, R. (2011). "Mixed Market Recovery For HDD." *Underground Construction,* 66(6), 24-26.

Cheng, E., and Polak, M. A. (2007a). "Theoretical model for calculating pulling loads for pipes in horizontal directional drilling." *Tunnelling and Underground Space Technology,* 22(5), 633-643.

Cheng, E., and Polak, M. A. (2007b). "Theoretical model for calculating pulling loads for pipes in horizontal directional drilling." *Tunnelling and Underground Space Technology,* 22(5), 633-643.

Chhabra, R. P., and Richardson, J. F. (2011). *Non-Newtonian flow and applied rheology: engineering applications.* Butterworth-Heinemann.

Constantin, P., and Foias, C. (1988). *Navier-stokes equations.* University of Chicago Press.

Duyvestyn, G. (2006). "Challenging ground conditions and site constrains not a problem for HD." *Proc., NASTT's No-Dig Show,*Nashville, TN.

Duyvestyn, G. (2009). "Comparison of predicted and observed HDD installation loads for various calculation methods." *Proc., NASTT's No-Dig Show, Toronto, Canada*.

Faghih, A., Ghimire, A., and Dupuis, D. (2015a). "Parametric Study of Pullback Forces on Pipelines Installed by Horizontal Directional Drilling." *Trenchless Technology Magazine*.

Faghih, A., Yi, Y., Bayat, A., and Osbak, M. (2015b). "Fluidic Drag Estimation in Horizontal Directional Drilling Based on Flow Equations." *Journal of Pipeline Systems Engineering and Practice,* 6(4), 04015006.

Grand View Research. (2015). "Horizontal Directional Drilling (HDD) Market Analysis By End-use (Utilities, Telecommunication), And Segment Forecasts To 2022." Grand View Research.

Haciislamoglu, M. (1989). *Non-Newtonian Fluid Flow in Eccentric Annuli and Its Application to Petroleum Engineering Problems.* UMI.

Hanks, R. W., and Larsen, K. M. (1979). "The flow of power-law non-Newtonian fluids in concentric annuli." *Industrial & Engineering Chemistry Fundamentals,* 18(1), 33-35.

Hassan, K., Alam, S., Bartlett, C., and Allouche, E. (2014). "Experimental Investigation of Soil-Pipe Friction Coefficients for Thermoplastic Pipes Installed in Selected Geological Materials." *NASTT's No-Dig Show Orlando, Fl.*

Huey, D., Hair, J., and McLeod, K. (1996). "Installation Loading and Stress Analysis Involved with Pipelines Installed by Horizontal Directional Drilling." *NASTT's No-Dig Show, New Orleans, LA*.

Malik, R., and Shenoy, U. V. (1991). "Generalized annular Couette flow of a power-law fluid." *Industrial and Engineering Chemistry Research,* 30(8), 1950-1954.

N.L. Baroid. (1998). *Baroid Fluids Handbook.* Baroid Petroleum Services Division/N.L. Industries.

Najafi, M., and Gokhale, S. (2005). *Trenchless technology: pipeline and utility design, construction, and renewal.* McGraw-Hill, New York; Toronto.

Nelson, A. (2009). *Engineering Mechanics: Statistics and Dynamics.* Tata McGraw-Hill Education.

NEN. (2007). *NEN 3650 (en) : requirements for pipeline systems.* Netherlands Standardization Institute, Delft, Netherlands.

Polak, M. A., and Chu, D. (2005). "Pulling loads for polyethylene pipes in horizontal directional drilling: theoretical modeling and parametric study." *Journal of Infrastructure Systems,* 11(2), 142-150.

Polak, M. A., and Lasheen, A. (2001). "Mechanical modelling for pipes in horizontal directional drilling." *Tunnelling and Underground Space Technology,* 16, 47-55.

Puckett, J. S. (2003). "Analysis of theoretical versus actual HDD pulling loads." *Pipeline Engineering and Construction International Conference 2003, Baltimore, Maryland*.

Rabiei, M., Yi, Y., Bayat, A., Cheng, R., and and Osbak, M. (2016a). "Estimation of Hydrokinetic Pressure and Fluidic Drag Changes in Horizontal Directional Drilling Pipe Installations Based on Identifying Slurry Flow Pattern Change within Borehole." *Submitted to the ASCE Journal of Pipeline Systems Engineering and Practice*.

Rabiei, M., Yi, Y., Bayat, A., Cheng, R., and and Osbak, M. (2016b). "Fluidic Drag Evaluation of Pipes Installed via Horizontal Directional Drilling Using Slot Flow Approximation." NASTT's No-Dig, Dallas, TX.

Rabiei, M., Yi, Y., Bayat, A., Cheng, R., and Osbak, M. (2016c). "Fluidic Drag Estimation in Horizontal Directional Drilling using Finite Volume Method." *Submitted to the Journal of Pipeline Engineering*.

Rabiei, M., Yi, Y., Bayat, A., and Cheng, R. (2016d). "General Method for Pullback Force Estimation for Polyethylene Pipes in Horizontal Directional Drilling." *Journal of Pipeline Systems Engineering and Practice,* 04016004.

Rabiei, M., Yi, Y., Bayat, A., Cheng, R., and and Osbak, M. (2015). "New method for predicting pullback force for pipes installed via horizontal directional drilling (HDD)." NASTT's No-Dig Show, Denver, Colorado.

Sarireh, M., Najafi, M., and Slavin, L. (2012). "Usage and applications of horizontal directional drilling." *ICPTT2012: Better Pipeline Infrastructure for a Better Life. Proceedings of the International Conference on Pipelinesand Trenchless Technology,* 1835-1847.

Slavin, L. M. (2010). "Parametric dependency and trends of HDD pull loads." *Journal of Pipeline Systems Engineering and Practice,* 1(2), 69-76.

Slavin, L. M. (2009). "Belowground Pipeline Networks for Utility Cables." American Society of Civil Engineers.

Slavin, L. M., and Najafi, M. (2013). "Maxi-HDD pull loads for entry and exit points at different elevations." *Journal of Pipeline Systems Engineering and Practice,* 6(3), A4014004.

Slavin, L. M., and Najafi, M. (2012). "Effect of pipe stiffness on maxi-HDD pull loads." *Journal of Pipeline Systems Engineering and Practice,* 3(1), 22-31.

Slavin, L. M., Najafi, M., and Skonberg, E. R. (2011). "Maxi-HDD pull loads for nonlevel grade for polyethylene pipe." *Journal of Pipeline Systems Engineering and Practice,* 2(2), 64-69.

Slavin, L. M., and Scholl, J. (2014). "Which method to use when estimating maxi-HDD installation loads: ASTM F 1962 or the PRCI method?" *Pipelines 2014, From Underground to the Forefront of Innovation and Sustainability,* ASCE, 722-733.

Slavin, L., and Petroff, L. (2010). "Discussion of ASTM F 1962, or 'How are the Pulling Load Formulas Derived and How are they Used?'" *NASTT's No-Dig Show, Chicago, IL*.

Willoughby, D. (2004). "Horizontal directional drilling: utility and pipeline applications." McGraw Hill Professional.

Zaisha, M., Chao, Y., and Kelessidis, V. C. (2012). "Modeling and numerical simulation of yield viscoplastic fluid flow in concentric and eccentric annuli." *Chin. J. Chem. Eng.,* 20(1), 191-202.